DEVELOPMENT AND CHARACTERIZATION OF PIG HAIR-REINFORCED POLYPROPYLENE COMPOSITES FOR POTENTIAL AUTOMOBILE APPLICATIONS

BY

BALOGUN, AUGUSTINE OLAMILEKAN

A THESIS SUBMITTED TO THE SCHOOL OF ENGINEERING, DEPARTMENT OF MANUFACTURING, INDUSTRIAL AND TEXTILE ENGINEERING IN PARTIAL FULFILMENT OF THE REQUIREMENTS FOR THE AWARD OF MASTER OF SCIENCE DEGREE IN INDUSTRIAL ENGINEERING

MOI UNIVERSITY

2025

DECLARATION

Declaration by Candidate

I, **Balogun Augustine Olamilekan**, hereby solemnly declare that this research to be carried out by me in the School of Engineering, Moi University, during the 2023/2024 academic year is original and in no part or whole will it be copied from any other work thereof or manipulated in any way. Any quotations from any source will duly be acknowledged.

Signature: _____ Date: _____

Balogun Augustine Olamilekan

MS/MIE/5291/23

Declaration by Supervisors

This research project has been submitted for examination with my approval as Moi University supervisor.

Signature: _____ Date: _____

Prof. David Njuguna

Department of Manufacturing, Industrial and Textile Engineering, Moi University, Kenya

Signature: _____ Date: _____

Prof. Fatai O. Aramide

Department of Metallurgical and Materials Engineering, School of Engineering and Engineering Technology, Federal University of Technology, Akure, Nigeria

ACKNOWLEDGEMENT

First and foremost, I give thanks to the Almighty God for His guidance, strength, and grace throughout this academic journey. Without His divine help, none of this would have been possible.

I am deeply grateful to the European Union and African Union for sponsoring the Strengthening Mobility and Promoting Regional Integration of Engineering Education in Africa (SPREE) Scholarship, which provided me with this invaluable opportunity. I also extend my appreciation to Moi University, the School of Engineering, and all the staff of the Department of Manufacturing, Industrial, and Textile Engineering for offering me such a great platform to pursue this degree.

My heartfelt gratitude goes to my supervisor, Prof. David Njuguna, for his selfless dedication, invaluable guidance, and constant support. His mentorship and readiness to assist at every stage made this work possible. I am equally indebted to Prof. Josphat Igadwa Mwasiagi, whose fatherly advice, encouragement, and inspiration have been a source of strength from the very beginning. Working under his mentorship has been a great privilege.

Special thanks also go to Prof. Fatai O. Aramide for his consistent encouragement and invaluable help throughout my research journey. I am sincerely grateful to Prof. Isiaka Oladele for his insightful reviews, guidance, and willingness to provide support whenever needed. I also acknowledge Mrs. Ann Cherus, our program coordinator, for her dedication and assistance, which contributed greatly to the smooth running of my studies.

Finally, I wish to express my profound gratitude to my family and friends for their love, care, prayers, and unwavering support from the very first day of this academic journey. Their encouragement has been my greatest source of motivation.

To all who contributed in one way or another, I say a heartfelt thank you. May the Almighty God bless you all abundantly.

ABSTRACT

The automotive industry's pursuit of lightweight, sustainable materials, coupled with the environmental challenge of managing agricultural waste, necessitates innovative material solutions. This research addresses this dual challenge by investigating the viability of using pig hair—an abundant and underutilized by-product of the pork industry—as a reinforcement in a polypropylene (PP) matrix. The study aimed to develop and optimize a novel biocomposite and characterize its mechanical and physical properties for potential automotive applications. Using a compression molding technique, pig hair fibers were pre-treated with a 5% NaOH solution and incorporated into a PP matrix. A Central Composite Design (CCD) under Response Surface Methodology (RSM) was employed to systematically optimize three key process parameters: Fiber length (7-15 mm), Fiber weight fraction (2-6 wt%), and molding temperature (170-190°C). The resulting composites were characterized for their tensile, flexural, and impact strength, as well as their morphology and thermal conductivity. The statistical analysis revealed that all three parameters significantly influenced the composite's mechanical properties. The optimized process conditions were identified as a Fiber length of 11.25 mm, a Fiber weight fraction of 4.5%, and a molding temperature of 183.4°C, which yielded a maximum predicted tensile strength of 24.16 MPa. The composite also demonstrated improved thermal insulation compared to virgin PP. The key conclusion of this study is that pig hair can be effectively utilized as a reinforcing fiber to produce a viable, lightweight composite with predictable mechanical properties suitable for non-structural automotive components like interior trim and door panels. It is recommended that future research explore the use of coupling agents to further enhance fiber-matrix adhesion. For policy and practice, it is recommended that abattoirs and agricultural bodies explore the implementation of collection and pre-processing systems to create a new value chain for pig hair, transforming this waste product into a valuable industrial feedstock

TABLE OF CONTENTS

LIST OF TABLES

LIST OF FIGURES

NOMENCLATURE

$\mathbf{T_1 - T_2}$	Temperature of steam chamber and lee's disc (kelvin)
$\mathbf{V_{fl}}$	Volume of fluid displaced. (cm^3)
$\mathbf{V_0}$	Initial volume of water filled inside the graduated measuring cylinder.
$\mathbf{V_1}$	Volume of water (cm^3)
$\mathbf{W_f}$	$Final\ weight$ of the composite after abrasion test (g)
$\mathbf{W_i}$	$Initial\ weight$ of the composite before wear test (g)
$\mathbf{m_{fl}}$	Mass of fluid displaced. (g)
$\mathbf{m_s}$	Mass of the pig hair fiber
$\mathbf{\theta_1 - \theta_2}$	Initial and final temperature of disk Lee's disk (kelvin)
$\mathbf{\rho_{fl}}$	Density of fluid. (g/cm^3)
$\mathbf{\rho_s}$	Density of pig hair fiber. (g/cm^3)
cN tex^{-1}	centi Newton/Tex
cp	specific heat capacity of the Lee's disk (kelvin)
D	diameter of the composite sample (mm)
m	mass of the Lee's disk (g)
PHF	Pig hair fiber
PP	Polypropylene
t	final time taken to reach a steady temperature (min)
x	Thickness of the composite sample (mm)

DEFINITION OF TECHNICAL TERMS

- **Alkaline Treatment:** A chemical process where a natural fiber is treated with an alkali solution (e.g., sodium hydroxide) to modify its surface by removing impurities and increasing surface roughness, thereby improving its adhesion to a polymer matrix.

- **Analysis of Variance (ANOVA):** A statistical method used to test for significant differences between the means of two or more groups. In this study, it is used to determine which process parameters significantly affect the composite's mechanical properties.

- **Composite:** A material made from two or more constituent materials with significantly different physical or chemical properties which, when combined, produce a material with characteristics different from the individual components.

- **Compression Molding:** A manufacturing process in which a pre-measured amount of molding material is placed into a heated mold cavity, which is then closed, and pressure is applied to force the material to fill the cavity and cure.

- **Flexural Strength:** The ability of a material to resist deformation under a bending or flexing load. It represents the highest stress experienced within the material at its moment of rupture.

- **Impact Strength:** A measure of a material's ability to withstand a suddenly applied load or shock without fracturing, typically measured in energy per unit area (e.g., KJ/m^2).

- **Interfacial Adhesion:** The force of attraction between the reinforcing fiber and the polymer matrix in a composite material. Good interfacial adhesion is critical for effective stress transfer and overall composite strength.

- **Keratin:** A fibrous structural protein that is the key structural material making up hair, feathers, horns, claws, and hooves. It is the primary component of the pig hair used in this study.

- **Matrix:** The continuous material in a composite that encloses and binds the reinforcement together. In this research, polypropylene (PP) serves as the matrix.
- **Morphology:** The study of the form and structure of a material at a microscopic level. In this thesis, it refers to the analysis of the composite's internal structure and the fiber-matrix interface, as observed via Scanning Electron Microscopy (SEM).

- **Polymer:** A large molecule, or macromolecule, composed of many repeated subunits, known as monomers. Polypropylene is the polymer used in this study.

- **Reinforcement:** The component in a composite material that provides strength and stiffness. The reinforcement is typically a fiber, such as the pig hair used in this work.

- **Response Surface Methodology (RSM):** A collection of mathematical and statistical techniques used for designing experiments, building models, and evaluating the effects of several factors to find the optimal conditions for a desirable response.

- **Tensile Strength:** The maximum stress that a material can withstand while being stretched or pulled before necking, which is when the specimen's cross-section starts to significantly contract.

- **Valorization:** The process of converting waste materials or by-products into more useful products with a higher economic value, such as converting pig hair waste into a reinforcing fiber for composites.

CHAPTER ONE

INTRODUCTION

1.0 Introduction

In this chapter, the subject matter of the research is exposed. The sections included in the chapter include the following: background of the study, problem statement, purpose of study, objectives of study, justification, and significance of the study, scope, and expected contribution to knowledge.

1.1 Background of Research

The global search for sustainable and cost-effective materials is increasingly focused on the valorization of abundant by-products from major industries, such as the pork industry. A prime example of this resource potential can be seen in global pig populations. According to the Food and Agriculture Organization (FAO) and Gale et al. (2012), the global pig population has exceeded 900 million, with China currently holding the largest swine population worldwide. In 2020, China's swine population was reported to be 412 million pigs, with an estimated annual pork production of 55 million tons, accounting for 46% of global pig production. Ortega et al. (2009) predict that pork consumption in China will rise in the upcoming years. The European Union, with a pig population of 150 million, represents the most prominent domesticated animal classification, exceeding that of cattle. The pork meat industry within the European Union is responsible for nearly half of the overall meat output in this region. In 2018, almost 75% of the total pig population in the European Union was concentrated in six member states: Spain (20.8%), Germany (17.8%), France (9.3%), Denmark (8.5%), the Netherlands (8.1%), and Poland (7.4%) (Marie-Laure, 2020).

This abundance is not limited to global superpowers but is also reflected in developing regions, establishing a widespread and consistent supply chain. According to the 2019 Population and Housing Census report findings, a significant proportion (70%) of pig farmers in Kenya are classified as small-scale farmers. Africa is projected to have 40 million pigs in 2022, with Kenya having an estimated 800,000 pigs and a per capita consumption of 0.4 kg, well behind poultry (0.6 kg), mutton/goat (2.2 kg), and beef (12.2 kg) (FAOSTAT, 2020). Between 2030 and 2050, pig output in Africa is predicted to rise from 125% to 268% (FAO, 2017). By 2030, the demand for pig and poultry products in East Africa is expected to have increased fourfold (Alexandratos, 2012). Between 2016 and 2020, Kenya recorded an average of 0.4 million pig deaths annually due to slaughter, valued at Sh3.8 billion, with a total supply of 27 million in 2020, putting the current per capita consumption at 13 kilograms yearly. Projections indicate a potential twofold increase by 2030 (Agcenture, 2022).

This vast, underutilized global bio-resource stream aligns perfectly with the needs of industries seeking sustainable material alternatives, chief among them being the automotive sector. The automotive industry has witnessed a growing demand for advanced materials that offer enhanced functionality and protection over the last five decades. Bio-composites have found diverse applications within this sector, including micro-car body shells, e-bikes, fullelectric vehicles, automotive interiors, and structural frame parts (Sreenivas et al., 2020). Driven by technological advancements, the scientific community has shown great interest in developing new functional materials for automobile applications, focusing on exploring the potential of natural fibers as reinforcement in thermoplastic resin matrices. Natural Fiber Reinforced Plastics (NFRPs) have emerged as a viable alternative to glass or carbon fibers due to their cost-effectiveness, biodegradability, renewability, and non-toxicity.

This drive towards new materials is largely a response to the significant environmental and economic pressures associated with the industry's reliance on fossil fuels. The transportation sector relies heavily on petroleum-based fuels and is crucial in the global economy. In 2017, the global demand for oil in various modes of transportation, such as road, rail, air, and maritime, was estimated to be 43.6, 1.8, 6.3, and 4 million barrels per day, respectively (OPEC, 2017). Given the finite nature of oil resources and the anticipated increase in passenger vehicles from 1,102 million in 2017 to 1,980 million by 2040, along with a corresponding increase in commercial vehicles from 230 million to 462 million over the same period (OPEC, 2017), it is imperative to minimize oil utilization. Moreover, the transportation industry is responsible for approximately 23% of global CO_2 emissions, with the automotive sector being the most significant contributor, accounting for around 72% of annual emissions (Sims et al., 2014). The escalating demand for automobiles has prompted significant attention towards developing materials with sound abatement capabilities that are renewable, biodegradable, and lightweight, intending to reduce fuel consumption and CO_2 emissions.

Studies by Verma et al. (2017), Akampumuza et al. (2017), and Agarwal et al. (2019) have highlighted that a 10% decrease in vehicle weight can lead to an estimated 7% enhancement in fuel efficiency, and a reduction of 1 kg in weight results in a decrease of 20 kg in CO_2 emissions.

In addition to market and environmental pressures, sustainability goals have been codified into law, further accelerating research into green materials. The non-renewable and nonbiodegradable nature of petroleum products has raised concerns regarding sustainability, highenergy consumption, and environmental impact, leading to an

increased carbon footprint. Consequently, research has been directed toward using natural fiber-reinforced composites for automobile applications. The European Union (EU) has played a significant role in guiding scientific research towards biodegradable eco-composite materials, mainly due to waste disposal issues and stringent environmental regulations outlined in the EU Packaging Directive (1997), the EU Landfill Directive (1999), and the EU Directive for Automotive Parts (2000). In 2022, Europe dominated the natural fiber composites market, accounting for the largest share, with the market's significant expansion attributed to the widespread utilization of these materials in various industries, such as automotive, aerospace, building, and construction (Partners, 2023).

As a direct result of these converging pressures, a tangible shift in material selection is already underway. Automotive manufacturers have demonstrated the ability to transition from steel alloys to aluminum alloys, and there is currently a trend toward replacing aluminum with fiber-reinforced polymer (FRP) composites in specific applications. Researchers speculate that a sizeable amount of automotive mass will be made of FRP composites in the future (Njuguna et al., 2011). FRP composites, comprising reinforcing or filling fibers and a polymer matrix, have been widely used in various fields, including construction, for a considerable period, and their prevalence is increasing in diverse industries. The fibers used in FRP composites can be classified into two categories: synthetic fibers (e.g., glass, carbon, and aramid) and natural fibers (e.g., plant, mineral, or animal). While synthetic fiber-reinforced polymer composites are prevalent in high-performance sectors like the aerospace and automotive industries due to their exceptional mechanical attributes and low mass, they are costly, energy-intensive to manufacture, and not environmentally sustainable. Improper recycling of these materials can lead to significant ecological issues (Ramamoorthy et al., 2015).

This drawback of synthetic fibers has renewed interest in natural alternatives, which have a long history as reinforcement materials. Throughout history, natural fibers have been utilized as reinforcement materials. From the earliest civilizations, grass and straw were commonly employed to reinforce bricks to construct mud walls. Natural fibers offer several benefits over traditional reinforcing materials, including low density, cost-effectiveness, improved energy recovery, favorable thermal properties, acceptable specific strength, and biodegradability (Cao et al., 2016). Natural fibers can be categorized into three distinct groups: animal fiber, plant fiber, and mineral fiber (Oladele et al., 2015). Animal fibers, such as wool and hair, are derived from various sources, including sheep, cows, grass cutters, pigs, and other animals. Plant fibers can be further classified into primary and secondary categories, with primary fibers (e.g., flax, hemp, jute, and sisal) being cultivated primarily for their fiber content and commonly used as reinforcement in polymers. In contrast, secondary fibers comprise byproducts such as coir, pineapple, and oil palm. Mineral fibers include materials such as asbestos, ceramic fibers (e.g., glass fibers, Al_2O_3, SiC, BiC), metal fibers, and other naturally occurring or minimally modified fibers (e.g., aluminum fibers).

Just as the choice of reinforcing fiber is critical, so too is the selection of the polymer matrix that binds the composite together. Polypropylene (PP) is a synthetic polymer with exceptional mechanical strength and chemical resilience, making it suitable for conversion processes such as injection molding and extrusion. PP is a viable option for a range of products, including bottles, carboys, funnels, instrument jars, pails, and trays, due to its ability to withstand high temperatures. Derived from the propylene olefin monomer via subsequent processing steps in the petrochemical industry, PP is synthesized through addition polymerization, whereby monomers are joined together using thermal energy, intense radiation, and a catalyst or initiator. PP's characteristics

can fluctuate based on process parameters, copolymer components, and molecular weight and distribution. According to The European Recycling Industries (2020), around 39 distinct varieties of plastics and polymers are utilized in automobile production, with PP accounting for 72 kg of the total 158 kg of plastic used (Emilsson et al., 2019). The annual consumption of PP by European manufacturers exceeds one million tons (Toni Gallone et al., 2019).

Therefore, by combining a widely used automotive polymer with a novel, abundant natural fiber, this research aims to develop a targeted material solution. The present research has opted for pig (swine) hair as the principal reinforcing fiber. This animal fiber has been employed in diverse sectors, including textile production, biomedical practices, and construction, but its potential application in the automotive sector remains largely unexplored. Pig hair fiber, also known as bristle, is a significant by-product of the pig slaughtering industry and is commonly used in producing brushes for domestic and industrial purposes. Recent studies have demonstrated that pig hair fiber exhibits a greater coarseness than other animal species, making it more appropriate for various industrial and household uses (Mohan et al., 2014; Mohan et al., 2022).

The choice of this specific by-product is further strengthened by its significant economic and logistical footprint. Domestic pigs are widely recognized for their exceptional feed conversion efficiency compared to other domesticated animals, and the procurement of hair or bristle fibers as a by-product of pig farming during the slaughtering process is of considerable importance. According to the United Nations Commodity Trade Statistics Database, the worldwide import and export of pig hair varied between 2008 and 2011, ranging from 124.86 to 100.62 million US dollars and 139.40 to 119.39 million US dollars, respectively. Pig waste production in Europe alone

amounts to approximately 890,000 metric tons annually, with associated management costs reaching up to EUR 20.68 million annually (Rauw et al., 2020).

Beyond its availability and economic context, the intrinsic properties of the fiber are paramount for its function as a reinforcement. The mechanical characteristics of an individual fiber play a pivotal role in determining its appropriateness for diverse applications in the manufacturing of consumer and industrial commodities. Using pig hair fibers requires distinct characteristics such as fineness, rigidity, and tensile strength. The use of fibers as a reinforcement for polymers or biocomposites has been observed, and the application of pig hair fiber may be considered a carbon-neutral commodity due to its inherent source. Selecting natural fibers over synthetic ones can promote sustainable development and reduce carbon footprints (Arayana et al., 2014; Van Dam, 2008).

Ultimately, this confluence of factors—an abundant waste stream, a pressing industrial need, and a promising material profile—forms the basis of this investigation. The growing demand for advanced materials in the automotive industry and the need for sustainable and ecofriendly solutions have increased interest in natural fiber-reinforced composites. Pig hair fiber, a by-product of the pork industry, has shown potential as a reinforcement material due to its unique properties and abundance. This study explores the viability of using pig hair fiber as a reinforcement in polypropylene matrix composites for automotive applications, focusing on characterizing these composites' mechanical properties and environmental benefits. The research will contribute to developing sustainable materials for the automotive industry and provide insights into the potential of utilizing waste materials from the pork industry in high value applications.

1.2 Problem Statement

The global automotive industry faces the pressing challenge of reducing its environmental impact, which requires the development of lightweight, sustainable, and renewable materials to improve fuel efficiency and lower CO_2 emissions. Concurrently, the global pork industry generates hundreds of thousands of metric tons of pig hair waste annually. This agricultural by-product is currently treated as an environmental liability, contributing to water and soil pollution while incurring significant disposal costs for producers.

A critical disconnect exists between the automotive industry's need for novel, low-cost reinforcing fibers and the pork industry's challenge of managing this problematic waste stream. While pig hair possesses desirable properties for a reinforcement material, such as coarseness and high tensile strength, a significant gap in knowledge has prevented its effective use. The specific processing parameters and characterization data required to create a viable and optimized composite from pig hair and polypropylene—one of the most common thermoplastics in the automotive sector—were unknown.

The aim of this study was therefore to address this problem by providing the first systematic investigation into the fabrication, optimization, and characterization of pig hair-reinforced polypropylene composites, with the goal of transforming a problematic agricultural waste into a value-added engineering material.

1.3 Objectives of the Study

1.3.1 Main objective

The main objective of this research is to develop pig hair-reinforced polypropylene composites and evaluate their fundamental properties to determine their potential for automobile applications.

1.3.2 Specific objectives

a. To characterize the length, surface profile, and treatment of pig fiber for composite production.
b. To fabricate pig fiber-reinforced composite at varying fiber lengths, weight ratios, and temperatures.
c. To determine optimal mechanical properties of a pig fiber reinforced composite.
d. To characterize the mechanical, morphological, and thermal properties of the developed pig fiber-reinforced composite to assess its potential for automotive applications.

1.4 Justification of Research

The exploration of composite materials has been ongoing since the early 1900s. However, it was not until the late 1980s that a surge of interest emerged as people sought ways to transform waste into valuable products, thus aiding in environmental cleanup efforts. Natural fibers have gained significant attention, as they offer advantages over synthetic fibers regarding accessibility, cost-effectiveness, and safety. Many examples exist, including cotton, coconut fiber, straws, hemp, sisal, silk, bird fiber, horsehair, alpaca hair, and even human hair. These natural fibers are eco-friendly alternatives to glass, carbon, and artificial fibers typically used in composite manufacturing. Their appeal lies in their availability, renewability, low density, non-toxicity, biodegradability, non-irritating nature, low energy consumption during production, and satisfactory mechanical properties (Chandramohan et al., 2011; Choudhry et al., 2012).

When it comes to the automotive industry, polypropylene (PP) has emerged as a favored choice. With the chemical formula C_nH_{2n}, this linear hydrocarbon polymer is

increasingly utilized due to its exceptional mechanical properties and moldability. Alongside polyethylene (HDPE/LLPE) and polybutene (PB), low-cost, high-performance polyolefins, PP has surpassed other polymer materials like ABS, PC, and PA, establishing itself as the dominant plastic used in automobiles. It accounts for more than half of all plastics employed in the industry. Out of the 3.75 million tons of global PP consumption in 2007, around 8% was allocated to the automotive sector. However, PP does exhibit certain drawbacks, such as high flexibility and low impact strength. In order to meet the critical technical requirements set by automobile manufacturers, PP compounds must strike a suitable balance between stiffness and toughness while also possessing good thermal resistance. Furthermore, the aim is to reduce dependency on imported raw materials, ultimately achieving more competitive pricing (Moritomi et al., 2010; Dias et al., 2019; Santos et al., 2013; Da Silva Spinacé et al., 2005).

Therefore, a critical need exists to enhance the strength of PP and achieve an optimal strengthto-weight ratio, a crucial factor in the automotive industry. Various studies (Fernandes et al., 2007; Hemais et al., 2003; Maddah, 2016; Moritomi et al., 2010) have demonstrated the utilization of PP in an array of automotive products, including trunk lids, battery trays, seat belt buckling boxes, rearview mirror boxes, bumpers, and glove boxes.

As livestock animals, pigs are prominent in global meat production and consumption. Regarding meat consumption by humans, pork takes the lead, accounting for approximately 36% of the total annual consumption, followed closely by poultry at 35% and cattle and buffalo at 22%. The Food and Agriculture Organization of the United Nations (FAO) reports that the global pig population reached approximately 1 billion in 2020. Among the significant pig producers, China stands out as the largest

contributor, accounting for half of the global production and consumption, trailed by the European Union at 23%, the United States at 10%, Brazil at 8%, and Vietnam at 6% (Giamalva, 2014). These figures highlight the significant role of pigs in the meat industry.

The production capacity of pigs varies across regions and farming practices, but on average, a sow can yield up to 20 piglets per year. However, alongside the benefits of pig farming, the industry generates substantial waste, including hair, blood, and wastewater from fat smelting processes. These waste products can pose significant environmental challenges, particularly regarding their impact on ground and surface water. To put it into perspective, Europe alone produces approximately 890,000 metric tons of pig waste annually. Africa contributes a staggering 28 million metric tons annually, of which 30% comprises pig hair (Iberwaste, 2015). The management costs of handling these by-products have been estimated to reach EUR20.7 million per year in Europe. Considering the growing utilization of pig by-products, the global pig population is projected to double within the next three decades (FAO, 2021).Figure 1.1 shows an infographic that provides a brief overview of the by-products of pigs.

Figure 1.1: Current uses of pig by-product.

(Source: Farm-Credit, 2020)

The global trade in pig hair and bristles is a notable aspect of the pig industry. In 2018, the worldwide export of pig hair and bristle reached an estimated 9.3 million kilograms, totaling USD 87 million. China was the leading exporter in this trade, accounting for $75 million and 5,525,280 kilograms. Germany, the Netherlands, the United States, and Italy contributed significantly to the export market (World Integrated Trade Solution Database, 2018).

While pig hair may not be the most prominent commodity in international trade, it still holds its place. It ranked as the 1170th most traded product globally, with a total trade value of USD 114 million. Between 2020 and 2021, the exports of pig hair experienced a notable growth rate of 29.4%, increasing from USD 88.2 million to USD 114 million. However, it is essential to note that the pig hair trade represents a small fraction,

accounting for only 0.00054% of the world trade. China, Germany, Ireland, the United Kingdom, and the Netherlands were the top exporters in this trade (OEC, 2022).

However, a significant portion of pig hair fibers is discarded without reaching the market for further processing. Over 90% of the fibers obtained during pig slaughter are wasted in India and Africa. Similarly, in Europe and China, around 68% and 40% of pig hair, respectively, face the same fate (Mohan, 2009). This highlights the need for proper waste management in the pig industry to prevent environmental pollution and address associated challenges. However, there is a positive aspect amidst these statistics. Innovative utilization of pig waste can offer sustainable solutions and alleviate the strain on waste management systems. Pig waste, including hair, can be utilized as a source for composite production, reducing dependence on non-renewable resources and promoting eco-friendly practices. By doing so, we can align with global efforts to reduce carbon emissions and embrace sustainable practices (Araya-Letelier et al., 2017; Ansari et al., 2020).

When it comes to the characteristics of the pig hair fiber, it is worth noting that it exhibits a coarser texture compared to other natural protein fibers such as wool and silk (Araya-Letelier et al., 2017). This unique characteristic may have implications for its thermal and mechanical properties. Studies by Mohan et al. (2014) and Mohan et al. (2017) have explored pig hair fiber's tensile and thermal properties, respectively. The results have shown similarities between pig hair and other keratin fibers derived from animals like wool, suggesting the potential for further research on its mechanical properties for both industrial and domestic applications.

1.5 Significance of the Study

The findings of this research are poised to make significant contributions to both the industrial and academic sectors, addressing critical environmental and economic challenges.

First, this study will establish a sustainable and value-added application for pig hair, an abundant agricultural by-product that currently poses an environmental and financial burden. By demonstrating its viability as a reinforcing fiber in polymer composites, this research provides a pathway to transform a problematic waste stream into a valuable industrial resource.

Second, the development of a lightweight, pig hair-reinforced polypropylene composite will provide the automotive industry with a novel, eco-friendly material alternative. This can contribute directly to the industry's lightweighting goals, leading to enhanced fuel efficiency and a reduction in CO_2 emissions, while also decreasing reliance on non-renewable, synthetic fibers like glass and carbon.

Furthermore, this research will create new economic opportunities. It will offer an additional revenue stream for pig farmers and has the potential to generate employment in rural communities through the collection, processing, and supply of pig hair fibers.

Academically, this work will contribute valuable new data to the field of natural fiber composites. It will provide a foundational understanding of the mechanical and physical properties of pig hair-polypropylene composites, filling a crucial gap in the existing literature and paving the way for future research and optimization of animal-based fiber composites.

1.6 Scope of the Study

This research focuses on the development and characterization of pig hair fiber-reinforced polypropylene composites for automotive applications. The study utilized pig hair fibers procured from Farmer's Choice Eldoret, Kenya, with polypropylene (PP) as the matrix material. Dioctyl Phthalate (DOP) was employed as a plasticizer, and sodium hydroxide (NaOH) was used for fiber treatment. The research encompassed fiber characterization, including the determination of fiber length, diameter, aspect ratio, and fiber fineness. Alkali treatment of pig hair fibers was conducted using 0.2M NaOH solution at 50°C for 1 hour. Composites were fabricated using the compression molding technique, with variables investigated including fiber length (7-15 mm), fiber weight fraction (0.6-6%), and processing temperature (170-180°C).

Property characterization involves the evaluation of mechanical properties such as tensile strength, flexural strength, impact strength, and hardness. Thermal properties, including thermal conductivity and conductance, were measured. Wear resistance was assessed using a Taber Abrasion tester, and morphological analysis was conducted using Scanning Electron Microscopy (SEM). Response Surface Methodology (RSM) optimized the composite formulation and processing parameters. This study does not include investigating other natural fibers or polymer matrices, full-scale automotive part production or in-vehicle testing, or longterm environmental exposure and fatigue testing of the composites. All experimental work was conducted at Moi University, Eldoret, Kenya, and partnering institutions as specified in the equipment and location section.

1.7 Structure of the Thesis

This thesis is organized into five chapters, each addressing a specific aspect of the research.

Chapter One provides a comprehensive introduction to the study. It establishes the research background, defines the problem statement, and outlines the main and specific objectives. The chapter concludes by detailing the scope and justification of the research.

Chapter Two presents a critical review of the relevant literature. It covers the fundamentals of polymer composites, the properties of natural fibers, and the characteristics of polypropylene. Special attention is given to the existing research on animal-based fibers, the chemical treatment of keratinous fibers, and the use of composites in automotive applications.

Chapter Three describes the materials and methods employed in the experimental work. This includes the sourcing and preparation of the pig hair fibers and polypropylene matrix, the fabrication process of the composite samples, and the detailed procedures for mechanical, morphological, and thermal characterization.

Chapter Four presents the experimental results and provides an in-depth discussion of the findings. The effects of various process parameters on the mechanical and physical properties of the composites are analyzed and interpreted with the support of statistical models and microscopic imaging.

Chapter Five concludes the thesis by summarizing the key findings of the study. It highlights the main conclusions drawn from the research, discusses the limitations of the work, and provides recommendations for future research in this area.

CHAPTER TWO

LITERATURE REVIEW

2.0 Introduction

This chapter outlines a related literature review by other researchers on bio-composites developed from natural fibers. It presented an overview of polypropylene and pig hair as a potential resource in the automobile sector and the need for research into sustainable and ecofriendly materials. It also highlighted some of the major areas of application of natural fibers in automobile industries.

2.1 Composites Materials

Composite materials combine two or more materials with different physical or chemical properties. The addition of reinforcing materials, also known as fillers, enhances the properties of the base material beyond what each component can achieve individually (Ramnath et al., 2014). In recent years, there has been a growing interest in natural Fiber-reinforced polymer composites due to their lightweight nature, biodegradability, and the abundance of resources available. Among the various types of natural Fibers explored, animal Fibers offer intriguing advantages as reinforcement materials thanks to their high strength, abrasion resistance, and sustainable sourcing as agricultural by-products (Manjusha et al., 2016).

The rapid advancement of technology on a global scale has prompted researchers to develop new classes of materials that can be utilized in various practical applications while meeting environmental and economic standards (Ramnath et al., 2014). This demand has led to the emergence of composite materials. Composites combine elements with distinct characteristics to produce innovative materials with enhanced properties (Nijssen, 2015). The two main components of composites are the matrix and

the reinforcement, which work together to provide improved mechanical, thermal, electrical, or chemical properties compared to the individual components alone (Ma et al., 2011; Schieler & Beier, 2015; Muflikhun, 2020). Composites possess the remarkable advantage of tailoring their properties to meet specific needs and applications. This is achieved by carefully selecting combinations of matrix and reinforcement materials, allowing composites to exhibit desired characteristics such as strength, stiffness, toughness, and more (Muflikhun, 2020; Manjusha et al., 2016). Such versatility enables their utilization across various industries and sectors, including aerospace, automotive, construction, electronics, and even biomedical applications (Loeliger et al., 2021; Manjusha et al., 2016).

Another notable benefit of composites lies in their exceptional strength-to-weight ratio. Renowned for their lightweight nature, composites excel in areas where weight reduction is paramount, as seen in the aviation industry (Brooks et al., 2017). Composites achieve a remarkable balance of strength and lightness by combining robust reinforcement materials like Fibers or particles with a lightweight matrix (Manjusha et al., 2016; Gama et al., 2021). Additionally, composites exhibit superior resistance to corrosion, chemicals, and environmental factors than traditional materials such as metals. For instance, thermoplastic matrix composites display reduced moisture absorption and enhanced corrosion resistance, rendering them suitable for applications in harsh and challenging environments (Schieler & Beier, 2015).

Moreover, composites can be engineered to have excellent thermal and electrical insulation properties, making them well-suited for environments requiring precise temperature control or efficient current flow regulation (Gama et al., 2021). Composites consist of two distinct materials: the continuous or matrix phase and the discontinuous

or reinforcing phase. Typically, the discontinuous phase exhibits greater strength and hardness compared to the matrix phase. The matrix phase can comprise various materials, including metals, polymers, or ceramics. When polymers serve as the matrix phase, the composite is called a polymer matrix composite (Agarwal et al., 2017).

The term "polymer" refers to long-chain molecules composed of repeating building blocks. Polymers have become ubiquitous in our daily lives due to their versatility, ease of fabrication, and ability to be shaped into various forms. The addition of fiber reinforcement can enhance the properties of polymers. These polymer matrix reinforcements can be synthetic or natural fibers (Puttegowda et al., 2018). Polymers have often replaced metals due to their superior characteristics, including better control over the structure, reduced physical effort, easier fabrication, lower cost, wider availability, and increased productivity. Most polymers used in composites fall into thermoplastic and thermosetting (Jawaid et al., 2013). Examples of useful polymers for composite applications include amino resins, starch, polyethylene, polyester, epoxy, polypropylene, polystyrene, phenolic resins, and polylactic acid (Puttegowda et al., 2018). Polymer matrices are generally resistant to chemical attacks and exhibit excellent adhesion properties. They also have minimal shrinkage during curing and do not emit volatile gases. However, their use may be limited in high-temperature applications (Matthew et al., 1994).

2.2 Polypropylene Matrix

Polypropylene (PP), a versatile thermoplastic polymer, finds widespread use in various manufacturing sectors due to its favorable properties and cost-effectiveness. PP boasts excellent resistance to chemicals, high stiffness, impressive impact strength, and low density, making it well-suited for a diverse range of applications (Singh et al., 2008;

Altay et al., 2021). The production of polypropylene involves the polymerization of propylene monomers utilizing catalysts. Various catalyst systems, including Ziegler-Natta catalysts, metallocene catalysts, and Phillips catalysts, can be employed to control the polymerization process and customize the properties of the resulting polypropylene (Mehtarani et al., 2013).

The choice of catalyst and process conditions can influence the polymer's molecular weight, crystallinity, and other characteristics (Singh et al., 2008). Polypropylene can be manufactured through different methods, such as bulk polymerization, slurry polymerization, and gas-phase polymerization. Gas-phase polymerization is a prevalent polypropylene production technique wherein propylene gas undergoes polymerization by a catalyst within a fluidized bed reactor (Patti & Acierno, 2020). Slurry polymerization involves the suspension of propylene monomers in a liquid medium, while bulk polymerization occurs in the absence of a solvent (Singh et al., 2008).

To further tweak the properties of polypropylene, additives or fillers can be incorporated during the production process. Additives like plasticizers, stabilizers, and flame retardants can enhance specific properties or improve processability (Yousef, 2022). Fillers, such as fibers, calcium carbonate, or talc, can be integrated to bolster mechanical properties, dimensional stability, and cost-effectiveness (Bhat et al., 2008; Altay et al., 2021). The properties of polypropylene can vary depending on factors like molecular weight, tacticity, and crystallinity.

The molecular weight of polypropylene can be regulated during the polymerization process, and it affects the polymer's mechanical properties and processability (Mehtarani et al., 2013). Tacticity refers to the arrangement of methyl groups along the polymer chain and can influence properties like crystallinity and melting behavior.

Crystallinity, conversely, dictates polypropylene's stiffness and heat resistance (Świetlicki et al., 2020).

Different types of polypropylene can be produced to meet specific application requirements. For instance, isotactic Polypropylene (iPP) is the most common form and boasts high crystallinity and stiffness (Michalska-Pożoga et al., 2017). Atactic Polypropylene (APP), characterized by a random arrangement of methyl groups, is amorphous, resulting in a lower melting point and increased flexibility (Michalska-Pożoga et al., 2017). Syndiotactic Polypropylene (sPP), with its regular alternation of methyl groups, exhibits unique properties such as a high melting point and excellent optical clarity (Michalska-Pożoga et al., 2017).

Polypropylene composites present both challenges and opportunities that require careful consideration. Some of the challenges include:

1. **Interfacial Adhesion:** The nonpolar nature of polypropylene (PP) can pose a challenge in achieving strong adhesion with certain reinforcement materials like glass fibers (Shi et al., 2017). Weak interfacial adhesion can compromise the composite's mechanical properties and overall performance (Serra-Parareda et al., 2020).
2. **Moisture Uptake**: Polypropylene composites may exhibit high moisture absorption because they are hydrophobic (Slapnik et al., 2021). This moisture uptake can lead to dimensional instability, reduced mechanical properties, and degradation of the composite (Slapnik et al., 2021).
3. **Thermal Stability:** Polypropylene has relatively low thermal stability, with a lower degradation temperature than certain reinforcement materials like plant fibers (Slapnik et al., 2021). Consequently, polypropylene composites'

processing temperature and potential applications may be limited (Slapnik et al., 2021).

4. **Agglomeration of Nanoparticles**: Incorporating nanoparticles, such as clay, into polypropylene can prove challenging due to the tendency of nanoparticles to agglomerate within the nonpolar matrix (Vimalathithan et al., 2018). The agglomeration of nanoparticles can negatively impact dispersion and the overall properties of the composites (Vimalathithan et al., 2018).
5. **Surface Energy and Adhesion**: The low surface energy of polypropylene can present difficulties in achieving strong adhesion with other materials, particularly metals, in hybrid composites (Yeole et al., 2019). Improving adhesion and interfacial bonding may necessitate surface treatment or modification (Yeole et al., 2019).

Table 2.1: Properties of thermoplastic polymers (Adapted and modified from Ku et al. (2011) and Agarwal et al. (2017))

Property	Polypropylene	Low-density polyethylene	High-density polyethylene	Polystyrene	Nylon
Density	0.899-0.920	0.910-0.925	0.94-0.96	1.04-1.06	1.12-1.14
Elastic modulus (GPa)	0.95-1.77	0.055-0.38	0.4-1.5	4-5	2.9
Elongation (%)	15-700	90-800	2.0-130	1-2.5	20-150
Izod impact strength (J/m)	21.4-267	>854	26.7-1068	1.1	42.7 - 160
Tensile strength (MPa)	26-41.4	40-78	14.5-38	25-69	43-79
Water absorption (24 hours in %)	0.01-0.02	>0.015	0.01-0.2	0.03-0.10	1.3-1.8

2.3 Natural Fiber Reinforced Polymer Composites (NFRPCs)

The utilization of fiber-reinforced polymer composites (FRPCs) has garnered significant attention from researchers due to the increasing awareness of environmental concerns and the demand for more sustainable materials. These materials offer many benefits, including their lightweight nature, high strength, and enhanced resistance to

corrosion and fatigue (Thakur & Thakur, 2014). FRPCs can be categorised into two main types: natural Fiber composites (NFCs) and synthetic Fiber composites (SFCs). The term "natural" refers to materials that occur in nature, while "Fiber" implies a structure resembling hair or thread with a high aspect ratio. In the case of polymer composites, the reinforcing phase can be fibrous or non-fibrous (particulates). Natural Fibers (NF) are specifically referred to as the fibrous reinforcing phase derived from plant or other biological sources, while the resulting composites are known as natural Fiber composites (NFCs) (Nirmal et al., 2015). Within natural Fibers, there are three primary categories: vegetable or cellulose Fibers, animal Fibers, and mineral Fibers (Nirmal et al., 2015).

2.3.1 Plant Fibers

Plant/cellulosic Fibers have grown in popularity and recognition in recent years due to their low environmental impact and potential to mitigate global energy consumption and environmental hazards (Faruk et al., 2012). These Fibers offer a range of options for various utility groups, including both primary and secondary applications. The primary utility groups encompass plants that serve multiple purposes, such as kenaf, jute, hemp, and more. On the other hand, the secondary utility groups involve agricultural waste products like pineapple peels and coir. These plant/cellulosic Fibers are available in various types, each with unique characteristics and applications (Ali et al., 2018; Sanjay & Yogesha, 2017).

Some examples of these Fiber types include leaf Fibers like banana, abaca sisal, and curaua; fruit Fibers such as oil palm and coir; bast Fibers like jute, hemp, ramie, and kenaf; seed Fibers like milkweed and kapok, grass/reeds Fibers including bagasse and bamboo, stalk Fibers such as maise, wheat, and rice, and wood Fibers from both

hardwood and softwood sources (Ali et al., 2018; Sanjay & Yogesha, 2017). These plant/cellulosic Fibers are lightweight and costeffective reinforcements in various products and industries. They find applications in automobile components, building and substructure projects (bridges, roof panels, beams), recreational equipment (tennis rackets, bicycle frames), consumer goods (chairs, tables, pipes, tanks), and even rotor blades (Shah et al., 2012).

2.3.2 Animal Fibers

Animal Fibers are a compelling alternative to plant Fibers for natural Fiber reinforcement in composites. These Fibers include sheep, bison, cashmere, alpaca, pigs, and more wool. Feathers from chickens, silk from silkworms, and hair from humans and other mammals also fall under animal Fibers. However, it is worth noting that these Fibers tend to be relatively expensive compared to plant Fibers, making them the second most accessible natural Fiber option. Often, these composites find applications in more sophisticated fields, such as the medical industry (Ramamoorthy et al., 2015).

Natural Fiber composites (NFCs) present a sustainable alternative to synthetic Fibers, offering a range of desirable characteristics. These include low cost, recyclability, low density, biodegradability, strong thermal properties, high specific stiffness, low tool wear, and minimal health concerns. NFCs are more environmentally friendly than synthetic Fiber composites (SFCs). However, it is important to acknowledge that NFCs have certain limitations due to using raw Fibers. These limitations include issues with Fiber quality, high moisture absorption, and low thermal stability, which can pose challenges in preparing composites using these Fibers (Begum & Islam, 2013; Puttegowda et al., 2018).

Figure 2.1 provides a classification of various Fibers, highlighting the diverse options available in natural Fibers for composite reinforcement.

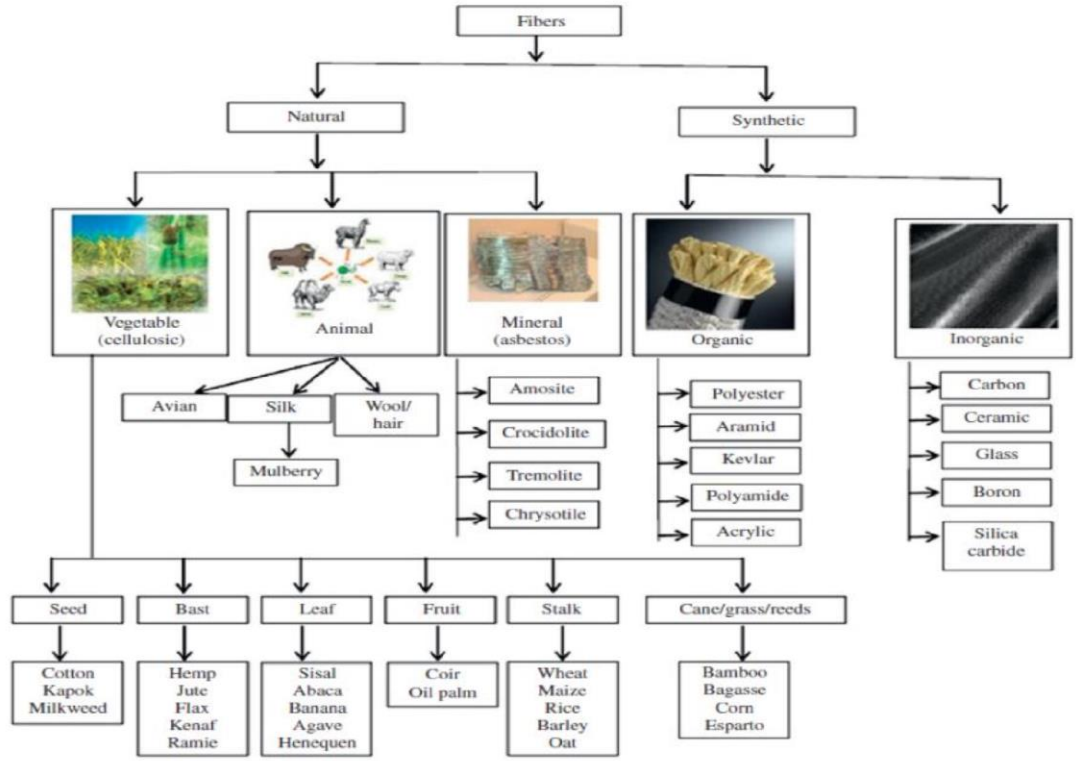

Figure 2.1: Sources of natural fibers (Puttegowda et al., 2018)

2.3.3 Sustainability of NFRPCs

In pursuing sustainable practices, industries recognise the importance of understanding how recycling and reprocessing NFRPC materials can contribute to environmental conservation while fulfilling new product requirements. It is crucial to approach each challenge with the appropriate level of expertise and knowledge (Putte Gowda et al., 2018). Figure 2.2 illustrates the limitations of utilising non-renewable resources while also showcasing potential solutions for NFRPCs based on the circular economy principles, which aim to create environmentally beneficial products and technologies.

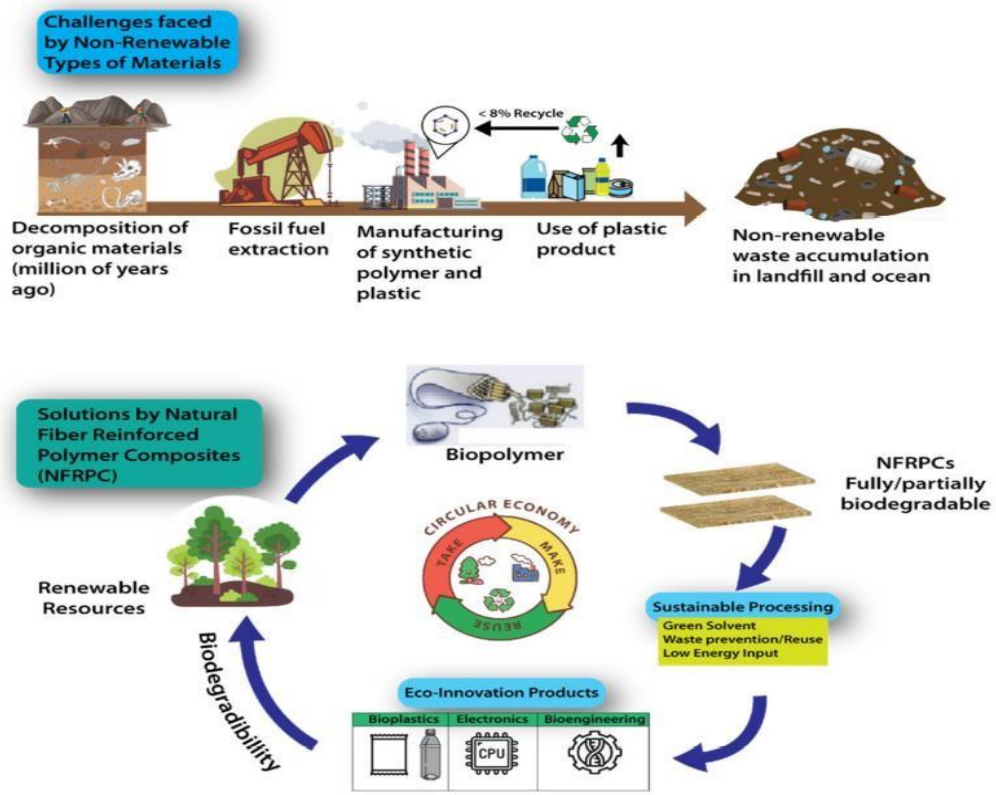

Figure 2.2: Challenges faced by non-renewable materials and solutions offered by NFRPC. (Putte Gowda et al., 2018)

With the expanding use of natural resources, there is a growing consensus among experts to transition from artificial alternatives. Using natural Fibers as reinforcements in composites offers many benefits, leading to their increased adoption. Researchers have been captivated by the remarkable properties of natural Fibers, including their biodegradability, low density, and exceptional processing flexibility (Raghavendra et al., 2014). Figure 2.3 illustrates the sustainability cycle of NFRPCs, highlighting their potential for long-lasting environmental impact.

Figure 2.3: Sustainability of NFRPC (Puttegowda et al., 2018)

Furthermore, as depicted in Figure 4, the design concept of sustainability in NFRPCs opens up a realm of new industrial applications. Natural fibers provide economic and ecological advantages over synthetic fibers when used as composite reinforcements, as shown in Table 2.2. This further emphasises the potential of NFRPCs as a sustainable and viable solution in various industries.

Table 2.2: Comparison between natural and synthetic fibers (Srinivas, 2017)

Properties		Natural fibers	Glass fibers	Carbon fibers
Economy	Annual global production (tonnes)	31,000	4,000,000	55,000
	Distribution for FRPs in EU (tonnes)	Moderate (60,000)	Wide (600,000)	Low (15,000)
	Cost of raw fiber(d/kg)	Low (0.5-1.5)	Low (1.3-20.0)	High (>12.0)
Ecological	Energy demand for raw fiber (MJ/kg)	Low (4-15)	Moderate (30-50)	High (>130)
	Renewable source	Yes	No	No
	Recyclable	Yes	Partly	Partly
	Biodegradable	Yes	No	No
	Health risk when inhaled	No	Yes	Yes

2.3.4 NFRPC for Sustainable Automotive Applications

NFRPCs possess modular properties that make them highly versatile for various applications, from everyday items to cutting-edge technologies. The automotive industry, in particular, has embraced using natural fiber-reinforced composites as reinforcing materials. The earliest documented use of NFRPCs can be traced back to the 1940s when Henry Ford employed hemp fiber composites to manufacture automobile parts. Subsequently, Mercedes-Benz adopted jute fiber in 1996 as a replacement for synthetic fibers in door panels (Peças et al., 2018). Driven by research endeavors, environmental concerns, and the implementation of new policies and regulations in the automotive sector, the utilization of NFRPCs experienced a significant surge. For instance, the EU's End of Life Vehicle Directive stipulates that 80% of a vehicle must be recyclable to facilitate proper recycling practices (2020).

Today, many interior and exterior car components are manufactured using NFRPCs, including boot linings, dashboards, noise insulation panels, door panels, headliners, decking, seat backs, hat racks, and more. The adoption of natural fiber-reinforced polymer composites in the automotive industry is driven by their ability to provide the necessary strength and durability (Fogorasi & Barbu, 2017). Furthermore, these composites offer cost-effectiveness, energy efficiency, recyclability, and the potential to reduce vehicle weight by up to 25 percent (Suriani et al., 2021). It is evident that NFRPCs present a promising solution that benefits technological advancements and contributes positively to environmental sustainability. Figure 2.4 showcases various car components manufactured using natural fiber-reinforced composites.

Figure 2.4: Car components are made up of natural fiber-reinforced composites. (Mohammed et al., 2015)

2.4 Fabrication of Natural Fiber-Reinforced Composites

The production of natural Fiber-reinforced composites entails the amalgamation of natural Fibers with a matrix material, resulting in a composite material that is both robust and lightweight (Jagadeesh et al., 2021). The fabrication of these composites involves various methods, which can be broadly classified into two major techniques: conventional manufacturing techniques and additive manufacturing techniques

2.4.1 Conventional Manufacturing Techniques

Conventional manufacturing techniques, such as injection molding, extrusion, compression molding, and resin transfer molding, have been widely employed in fabricating natural Fiberreinforced composites (Jagadeesh et al., 2021). These techniques involve the impregnation of natural Fibers with a polymer matrix and shaping them into the desired form.

1. Injection Molding

Injection molding is a highly utilised technique that involves injecting molten material, typically a thermoplastic polymer, into a mold cavity under high pressure. This technique is commonly employed for composites with shorter natural Fibers or Fiber fillers. The Fibers are mixed with a polymer melt and injected into a mold cavity under high pressure. The composite is subsequently cooled and solidified. Injection molding offers advantages such as high production efficiency, precise control over part dimensions, and the ability to produce complex geometries with excellent surface finish. However, it should be noted that there may be limitations regarding material selection and high initial tooling costs (Fu et al., 2020). Injection molding finds extensive applications in the production of plastic parts for automotive, consumer electronics, medical devices, and various other industries.

2. Extrusion

Extrusion is a process that involves the forcing of a molten material, typically a thermoplastic polymer, through a die to produce a continuous profile with a consistent cross-section. The extruded material is then cooled and cut into the desired length. Extrusion is commonly employed in the production of plastic pipes, tubes, sheets, and profiles (Fu et al., 2020). This technique offers high production rates, good dimensional control, and the ability to process various materials. However, it should be noted that producing complex shapes may pose limitations when using extrusion techniques.

3. Compression Molding

Compression molding is widely used to fabricate composite parts, such as Fiberglassreinforced plastics (FRP) and rubber products (Srebrenkoska et al., 2009). This method involves the placement of a preheated material, typically a thermosetting

polymer, into a heated mold cavity. Subsequently, the material is subjected to high pressure, ensuring its complete filling of the mold cavity and curing to attain the final product. Compression molding remains a preferred choice with advantages like good dimensional accuracy, high production efficiency, and the ability to manufacture large and complex parts. However, it is worth noting that challenges may arise in terms of cycle time and material flow control (Jagadeesh et al., 2021).

4. Resin Transfer Molding (RTM)

Resin transfer molding (RTM) is an esteemed closed-mold process renowned for its ability to produce high-quality composite parts with impeccable surface finish and dimensional accuracy (Oliveira et al., 2015). The RTM process involves placing a dry Fiber preform into a mold cavity and injecting a liquid resin under pressure, typically a thermosetting polymer. The resin infiltrates the Fibers, creating a strong bond, and undergoes curing to form a solid composite part. The aerospace, automotive, and marine industries greatly appreciate the advantages RTM offers, particularly in producing lightweight and high-strength composite components.

5. Filament Winding

Filament winding, a captivating method of composite manufacturing, is renowned for its ability to produce structures with exceptional strength and stiffness. This technique involves the continuous winding of Fibers, typically glass or carbon, onto a rotating mandrel in a predetermined pattern. As the Fibers are wound, they are impregnated with a resin matrix, such as epoxy. Filament winding finds its application in the production of cylindrical or tubular structures, including pipes, pressure vessels, and rocket motor casings (Özbek et al., 2020). The meticulous control over Fiber orientation achieved through filament winding results in structures exhibiting outstanding mechanical

properties and dimensional accuracy. It is important to note, however, that filament winding is best suited for producing rotationally symmetric shapes (Li & Ma, 2022).

6. Pultrusion

Pultrusion is a continuous manufacturing process widely employed in the production of composite profiles with a consistent cross-section. This method involves pulling continuous Fibers, such as glass or carbon, through a resin bath and a heated die. The resin used is typically a thermosetting polymer like polyester or epoxy. As the Fibers pass through the die, they are impregnated with the resin and cured to form a solid composite profile. Pultrusion finds extensive application in the fabrication of high-strength and high-stiffness profiles, including beams, rods, and tubes (Irfan et al., 2020). This process offers advantages such as high production efficiency, precise dimensional control, and the creation of long and continuous profiles. However, it is important to note that pultrusion is limited to linear profiles (Ashraf et al., 2019).

7. Hand Layup

Hand layup is a manual process employed for the fabrication of composite parts, wherein layers of Fibers, often in the form of woven fabrics or mats, are meticulously positioned by hand onto a mold or tool surface. The Fibers are subsequently impregnated with a resin matrix, such as polyester or epoxy, using brushes or rollers. This process is repeated layer by layer until the desired thickness and Fiber orientation are achieved. Hand layup offers versatility and cost-effectiveness, allowing for the production of complex shapes and customised parts. However, it is important to acknowledge that hand layup is labour-intensive and may result in variations in Fiber alignment and resin distribution (Ahmed et al., 2021).

8. Vacuum Bagging

Vacuum bagging is a technique employed in conjunction with other manufacturing methods, such as hand layup or resin transfer molding (RTM), to enhance the consolidation and compaction of composite laminates. A flexible film or bag is carefully placed over the layup or mold, and a vacuum is applied to create a pressure differential. The vacuum pressure removes air voids and ensures the intimate contact and compaction of the composite layers.

Vacuum bagging is commonly adopted in the production of aerospace components, wind turbine blades, and high-performance structures (Takagaki et al., 2016). This technique enables better control over resin infusion, improving mechanical properties and surface finish. However, it is essential to consider that vacuum bagging requires additional equipment and processing time (Khan et al., 2018).

2.4.2 Additive Manufacturing

Additive manufacturing, also referred to as 3D printing, is a swiftly advancing technology that has found its application in the fabrication of natural Fiber-reinforced composites (Ning et al., 2017). This innovative method enables precise material deposition layer by layer, allowing for the seamless integration of natural Fibers within the composite structure. Among the various additive manufacturing techniques, fused deposition modelling (FDM) is prominent in fabricating Fiber-reinforced composites (Ning et al., 2017). However, it is crucial to acknowledge that the mechanical properties of the printed components may exhibit lower strength than conventionally manufactured products (Ismail et al., 2022). While additive manufacturing presents exciting possibilities for composite production, careful consideration must be given to ensure optimal mechanical performance in the final printed parts.

2.5 Pig Hair Fiber as a Potential Reinforcement

2.5.1 Characteristics of Pig Hair Fibers

Hair, a proteinous Fiber, possesses a remarkable hierarchical organisation comprised of subunits that intricately form α-keratin chains through intermediate filaments within the Fibers. This unique structure contributes to the exceptional properties exhibited by hair, including its chemical composition, slow degradation rate, thermal insulation, high tensile strength, elastic recovery, and distinctive interaction with water and oils. These remarkable attributes have paved the way for diverse applications, with hair finding its place as a reinforcing material in composites (Kumar, 2014).

Being a proteinous fiber, hair shares similarities with other keratin-based materials such as human hair, animal fur, feathers, and nails. This keratin composition imparts strength and durability to hair, making it a formidable fiber. Notably, pig hair fibers exhibit a coarse and robust nature, granting them excellent resistance to abrasion and rendering them potentially suitable for reinforcement purposes. Furthermore, pig hair fibers' natural curvature and crimped structure provide an added advantage by enhancing their bonding capability with polymer matrices. It is important to mention that pig hair fibers have coarser properties than other natural animal protein fibers, such as wool and silk (Mohan et al., 2014).

The physical properties of pig hair fibers, including density, fineness, tensile strength, and maximum load at rupture, can vary depending on the pig breed and the specific location on the body from which the hair is obtained. Extensive studies have been conducted on breeds such as Ghungroo, Ninag Megha, Hampshire, and Duroc, revealing intriguing insights into the characteristics of pig hair fibers. For instance, the mean density of fibers on the pig's body surface ranged from 0.079 to 0.154 per mm^2.

The fineness of these fibers varied between 29.1 and 124.2 tex (Mohan et al., 2014). In terms of tensile strength, the average value for pig hair fibers was 14.05 cN tex^{-1}, with an average extensibility and Young's modulus of 31.53% and 6.39 ± 0.19 GPa, respectively. The maximum load at rupture of the fibers ranged from 9.2 to 13.8 N. Furthermore, pig hair fibers' mean work of rupture and flexural rigidity were determined to be 3.61 × 10−2 Jm^{-1} tex^{-1} and 1059 ± 321 mN mm^2 mm^{-1}, respectively (Mohan et al., 2014).

Interestingly, pig hair shares similarities with human hair in terms of thickness and density. The thickness of pig hair, ranging from 18 to 49 mm, closely aligns with that of human hair, which falls within the range of 16 to 42 mm (Otberg et al., 2004). Additionally, the hair density of pig hair on the back (24–28/cm²) and limbs (13–27/cm²) closely resembles that of human hair on the back (29/cm²) and limbs (14–32/cm²) (Otberg et al., 2004). Although the hair density of human scalp hair (292/cm²) is significantly higher than that of pig hair on the head (46–53/cm²), both species exhibit the trend of higher hair follicle density on the head compared to other body parts (Jiang et al., 2021). Figure 2.5 highlights the five major types of pig hair, illustrating the diversity within this intriguing fiber (Mohan et al., 2014).

Hair Type	Phenotype Characteristics	Position									
		Back	Limb	Hoof	Shoulder	Buttocks	Head	Beard	Ear	Eyebrow	Eyelash
Awl	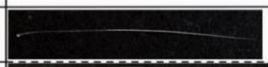	8%	42%	12%	54%	40%	NA	42%	NA	12.5%	100%
Guard_1		46%	32%	34%	38%	60%	48%	56%	100%	62.5%	NA
Guard_2		30%	16%	46%	NA	NA	NA	NA	NA	25%	NA
Auchene		10%	6%	NA	4%	NA	NA	NA	NA	NA	NA
Zigzag		6%	4%	8%	4%	NA	52%	2%	NA	NA	NA

Figure 2.5: Five different hair types found on different body parts of a pig; NA, not this hair type. (Jiang et al., 2021)

2.5.2 Availability of Pig Hair Fibers

Amongst the domesticated livestock, the pig is a remarkable creature known for its efficient feed conversion capabilities. The abundance of pig hair is a direct result of the widespread and large-scale pig farming practices across the globe. Pigs are widely raised and consumed livestock animals, with staggering numbers to support their significance. According to the insightful research conducted by Shahbandeh (2023), the world's pig population reached a staggering 778.64 million as of April 2022. Noteworthy pig-producing countries include China, the European Union, the United States, Brazil, and Vietnam, with China reigning as the largest pork producer and consumer.

In pig farming, pig hair or bristle Fibers are obtained as a valuable by-product during slaughter. The Fiber content may vary depending on factors such as the breed, age, and specific body region of the pig, with an average Fiber content of approximately 2-4% within the pig's body (Mohan et al., 2009). While pig hair has traditionally found its use in applications such as brushes, bristles, and brooms, its potential as a reinforcement material for composites is rapidly gaining attention (Araya-Letelier et al., 2017). The global import and export data for pig hair during 2008-2011 fluctuated between 124.86 to 100.62 million US$ for imports and 139.40 to 119.39 million US$ for exports (United Nations Commodity Trade Statistics Database, 2012). Furthermore, between 2020 and 2021, the exports of pig hair witnessed an impressive growth rate of 29.4%, reaching from $88.2M to $114M (OEC, 2023).

The presence of pig hair Fibers as a readily accessible by-product of the thriving pig farming industry presents an enticing opportunity for enhancing composite materials' mechanical properties and sustainability (Araya-Letelier et al., 2017). As the pig

population continues to thrive, so does the potential supply of pig hair Fibers, making them a viable and sustainable choice for reinforcing composite applications. The utilisation of these Fibers adds value to the pig farming industry and contributes to the development of eco-friendly composite materials that align with global sustainability goals.

2.5.3 Comparison with Other Natural Fibers

Wool, a highly prized textile Fiber, can be sourced from diverse animals, including sheep, goats, camels, rabbits, and other mammals. However, wool from sheep has gained unparalleled popularity due to its abundant availability and cost-effectiveness (Ramamoorthy et al., 2015). In comparison to pig hair Fibers, shear wool Fibers exhibit greater elasticity. The fineness of wool can vary significantly, typically between 16 and 40 microns, depending on the breed. Furthermore, wool Fibers possess a complex physical structure, contributing to their remarkable characteristics of elasticity, resilience, absorbency, and thermal retention (Arunkumar et al., 2013).

Human hair, on the other hand, possesses a unique composition and structure that imparts a silky yet robust and flexible nature. Unlike the aforementioned Fibers, human hair is a keratinous Fiber, distinguished by its exceptional tensile strength, high extensibility, and moisture absorption properties (Saxena et al., 2011). While pig hair tends to be shorter and coarser compared to human hair, human hair can exhibit greater length. In contrast to sheep wool, alpaca Fiber boasts a nearly pristine white hue and is warmer and lighter in weight. Moreover, alpaca Fiber is hypoallergenic, as it lacks lanolin or grease. When comparing the versatility and softness of pig hair to the exquisite qualities of alpaca Fiber used in the production of premium garments and household goods, pig hair pales in comparison (Arunkumar et al., 2013).

Cashmere is a truly exquisite wool Fiber sourced from the Cashmere goat, known for its luxurious silky texture. Cashmere offers a remarkable warmth-to-weight ratio and provides unparalleled comfort when worn. Cashmere is known for its exceptional softness and impressive tensile strength, making it a highly sought-after material (Saxena et al., 2011).

Chickens, being vertebrates, possess feathers as part of their integumentary system. These feathers originate from microscopic follicles present on the outer layer of the chicken's skin. Feathers comprise keratin proteins and exhibit a complex structure (Saxena et al., 2011). Feathers from chickens possess unique characteristics, including low density and exceptional thermal and acoustic insulation properties. Chicken feathers are suitable reinforcing materials in composite applications with a composition consisting of 91% keratin (protein), 1% lipids, and 8% water (Arunkumar et al., 2013).

Table 2.3: Mechanical Properties of Animal fibers

Fiber	Density (g/cm3)	Elongation (%)	Tensile strength (MPa)	Young's modulus (GPa)	References
Pig hair	7.9 –15.4	31.53	126.45	6.39	Mohan et al. (2014)
Alpaca fiber	1.3	25	45 - 60	4.25	Vinoth et al. (2021)
Cashmere fiber	1.345	30.79±11.48	105.81±36.51	1.51±0.42	Madueke et al. (2022)
Chicken feather	0.5 – 0.91	10.83	203	3-50	Vinodh Kumar et al. (2021)
Cow hair	1.34	8 - 20	75.6	0.73	Arinze et al. (2022)
Human hair	1.32	-	76 - 251	2 - 5	Mishra et al. (2016)
Sheep hair	1.30	25–35	50	1.2	Arinze et al. (2022)
Grasscutter hair	0.4285	23-45	40.22	0.37±0.66	Oladele et al., (2020)

2.6 Characterization of Fiber Length and Surface Profile

Fiber length, a crucial parameter in natural fibers derived from plants, animals, or minerals, encompasses the size and dimensions of individual fibers. The length of these

fibers can vary significantly depending on their source and the methods employed during processing. Understanding the characterization of natural fiber length is vital to comprehending their mechanical, thermal, and physical properties and determining their suitability for diverse applications (Oliveira et al., 2020).

When it comes to fiber-reinforced composites, the length of the natural fibers used plays a significant role in their performance. Longer fibers are preferred for mechanical properties such as tensile strength and stiffness since they facilitate a more even stress distribution (Prakash et al., 2021). The utilization of longer fibers not only enhances load transmission but also promotes improved interfacial bonding between the fibers and the matrix, ultimately enhancing the overall performance of the composite (Datta et al., 2021). However, applications that require greater impact resistance and energy absorption may benefit from using shorter fibers (Oliveira et al., 2020).

Characterizing the length of natural fibers can be challenging, given the multitude of fibers present even in a small sample (Goris et al., 2017). Various methods have been developed for measuring and analyzing the length distribution of natural fibers. These methods include optical microscopy, image analysis, scanning electron microscopy (SEM), and other techniques (Goris et al., 2017; Codispoti et al., 2013). By applying these methodologies, researchers have accurately measured the length distribution and average length of natural fibers, providing crucial data for product development and fabrication processes.

The surface profile of natural fibers can vary, exhibiting either a smooth or rough texture. This surface profile plays a significant role in the adhesion properties, frictional behavior, and interfacial interactions of fibers with other materials. To fully understand the performance of natural fibers in diverse applications, such as their use as

reinforcement in composites, it is crucial to characterize their surface profile. Factors such as surface treatment techniques (Saravanan et al., 2023; Hossain et al., 2013), inter-fiber entanglement (Lu et al., 2012), and the presence of a soft and compliant layer on the fiber's surface can influence the surface profile of natural fibers.

For instance, the presence of a liquid-like layer on the fiber's surface can enhance its adhesion and frictional properties, allowing the fiber to conform to the roughness profile of the substrate (Saravanan et al., 2023). Chemical modifications of the fiber's surface profile through surface treatment techniques can also improve the compatibility of fibers with matrix materials (Hossain et al., 2013). However, characterizing the surface profile of natural fibers can be challenging due to their heterogeneous and complex surfaces. Various methods, including atomic force microscopy (AFM), scanning electron microscopy (SEM), and contact angle measurements, have been employed to investigate the surface roughness and topography of natural fibers (Karliati et al., 2019; Hamieh, 2011). These methods provide valuable insights into the surface properties of fibers, which can be utilized to enhance the performance of materials.

2.7 Fiber Treatment Techniques

Fiber treatment techniques are pivotal in enhancing the properties of natural fiber-reinforced polymer composites (NFRPCs). These treatments aim to address the limitations of natural fibers, such as poor interfacial adhesion, low melting point, and high moisture absorption (Kalia et al., 2011). By employing surface treatment, the hydrophobicity of fibers can be improved, leading to enhanced interfacial bonding between the fibers and the polymer matrix, reduced moisture absorption, and increased fiber roughness and wettability (Ku et al., 2011). Ranges of fiber treatment techniques

are available to achieve these objectives, including surface chemical modification, physical treatments, and hybrid treatments.

2.7.1 Surface Chemical Modification

Surface chemical modification is a commonly employed technique for altering the surface of natural fibers. Before their reinforcement use, fibers undergo treatment with various chemicals to enhance their performance. These chemicals encompass a range of substances, including alkali, potassium permanganate, silane, enzymes, sulfuric acid, saltwater, benzoyl peroxide, and more (Mansingh et al., 2022). Kalia et al. (2011) state that these chemical treatments increase surface roughness, cleanse the fiber surface, and induce chemical changes on the surface.

The modification of fiber surfaces through chemical treatments contributes to the improvement of mechanical and thermal characteristics in natural fiber-reinforced polymer composites (NFPCs). This is achieved by enhancing the interfacial adhesion between the natural fibers and the polymer matrix (Nurazzi et al., 2021). Alkali treatments, in particular, have been extensively studied for their effects on natural fibers and composites. Researchers have focused on developing methods to enhance compatibility between hydrophobic thermoplastic polymers and hydrophilic natural fibers, and alkali treatment has emerged as a viable solution (Serrano et al., 2013).

Among the various techniques employed for surface modification of natural fibers, alkali treatment is a commonly used and cost-effective approach. It facilitates the removal of wax, hemicellulose, and inorganic impurities, resulting in an increased effective surface area and improved adhesion to the polymer matrix (Wang et al., 2017). In addition, this treatment method has been found to enhance fiber-matrix compatibility by increasing surface roughness and thickness (Hong et al., 2019).

The influence of alkali treatments on the characteristics of natural fibers has been extensively investigated in numerous studies. For instance, Mohammed et al. (2015) observed that hemicellulose and pectinase treatments can enhance the thermal characteristics of fibers. It has been demonstrated that alkali treatments can improve the wettability, surface structure, chemical composition, and tensile strength of natural fibers by effectively removing contaminants such as lipids, lignin, and pectin (Nurazzi et al., 2021). Furthermore, alkali treatments have been linked to improved interfacial adhesion between the fibers and the polymer matrix, primarily through increased cellulose content on the fiber surface (Awad et al., 2022).

Several studies have also investigated the mechanical properties of natural fiber composites following alkali treatment. Verma et al. (2022) examined the impact of alkali treatment on the mechanical properties of kenaf-epoxy composites and found that chemical treatments, including alkali treatment, can enhance the bondability between the fibers and the matrix. Similarly, Hao et al. (2018) explored the improvement of interface bonding in sisal fiberreinforced polylactide composites with the addition of epoxy oligomer and found that alkali treatment enhances the interfacial adhesion between the fiber and the matrix. In a study by Subramonian et al. (2016) on the effect of fiber loading on the mechanical properties of bagasse fiber-reinforced polypropylene composites, it was reported that alkali treatment of the fibers enhances the adhesion between the fibers and the polypropylene matrix, resulting in increased tensile strength and modulus of the composites.

In a study conducted by Motaleb et al. (2018), pineapple leaf fiber-reinforced polypropylene composites were developed, and the impact of alkali treatment on their physicomechanical characteristics was investigated. The findings revealed that the

alkali treatment of the fibers led to enhancements in the tensile strength, tensile modulus, elongation at break, bending strength, and bending modulus of the composites. Furthermore, the water absorption of the composites was reduced. Similarly, Hermawan et al. (2019) explored the physical and mechanical properties of green thermoplastic composites reinforced with oil palm microfibers. They observed that alkali treatment of the fibers resulted in improved mechanical characteristics of the composites, primarily due to enhanced interfacial adhesion between the fibers and the polypropylene matrix.

Alkali treatment has also been shown to influence the thermal characteristics of natural fiber composites and their mechanical properties. Hong et al. (2019) researched bagasse fiber-based composites and found that alkali treatment improved the interfacial compatibility between the fiber and the polymeric components, thereby affecting the thermal and mechanical characteristics of the composites. Similarly, using thermal and structural analysis, Kamarudin et al. (2020) investigated kenaf fiber-reinforced poly(lactic acid) bio-composites. They discovered that alkali treatment enhanced the interfacial adhesion between the fiber and the matrix, improving mechanical properties.

Furthermore, Ramlee et al. (2022) examined the thermal and acoustical characteristics of biophenolic hybrid composites made from oil palm and bagasse fibers after undergoing silane and hydrogen peroxide treatment. The chemical surface treatment improved the composites' thermal stability, as it increased the adhesion and interfacial bonding between the fibers and the polypropylene matrix. Furthermore, applying alkali treatment with other surface alteration methods has demonstrated synergistic effects. A study conducted by Gieparda et al. (2021) revealed that the combined treatment of alkali and silane on the surface resulted in the strongest interfacial adhesion between the

natural rubber matrix and jute fibers. This combined treatment not only enhanced the interfacial adhesion but also improved the mechanical characteristics of the composites.

To summarize, alkali treatments have been extensively utilized for surface chemical modification of natural fibers, aiming to enhance their compatibility with polymer matrices. These treatments eliminate impurities, increase surface roughness, and improve the interfacial adhesion between the fibers and the matrix. As a result, alkali treatments have significantly enhanced natural fiber composites' mechanical and thermal properties. It is important to note that the effectiveness of alkali treatments may vary depending on the specific type of fiber and the treatment conditions employed.

2.7.2 Physical Treatment

In addition to chemical processes, physical treatments offer an alternative approach to modifying natural fibers' surface and structural properties. Techniques such as fibrillation, electric discharge (cold plasma, corona), steam explosion, and mechanical hot-pressing have been utilized as physical treatments (Nurazzi et al., 2021). These treatments aim to enhance the bonding between the polymer matrix and reinforcing fibers, thereby increasing the strength of the resulting composites (Nurazzi et al., 2021).

Fibrillation, in particular, involves the mechanical separation of individual fibrils from natural fibers. This process effectively increases the surface area of the fibers, leading to improved interfacial adhesion with the polymer matrix. Nurazzi et al. (2021) discussed the application of fibrillation as a surface treatment for natural fiber-reinforced polymer composites. They highlighted its potential to enhance stress transfer between the fibers and the matrix, ultimately resulting in improved mechanical properties of the composites.

Electric discharge techniques, such as cold plasma and corona treatment, have also been explored to enhance the surface characteristics of natural fibers. These processes involve the application of electrical energy to the fibers, activating their surfaces and inducing chemical changes. Zwawi (2021) mentioned plasma treatment as a green technology that can be employed to clean, etch, deposit, and polymerize the surface of natural fibers. These treatments enhance the composites' mechanical properties by strengthening the bond between the fibers and the polymer matrix.

2.7.3 Hybrid Treatment

Hybrid treatments, combining multiple fiber treatment methods, have emerged as promising to achieve additive effects. A notable study examined the impact of surface modification on the mechanical and thermal properties of epoxy hybrid composites reinforced with flax, sisal, and glass fibers. The researchers discovered that the alkaline treatment of sisal and flax fibers significantly enhanced their tensile, flexural, and impact strength (Meenakshi & Krishnamoorthy, 2019).

Another study investigated the water absorption and mechanical properties capabilities of woven bamboo/flax composites while considering the effects of stacking order and hybridization. The findings revealed that various factors, including the choice of polymer matrix, fiber treatment method, individual fiber loading, and fiber selection, influenced the mechanical characteristics of the hybrid composites (Shesan et al., 2019).

In an interesting exploration of alternative approaches to chemical treatments, Jagadeesh et al. (2021) delved into the concept of hybridization for reducing the hydrophilicity of natural fibers. They emphasized the potential of hybridization in combining natural fibers' hydrophilicity with synthetic fibers' hydrophobicity, ultimately leading to improved characteristics in the composites.

Indeed, fiber treatment techniques play a crucial role in enhancing the properties of natural fiber-reinforced polymer composites. By implementing surface chemical modification, physical treatments, and hybrid treatments, we can unlock various benefits for fibers. These treatments are designed to improve the hydrophobicity of the fibers, foster stronger interfacial bonding, reduce moisture absorption, and enhance the roughness and wettability of the fibers. As a result, the mechanical and thermal properties of the composites experience a significant boost.

2.8 Chemical Treatment of Animal (Protein-Based) Fibers

The performance of a natural fiber-reinforced composite is highly dependent on the interfacial adhesion between the fiber and the polymer matrix. For animal fibers like pig hair, which are protein-based, surface treatments are employed to clean the fiber surface and modify its topography and chemistry to promote better bonding with a hydrophobic matrix like polypropylene (PP) (Manikandan et al., 2017). While various treatments such as plasma, enzymatic, and silane coupling agents have been explored, alkaline treatment using sodium hydroxide (NaOH) remains one of the most common and cost-effective methods for modifying protein-based fibers (Akin et al., 2011; Sharma, Singh, and Singh, 2018).

2.8.1 The Structure of Pig Hair (Keratin)

Pig hair is primarily composed of the protein α-keratin, a fibrous structural protein. Keratin consists of long chains of amino acids organized in a helical structure and linked by peptide bonds (Monteiro et al., 2019). These chains are cross-linked by various interactions, including hydrogen bonds, salt bridges, and most notably, strong covalent disulfide bonds (-S-S-) from the amino acid cystine. This robust, cross-linked structure gives hair its characteristic mechanical strength, chemical resistance, and thermal

stability (Jones, 2001). The surface of the hair fiber is covered by a smooth, scaly layer called the cuticle, which is hydrophobic due to a covalently bonded layer of fatty acids, primarily 18-methyleicosanoic acid (18-MEA) (Rouse & Van Dyke, 2016). This hydrophobic surface, while seemingly compatible with a nonpolar matrix like PP, is too smooth to form a strong mechanical interface, leading to poor adhesion and stress transfer (Monteiro et al., 2019).

2.8.2 The Effect of Alkaline (NaOH) Treatment on Keratin

Unlike the treatment of plant fibers, where NaOH primarily removes cementing agents like lignin and hemicellulose, its effect on keratin is a process of controlled surface degradation and chemical modification. The chemical reactions are multifaceted. A primary reaction is the hydrolysis of peptide bonds (-CO-NH-) in the protein chains, particularly at the surface of the fiber (Aluigi et al., 2008). Critically, the alkali also attacks and cleaves the strong disulfide cross-links through a process of hydrolysis. This reaction, known as keratinolysis, disrupts the tightly packed protein structure and can lead to the formation of more reactive thiol (-SH) and dehydroalanine groups on the fiber surface (Saravanan & Dhurai, 2012; Sharma, Singh, and Singh, 2018).

The extent of this chemical attack is dependent on the concentration of the NaOH solution, the treatment duration, and the temperature (Manikandan et al., 2017). The goal is to induce a controlled level of degradation, sufficient to alter the surface morphology without compromising the bulk integrity of the fiber.

2.8.3 Impact of Treatment on Composite Properties

The objective of this controlled chemical treatment is to modify the fiber's surface to enhance its function as a reinforcement. The primary benefit of the alkaline treatment is the roughening of the fiber surface, which directly improves interfacial adhesion. By

hydrolyzing the surface proteins and removing the fatty acid layer, the treatment etches away the smooth cuticle scales, increasing the surface area and creating a more irregular topography (Fiore et al., 2014; Monteiro et al., 2019). This allows the molten polypropylene matrix to flow into the newly created pits and grooves, promoting strong mechanical interlocking at the fiber-matrix interface. This enhanced interlocking facilitates more efficient stress transfer from the matrix to the fiber, which can significantly improve the mechanical properties of the composite, including its tensile strength, flexural modulus, and impact strength (Sharma, Singh, and Singh, 2018; Reddy et al., 2009).

However, a critical trade-off exists, as the treatment carries the risk of excessive fiber damage. If the treatment is too aggressive—for instance, if the NaOH concentration is too high or the duration is too long—the chemical degradation will not be confined to the surface. It will penetrate deep into the fiber's cortex, severely cleaving the keratin chains and disulfide bonds. This excessive damage reduces the intrinsic strength and stiffness of the pig hair fiber itself (Aluigi et al., 2008; Goud et al., 2011). A weakened fiber cannot act as an effective reinforcement, and the resulting composite will exhibit poor mechanical properties, often worse than those with untreated fibers, regardless of the improved surface adhesion (Manikandan et al., 2017).

Therefore, the concentration of the NaOH solution is a critical parameter that must be optimized. The ideal treatment creates sufficient surface roughness to enhance adhesion while minimizing the loss of the fiber's inherent tensile strength. This study's investigation into varying NaOH concentrations is aimed at identifying this optimal balance for the pig hairpolypropylene system, a common challenge noted throughout the literature on protein-based fiber composites (Fiore et al., 2014).

2.9 Mechanical Properties of Natural Fiber Composites

2.9.1 Principles of Natural Fiber-Reinforced Composites

The performance of a natural fiber-reinforced composite is fundamentally governed by the efficiency of stress transfer from the polymer matrix to the reinforcing fiber. This is highly dependent on the interfacial adhesion between the two components, a principle highlighted by Ku et al. (2011). The quality of this interface, along with several physical parameters, dictates the composite's overall mechanical properties, including tensile, flexural, and impact strength (Rajini, 2013; Khalid et al., 2021). Key parameters that have been consistently shown to influence these properties are fiber length and fiber weight fraction.

The length of the reinforcing fiber plays a crucial role in determining the mechanical qualities of the final composite. As demonstrated by Anand et al. (2022) in their work on pineapple leaf fiber composites, longer fibers can contribute to greater tensile strength. This is because a certain minimum "critical fiber length" is required for the matrix to effectively transfer the applied load to the fiber. Milosevic et al. (2017) further emphasized that fiber length, alongside alignment and dispersion, is a determining factor in composite performance. A comprehensive review by Datta et al. (2021) confirmed the importance of regulating the contact between the fiber and matrix via fiber length to achieve desired mechanical characteristics.

Similarly, the fiber weight fraction, or the amount of fiber in the composite, is a critical optimization parameter. Studies have repeatedly shown that mechanical properties like tensile strength and hardness tend to increase with fiber volume up to an optimal point (Prakash et al., 2021). For example, Bhuvaneshwaran et al. (2019), in a detailed investigation on Coccinia indica fiber-reinforced epoxy composites, found that a fiber

loading of 35 wt% with a fiber length of 30 mm yielded the most superior mechanical capabilities. Beyond this optimal loading, issues such as poor fiber wetting, increased porosity, and fiber-to-fiber agglomeration begin to dominate, leading to a decline in performance. This trend was also observed by Ameer et al. (2019) in jute/polypropylene composites, where a fiber volume fraction of 0.30 exhibited the best flexural and impact properties, while a fraction of 0.40 showed the best tensile properties, indicating a clear trade-off and the need for careful optimization.

2.9.2 Overview of Natural Fiber Applications in Various Matrices

The application of natural fibers as reinforcement is diverse, extending beyond the thermoplastic composites that are the focus of this study. For instance, researchers have investigated the use of pig hair to improve the impact strength of cementitious mortars (ArayaLetelier et al., 2017) and the compressive strength of concrete, sometimes in combination with other waste materials like crushed mussel shells (Gagan & Lejano, 2016). While these studies validate the reinforcing potential of keratin fibers, the bonding mechanisms and failure modes in an inorganic, brittle matrix like concrete are fundamentally different from those in a ductile, organic polymer matrix like polypropylene.

A significant body of research also exists for natural fibers in thermoset matrices like epoxy. Hashim et al. (2019) explored chicken feather fibers in epoxy for automobile interiors, finding an optimal concentration at 4 wt% for tensile and flexural strength. Similarly, Oladele et al. (2020) developed a hybrid composite using coir and chicken feather fibers in an epoxy matrix. However, the rigid, cross-linked chemical structure of thermosets creates a different interfacial condition and processing reality compared to the melt-processed interface in thermoplastics. Therefore, while these studies are

valuable for context, their results are not directly transferable to a pig hair/polypropylene system.

2.9.3 Keratin Fibers as Reinforcement in Thermoplastic Composites

Research on keratin fibers within thermoplastic matrices provides a more direct context for the present study. Various animal fibers have been explored, each with unique properties and challenges. Oladele (2014) investigated fowl feathers and cow tail hair in high-density polyethylene (HDPE), noting that different fiber types and concentrations were optimal for different properties (flexural vs. tensile). Choudhry & Pandey (2013) found that incorporating human hair into polypropylene decreased tensile strength but improved flexural and impact strengths, highlighting the complex effects of fiber addition. Studies using horn fiber (Kumar & Boopathy, 2014) and chicken feathers (Caavate et al., 2016) in PP and PLA, respectively, also reported mixed results, often observing a trade-off between stiffness and ultimate strength.

These studies collectively demonstrate the potential of keratinous by-products as reinforcements but also reveal a consistent challenge: achieving strong interfacial adhesion with hydrophobic thermoplastic matrices. This often leads to suboptimal performance and highlights the need for a more critical, systematic approach to material development, which is detailed in the following analysis. Table 2.4 provides a critical analysis of past studies on animal fiber-reinforced polymer composites.

Table 2.4: Critical Analysis of Recent Studies on Animal Fiber-Reinforced Polymer Composites

Author(s) & Year	Fiber Type & Matrix	Key Methodology	Key Findings	Critical Analysis & Limitations
Tusnim et al. (2022)	Hybrid: Jute + Sheep Wool fibers; Polypropylene (PP) matrix	Hot compression molding; jute fibers treated with 5% NaOH and diazonium salt.	Best performance from composites using neutral-pH diazonium-treated jute combined with untreated sheep wool, yielding highest tensile, flexural, and hydrophobic properties.	Relies on complex chemical modification of jute. Lacks statistical optimization (DoE/RSM). As a hybrid composite, it does not isolate the effects of the keratin (wool) fiber, making it difficult to draw conclusions for single-fiber systems like pig hair.
GarridoSoriano et al. (2018)	Chicken Feather fibers; Polypropylene (PP) and LDPE	Melt blending with 20 vol% ground feathers; chemical modifications (acetylation, silanization) and coupling agents (MAPP).	Addition of 20 vol% untreated feathers drastically reduced tensile strength. Chemical treatments and MAPP only partially improved bonding; mechanical properties remained degraded at high loading.	Required both MAPP and chemical surface treatments, yet the interface remained weak. Highlights the significant challenge of keratin-polyolefin adhesion. Uses hollow chicken feathers, which differ morphologically from solid pig hair.
Melo et al. (2018)	Wool fibers; Polypropylene (PP)	Melt blending and injection molding; used MAPP as a coupling agent.	Increasing MAPP concentration improved stress transfer and tensile/flexural strength. Without MAPP, poor adhesion was observed.	Success is entirely dependent on the use of a MAPP compatibilizer. The study did not investigate fiber surface pre-treatments (like NaOH) as an alternative to improve adhesion, which is a key part of your study's methodology.
Sek-Kudłacik et al. (2020)	Chicken Feather fibers; Polypropylene (PP)	Extrusion and injection molding; surface treatment	Silane treatment improved thermal stability and mechanical properties (tensile and flexural	Relies on a silane coupling agent, not a simple alkaline treatment. Also uses hollow chicken feathers. The study did not systematically optimize other

		with BQTMS silane coupling agent.	strength) compared to untreated feather composites.	process variables like fiber length or temperature.
Verma & Gope (2021)	Human Hair; Polypropylene (PP)	Compression molding; investigated fiber loading (315 wt%).	Optimal performance was found at 5 wt% fiber loading. Higher concentrations led to agglomeration and a decrease in mechanical properties.	Validates the concept of an optimal fiber loading but lacks a systematic statistical optimization (RSM) to study the interaction effects of other crucial parameters like fiber length and processing temperature.
Oladele et al. (2020)	Cow Hair; Recycled Polypropylene (rPP)	Compression molding; investigated fiber length and weight %.	Tensile and impact strength increased with fiber loading up to an optimal point (30 wt%) before decreasing.	Used recycled PP (rPP), which can have inconsistent properties compared to virgin PP. The study did not include chemical pre-treatment of the fibers, likely resulting in sub- optimal interfacial adhesion.
Atagur et al. (2021)	Angora Goat Hair; Polypropylene (PP)	Twin-screw extrusion and injection molding.	Increasing fiber content (up to 30%) decreased tensile strength but increased flexural modulus. SEM showed poor adhesion.	Highlights the challenge of keratinPP adhesion but did not include any fiber surface treatment (like NaOH), which is a critical step in your study to enhance mechanical interlocking without extra compatibilizers.
Nien et al. (2021)	Hybrid: Rice Straw + Chicken Feather fibers; Epoxy matrix	Hand lay-up; 3D fiber mats; NaOH treatment on straw fibers.	Hybrid straw+feather laminates exhibited synergistic gains: higher flexural and impact strength than single-fiber composites.	Utilizes a thermoset matrix (epoxy) and a non-standard hand lay-up process, limiting direct comparison. The "synergy" in a hybrid might be a test artifact and doesn't inform on single-fiber performance in a thermoplastic.

2.9.4 A Critical Comparison of Pig Hair with Other Keratin Fibers

While keratin is the fundamental protein in animal fibers such as wool, human hair, and chicken feathers, the physical and morphological characteristics of these fibers differ significantly, which has profound implications for their performance as composite reinforcements. Pig hair, also known as bristle, is distinguished primarily by its exceptional coarseness, rigidity, and large diameter. These properties set it apart from other keratinous fibers and are critical to understanding its potential as a reinforcement material.

Compared to the fine, flexible, and often crimped structure of wool or the smaller diameter of human hair, pig bristles possess a much larger diameter—often exceeding 150 μm—and greater inherent stiffness (Franbourg et al., 2003). This distinction is critical for composite performance. A larger, stiffer fiber can provide more substantial reinforcement against bending (flexural forces), but it can also act as a larger stress concentration point at the fibermatrix interface. This may lead to a different failure mechanism, such as interfacial debonding, compared to the behavior of finer, more flexible fibers which might fail by fracture (Hughes, 2012).

Furthermore, the surface topography of the cuticle layer on pig hair differs from that of wool, which can affect the efficiency of chemical treatments and the degree of mechanical interlocking with the polymer matrix. Another key differentiator is the fiber's structure. Unlike chicken feathers, which have a complex, hollow, and lightweight structure consisting of a rachis and barbs, pig hair is a solid, dense fiber. This makes it less prone to crushing or collapsing during high-pressure manufacturing processes like compression molding, ensuring a more consistent and robust transfer of stress from the matrix to the fiber.

Therefore, while general principles can be learned from studies on other keratin fibers, the unique morphological properties of pig hair, specifically its large diameter, high stiffness, and solid cross-section necessitate a dedicated investigation. Extrapolating results from composites made with wool, human hair, or chicken feathers would be scientifically unsound, as these differences will fundamentally alter the processing behavior, interfacial dynamics, and ultimate mechanical properties of the final composite.

2.10 Research Gap

After a comprehensive review of the existing literature, it is clear that while significant progress has been made in the field of natural fiber composites, several critical research gaps persist. The preceding analysis highlights a consistent need for more systematic and targeted research. This study is therefore designed to address the following specific gaps:

1. **Lack of Focus on Pig Hair in Thermoplastic Composites:** While extensive literature exists for plant-based fibers (Sanjay et al., 2018) and other animal fibers like chicken feathers (Tesfaye et al., 2017) or human hair (Choudhry & Pandey, 2013), there is a notable absence of comprehensive research on pig hair as a reinforcement in a thermoplastic matrix like polypropylene. The unique morphology of pig hair means its performance cannot be reliably predicted from studies on other keratin fibers, necessitating a dedicated investigation.
2. **Absence of Systematic Process Optimization:** Many previous studies on natural fiber composites (e.g., Pickering et al., 2016) have focused on a limited range of processing parameters. A systematic investigation using statistical tools like Response Surface Methodology (RSM) to model and optimize the

interacting effects of fiber length, weight fraction, and processing temperature for pig hair-PP composites has not been conducted, which is crucial for moving beyond proof-of-concept to developing a material with predictable and optimized properties.

3. **Need for Comprehensive, Application-Focused Characterization:** While natural fiber composites have been studied for various applications, there is limited research specifically targeting their use in automotive components with a full suite of property characterizations (Ramesh et al., 2017). This research aims to provide a holistic analysis, including mechanical (tensile, flexural, impact), thermal, and morphological properties, evaluated within the specific context of automotive material requirements.
4. **Under-Explored Potential for Waste Valorization:** Despite the growing interest in sustainable materials, the potential of pig hair—a globally abundant by-product of the pork industry—remains largely unexplored in materials science (Araya-Letelier et al., 2017). There is a clear gap in research that demonstrates a viable pathway for valorizing this agricultural waste, transforming a costly environmental liability into a value-added industrial product for a high-demand sector.

By addressing these research gaps, this study will contribute new and valuable knowledge to the field of natural fiber composites. The findings will provide the first systematic optimization of pig hair-reinforced polypropylene composites, offering crucial insights for the automotive industry in its pursuit of more sustainable material solutions and paving the way for the industrial-scale implementation of this novel bio-composite.

CHAPTER THREE

MATERIALS AND METHODS

3.0 Introduction

This chapter presented the methodological process used for the development of the biocomposites from pig hair fiber. The development process includes fiber screening, fiber treatment, the experimental design technique, composite fabrication, thermal conductivity, and optimization of the developed composites.

3.1 Materials

3.1.1 Pig hair fiber

As the primary material for this research, pig hair fiber was sourced from Sukunagas Pork Slaughterhouse located in Eldoret, Uasin Gishu County, Kenya. The fibers were extracted from slaughtered (duroc) pigs by scraping them with scissors. A thorough cleaning process was carried out on the fibers using mild water and non-ionic detergents to eliminate debris, oil, and other contaminants. After being sun-dried, the fibers were cut into various lengths and divided into two groups: one untreated and the other chemically treated.

Figure 3.1 provides a visual overview of the stages involved in the preparation of pig hair fibers for composite fabrication: (a) the Duroc pig, which is the source of the fibers, (b) the extracted pig hair, and (c) the washed and sun-dried pig hair fibers. These images illustrate the raw material and its processing stages before incorporation into the polypropylene matrix for composite development.

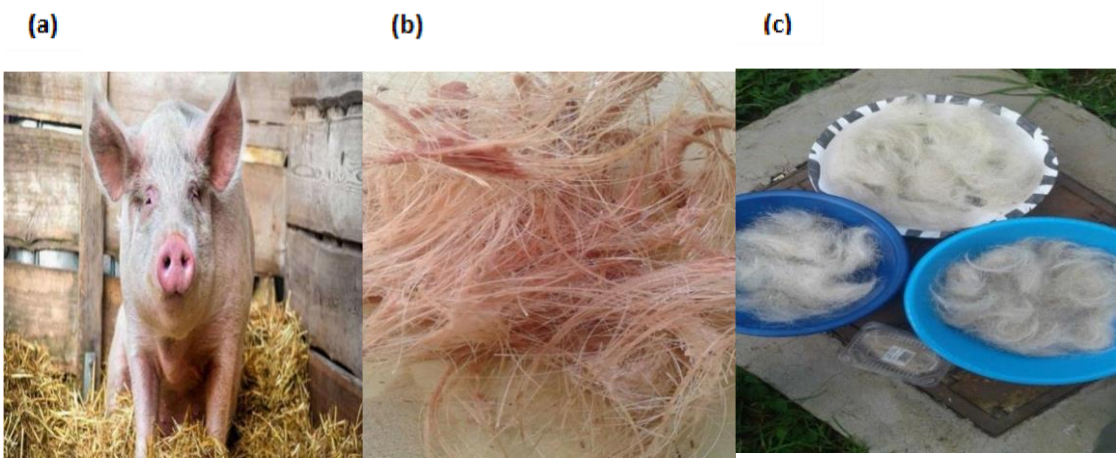

Figure 3.1: Macroscopic Image of: (a) Duroc pig, (b) Extracted Pig hair (c) Wash and sundried Pig hair fiber

3.1.2 Chemicals and Reagents

Polypropylene (PP), plasticizer (Dioctyl Phthalate), aluminum foil/Teflon sheets, and Sodium hydroxide (NaOH) were procured from commercial suppliers. The compression molding machine and metal molds were obtained from Rivatex East Africa Textile Limited, Eldoret. Distilled water was sourced from the Chemistry Department, Moi University, Eldoret.

3.1.3 Sustainability and Ethical Considerations in Material Sourcing

The sourcing of all materials for this research was guided by principles of sustainability and ethical responsibility. The pig hair used as reinforcement was sourced as a post-slaughter byproduct from a local abattoir in Eldoret, Kenya. It is critical to state that no animals were raised or harmed for the purpose of this study. The use of this material is an act of waste valorization which is the process of converting a low-value waste stream into a higher-value commodity. The pig hair would otherwise have been discarded, contributing to environmental waste management challenges and associated costs. By repurposing it as a reinforcing fiber, this research aligns with the principles of a circular economy, promoting the sustainable use of existing resources and reducing the environmental footprint of the pork industry. This approach provides an ethical and

environmentally sound basis for the research, ensuring that the study contributes positively to sustainable material development.

3.2 Equipment

The experimental work was conducted using the equipment detailed in Table 3.1, which lists the specifications and locations for each instrument.

Table 3.1: Research Equipment and Location

Equipment	Specification (Accuracy/Precision)	Location
Electronic Weighing Balance	± 0.01 g	Department of Manufacturing, Industrial and Textile Engineering, Moi University, Eldoret, Kenya.
Shaking Water Bath	Temperature Stability: ± 0.5 °C	Department of Manufacturing, Industrial and Textile Engineering, Moi University, Eldoret, Kenya.
Digital Vernier Caliper	± 0.02 mm	Department of Manufacturing, Industrial and Textile Engineering, Moi University, Eldoret, Kenya.
pH Meter	± 0.01 pH	Department of Chemistry, Moi University, Eldoret, Kenya.
Universal Tensile Testing Machine	Load Cell Accuracy: ± 0.5% of reading	Rivatex East Africa Textile Limited, Eldoret, Kenya.
Izod Impact Testing Machine	Energy Reading Accuracy: ± 1%	Rivatex East Africa Textile Limited, Eldoret, Kenya.
Scanning Electron Microscope	Resolution: ~3 nm	Obafemi Awolowo University, IleIfe, Nigeria.
Lee's Disk Apparatus	Dependent on caliper and thermometer accuracy (typically ± 0.02 mm and ± 0.1 °C)	Federal University of Technology Akure, Ondo state, Nigeria.
Compression Molding Machine	Temperature Control: ± 2 °C; Pressure Control: ± 1%	Rivatex East Africa Textile Limited, Eldoret, Kenya.

Figure 3.2 presents a series of macroscopic images of the equipment used for testing the mechanical and physical properties of the developed composites: (a) Izod impact machine, (b) Digital Shore Hardness tester, (c) 5 KN Universal Testing Machine, (d) Taber Abrasion tester machine, (e) Thermal Conductivity measuring machine, and (f) Scanning Electron Microscope.

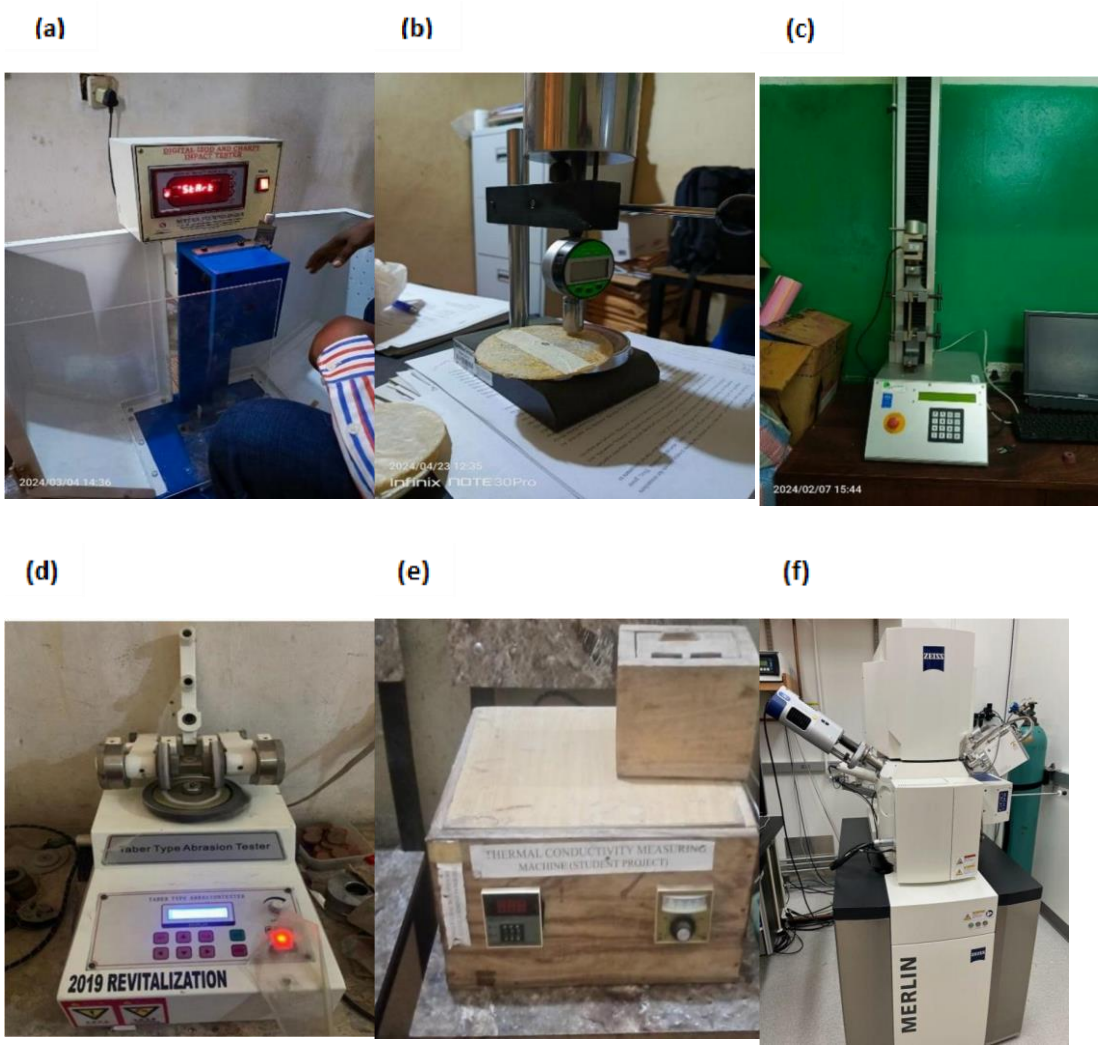

Figure 3.2: Macroscopic Image of (a) Izod impact machine, (b) Digital Shore Hardness tester (model: LX-D-Y), (c) 5 KN Universal Testing Machine, (d) Taber Abrasion tester machine, (e) Thermal Conductivity measuring machine. (f) Scanning Electron Microscope

3.3 Extraction and Alkali Treatment of Fibers

3.3.1 Extraction of pig hair fiber

The sourced pig hair was thoroughly washed with distilled water and detergent to remove dirt and bloodstains. The fibers were then sun-dried for 5 days in order to ensure moisture removal (Mohan et al., 2018; Oladele et al., 2014).

3.3.2 Alkaline treatment of the fiber

To enhance the interfacial adhesion between the hydrophilic pig hair fibers and the hydrophobic polypropylene matrix, a controlled alkaline treatment was performed. The raw pig hair fibers were submerged in a 5% weight by volume (w/v) sodium hydroxide (NaOH) solution. This concentration was chosen based on literature indicating its effectiveness in roughening the keratin surface without causing excessive fiber degradation.

The treatment was conducted in a shaking water bath maintained at a constant temperature of 30°C for a duration of 45 minutes to ensure uniform treatment of all fibers. Following the alkaline soak, the fibers were thoroughly washed with distilled water multiple times until the pH of the rinse water became neutral (pH ≈ 7), as verified with a digital pH meter. This step is critical to remove any residual NaOH, which could otherwise degrade the polymer matrix during processing. Finally, the cleaned fibers were dried in a laboratory oven at 80°C for 24 hours to completely remove moisture before being stored in sealed bags. The specific concentration and duration of the treatment were determined based on a review of existing literature (e.g., Oladele et al., 2015; Hai et al., 2009) to optimize fiber-matrix adhesion and minimize moisture absorption.

Figure 3.3 provides a visual depiction of the stages involved in the treatment of pig hair fibers: (a) fiber measurement, (b) alkali treatment of the fibers, (c) initial pH of the fibers after treatment, and (d) the treated fibers after being oven dried at 120°C for 1 hour using an Olab tech Oven (model number LDO-150F).

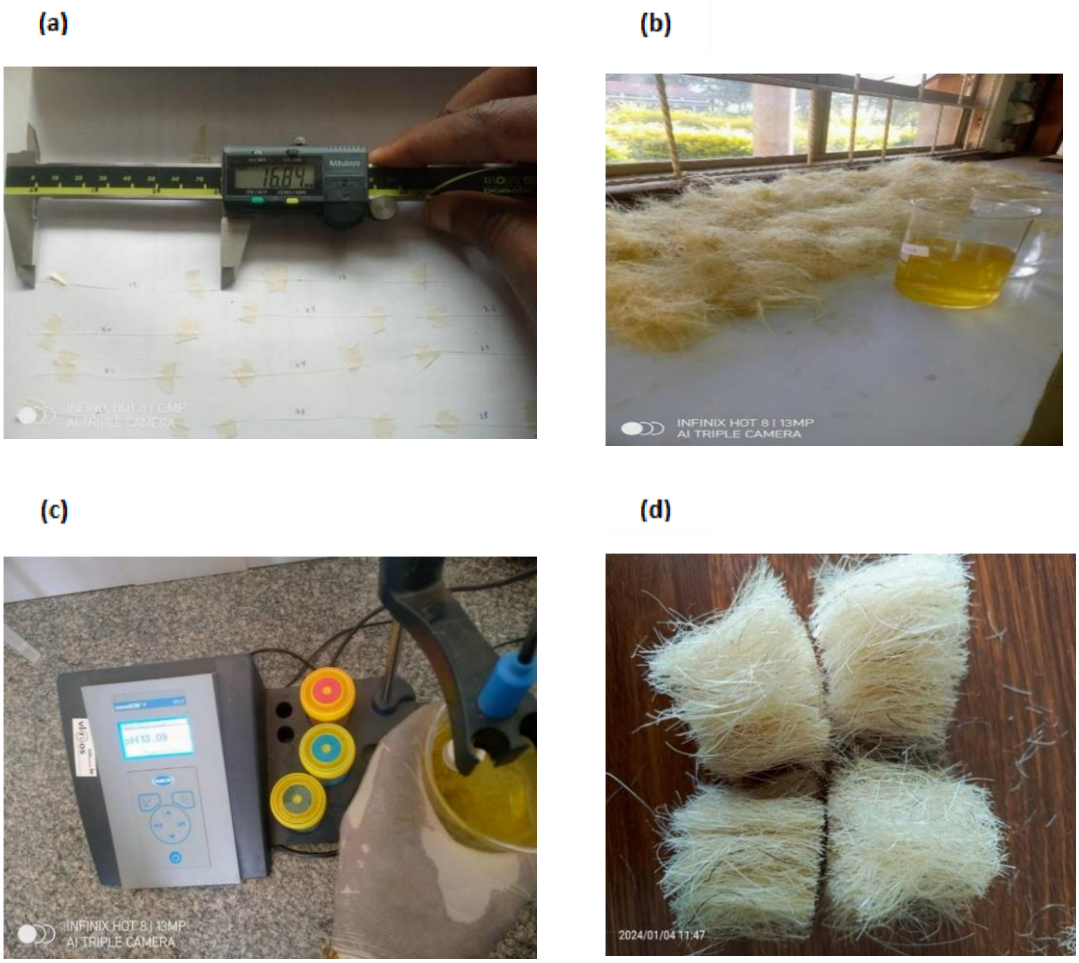

Figure 3.3: Macroscopic Images of (a) Fiber measurement (b) Alkali treatment of fiber (c) Initial pH of fiber after treatment (d) treated fiber after oven dried at 1200C for 1 hour using Olab tech Oven with the model number (LDO-150F).

3.4 Physio-chemical Properties of Pig Hair Fiber

3.4.1 Density measurements of pig hair fiber

The density of treated and untreated pig hair Fibers was determined using Archimedes' principle, also known as the buoyancy method (Wirawan et al., 2010; Oladele et al., 2020). The pig hair fiber was measured using a digital metric weight balance (m_s), measuring the weight of an empty container filled with distilled water and taking the record (V_0), then placing the pig hair Fiber sample into the water in the container making sure it submerges and take the record (V_1). The values obtained were used to calculate the volume of water displaced by the pig hair fiber (V_{fl}) and the result was used to calculate the mass of water displaced by the fiber (m_{fl}). The density of PHF (ρ_s) was calculated using the Equation in (3.1)

$$\rho_s = \rho_{fl} \times \frac{m_s}{m_{fl}} \; or \; \rho_{fl} = \frac{m_{fl}}{V_s} \text{g/cm}^3. \tag{3.1}$$

Where;

ρ_{fl} is the density of water, m_s is the mass of the fiber sample, and m_{fl} is the mass of the displaced water, is the volume of fiber displaced. The obtained density values were then compared with findings from previous research (Mohan et al., 2018). For this research, 20g of treated and untreated pig hair fiber was submerged in water with a density of 1g/cm3 with a displaced volume of treated and Untreated PHF 240 cm^3 and 250 cm^3, respectively.

3.4.2 Average hair length and diameter

The average length and mid diameter of the pig hair fibers were determined by randomly selecting 50 strands from Duroc, Hampshire, and Large white pigs and were measured using a digital vernier caliper; the average was then computed. This was done

to know which of these commonly available breeds in Kenya was well suited for this research work. The obtained values were then compared with observations made by Araya-Letelier et al. (2017).

It is important to acknowledge the potential limitations associated with using a Vernier caliper for measuring the dimensions of pig hair fibers. While a Vernier caliper is a readily available tool, its application to soft, flexible, and microscopic fibers presents several demerits that can impact the accuracy and repeatability of the measurements (Saville, 2004). The most significant demerit for diameter measurement is the compression of the fiber by the caliper's jaws. Pig hair is a soft, pliable material, and the pressure required to close the jaws, even when carefully applied, inevitably deforms and flattens it. This leads to a measured diameter that is systematically smaller than the true diameter, introducing a significant source of error into subsequent calculations that rely on this value, such as cross-sectional area and tensile stress (ASTM D3822/D3822M-14, 2020).

Furthermore, the typical diameter of pig hair falls within a range where the resolution of a standard digital Vernier caliper (typically 0.01 mm or 10 μm) is insufficient for precise characterization. Attempting to measure a dimension that is only a few multiples of the tool's resolution limit is inherently imprecise (Taylor & Kuyatt, 1994). This issue is compounded by the fact that pig hair does not have a perfect cylindrical shape; a caliper measures only a single axis and cannot account for the fiber's potentially elliptical or irregular cross-section.

Similar challenges exist for length measurement. Pig hair fibers are flexible and often curved, making it difficult to hold them perfectly straight for measurement without introducing error. If the fiber is not perfectly taut, its length will be underestimated.

Conversely, if too much tension is applied to straighten it, the fiber will stretch, leading to an overestimation of its true length. This process introduces significant operator-dependent variability into the results.

3.4.3 Fiber fineness

Fiber fineness, a measure of the fiber's linear density, was calculated using the average diameter and density of the pig hair fibers. The obtained values were computed using Equation 3.2 according to (Steinmann & Saelhoff, 2016) and then compared with the findings of ArayaLetelier et al. (2017).

$$D = \sqrt{\frac{4}{\pi.\rho}\, x\, T} \tag{3.2}$$

Where D is the Diameter of the Duroc pig hair fiber, ρ is the density of the PHF, and T is titer or fiber fineness. For this research, the fiber fineness of the three most common pig breeds in Kenya was carried out, where D = 0.012cm, 0.01cm, and 0.07cm for Duroc, Hampshire, and Large white, respectively, and ρ = 0.083g/cm3, which is the density for treated PHF.

3.5 Experimental Design and Statistical Analysis

3.5.1 Central Composite Design/Surface Response Methodology

A five-level, three-factor inscribed, and rotatable central composite design (CCD) was employed to investigate the relationship between the response functions (tensile strength, flexural strength, impact resistance, and wear resistance) and the process variables (fiber length, fiber weight fraction, and molding temperature) using Design Expert13 software (StatEase Inc, USA). A total of 20 runs, each with three replicates, were conducted for each mix design. The mixing proportions and the effect of these independent variables, weight fraction, Fiber length, and temperature, have been

identified and studied by various researchers such as Oladele et al. (2020) and Lejano (2017). Two levels of full factorial with three factors were considered: pig hair fiber (PHF) length, fiber weight fraction, and temperature. For PHF length, 7mm and 15mm were selected, and 2% and 6% were chosen for fiber weight fraction. These combinations were investigated across different temperatures between 170°C and 180°C. Each independent variable was tested at low, high, and center-point levels, represented as -1, +1, and 0^a, respectively.

Table 3.2 shows the design variables' limits, while Table 3.3 shows the independent variables and their corresponding values.

Table 3.2: Design variables with their levels

Factor	Lower Limit	Upper Limit
Fiber Length	7 mm	15 mm
Fiber Weight Fraction	2 %	6 %
Molding Temperature	170 ℃	180 ℃

Table 3.3: Independent variables and their corresponding levels

Independent Variables	Symbol	Coded Levels				
		$-\alpha$	-1	0^a	1	$+\alpha$
Fiber Length (mm)	X_1	4.27	7.0	11.0	15.0	17.73
Fiber weight Fraction (%)	X_2	0.64	2.0	4.0	6.0	7.36
Molding Temperature (°C)	X_3	166.59	170.0	175.0	180.0	183.41

After conducting the experiment according to the experimental design matrix using Design Expert13, the matrix is provided in Table 3.4 alongside the corresponding responses.

Table 3.4: Experimental Design Matrix

		Coded variables			Actual variables		
Run	Space Type	X1: PHF length	X2: PHF Weight Fraction	X3: Temperature	X1	X2	X3
					mm	%	°C
1	Factorial	-1	-1	1	7.0	2.0	180
2	Center	0	0	0	11.0	4.0	175
3	Factorial	1	1	1	15.0	6.0	180
4	Factorial	-1	1	-1	7.0	6.0	170
5	Axial	0	-1.682	0	11.0	0.6	175
6	Center	0	0	0	11.0	4.0	175
7	Axial	1.682	0	0	17.7	4.0	175
8	Factorial	-1	1	1	7.0	6.0	180
9	Center	0	0	0	11.0	4.0	175
10	Axial	0	0	-1.682	11.0	4.0	167
11	Axial	-1.682	0	0	4.3	4.0	175
12	Factorial	1	1	-1	15.0	6.0	170
13	Center	0	0	0	11.0	4.0	175
14	Factorial	-1	-1	-1	7.0	2.0	170
15	Center	0	0	0	11.0	4.0	175
16	Factorial	1	-1	1	15.0	2.0	180
17	Axial	0	0	1.682	11.0	4.0	183
18	Center	0	0	0	11.0	4.0	175
19	Axial	0	1.682	0	11.0	7.4	175
20	Factorial	1	-1	-1	15.0	2.0	170

3.5.2 Justification for Experimental Variable Ranges

The ranges for the independent variables in the Central Composite Design were selected based on a combination of established principles in composite science and practical processing considerations to ensure both meaningful results and manufacturability.

1. **Fiber Length (7 mm to 15 mm):** The selection of this range is based on the concept of critical Fiber length (Lc), the minimum length required for a fiber to achieve its maximum reinforcing potential through effective stress transfer from the matrix (Arbelaiz et al., 2005). While the exact Lc for pig hair in polypropylene is unknown, this range was chosen to explore lengths likely to be above this critical threshold. The lower bound of 7 mm ensures the fibers are long enough to act as effective reinforcement, while the upper bound of 15 mm

was chosen to mitigate processing challenges. In short-fiber thermoplastic composites, fibers longer than this can be difficult to disperse uniformly in the viscous polymer melt, leading to clumping (agglomeration) and entanglement, which creates weak spots and degrades mechanical performance (Fu & Lauke, 1996).

2. **Fiber Weight Fraction (2% to 6%):** This range was selected to identify the optimal loading level for reinforcement. A loading below 2 wt% is often insufficient to impart a significant reinforcing effect to the composite. Conversely, as the weight fraction of natural fibers increases, issues such as poor wetting of fibers by the hydrophobic polymer matrix, increased porosity, and dominant fiber-to-fiber interactions can arise. These factors hinder proper stress transfer and often lead to a decrease in mechanical properties at higher loadings (Verma & Gope, 2021). The 2-6 wt% range is therefore a strategic choice to investigate the positive effects of reinforcement while staying below the threshold where negative processing-related effects typically begin to dominate.

3.5.3 Numerical optimization procedure

Numerical optimization was performed on the response variables (tensile strength, flexural strength, impact resistance, and wear resistance) using Design Expert 13 software. This procedure provided the optimal levels of fiber length, fiber weight fraction, and molding temperature to achieve the best mechanical properties of the composites. For numerical optimization, the goal for each predictor variable was minimized within the studied range, while the response variables were maximized within the reported experimental ranges.

Three-dimensional (3D) response surface plots and contour plots were generated to visualize the correlation between each response variable and the experimental levels of the process variables. This was achieved by maintaining one predictor variable at the center point and varying the other two independent variables within the studied range. The interaction effects of two predictor variables on each response variable were determined and presented using 3D response surface plots. The accuracy and predictability of the developed regression models were validated by conducting confirmatory experiments using the optimized process parameters. The experimental results were compared with the predicted values to assess the model's adequacy.

3.5.4 Statistical analysis

The experimental data were analyzed using Analysis of Variance (ANOVA) to determine each factor's significance and interactions with the response variables. Regression analysis was performed to develop mathematical models that describe the relationship between the process variables and the response variables.

3.6 Fabrication of the Composite Panels

The composite panels were fabricated using a compression molding technique, adhering to the principles outlined in ASTM D 4703 – 03. Prior to mixing, the polypropylene granules were dried according to the manufacturer's instructions to prevent moisture-induced defects. The required amounts of dried polypropylene and pre-treated pig hair fibers were weighed using an electronic balance (± 0.01 g) and then thoroughly mixed for 5 minutes to ensure a homogenous blend. A small amount of dioctyl phthalate was added to the mixture as a plasticizer to enhance the flow and thermoplasticity of the polypropylene melt during molding.

A hydraulic press with heated platens was used for the molding process. To prevent the composite from sticking, the internal surfaces of the 150 mm x 150 mm x 3 mm steel mold were treated with a silicon oil release agent. The prepared PP-PHF mixture was then distributed evenly within the mold, which was placed in the press preheated to the specific temperature dictated by the experimental design (170°C, 180°C, or 190°C).

The material was allowed to preheat in the mold for 5 minutes to ensure the polypropylene had completely melted. A compression pressure of 5 MPa was then applied and held for a duration of 10 minutes to ensure proper compaction and consolidation of the composite. Following this stage, the mold was removed from the press and allowed to cool to room temperature under the load of a 34 kg concrete block. This controlled cooling under pressure is essential to ensure consistent crystallization, minimize warpage, and produce a panel of uniform thickness. Finally, the finished composite panel was carefully demolded.

The materials used in this study included pig hair fibers and polypropylene. The chopped fiber lengths, as shown in Figure 3.4 (a), were used in the composite fabrication. Pig hair fibers and polypropylene were laid up, as depicted in Fig. 3.4(b) and Fig. 3.4(c), and then processed using a compression molding machine (Fig. 3.4 (d)). The developed composites, prepared for tensile, flexural, impact, and wear testing, are shown in Fig. 3.4 (e) and Fig. 3.4 (f).

Figure 3.4: Macroscopic Image of (a) chopped fiber lengths, (b) & (c) mold lay-up with PHF and Polypropylene, (d) Compression molding machine for composites development, (e) & (f) developed composites (tensile, flexural, impact and wear)

3.7 Surface Morphology of Fibers and Composites

This section examines the surface characteristics and elemental composition of pig hair fibers and their polypropylene composites using advanced microscopy and spectroscopy techniques. Scanning Electron Microscopy (SEM) was employed to investigate the surface morphology of both treated and untreated pig hair fibers and the fracture surfaces of the composites. Complementing this, Energy Dispersive X-ray Spectroscopy (EDS) analysis provided insights into the elemental composition of the fibers and composites. These analyses were crucial for understanding the effects of chemical treatments on the fibers and the nature of fiber-matrix interactions in the composites.

3.7.1 Scanning Electron Microscopy (SEM) of pig hair fiber

The surface morphology of untreated and treated pig hair fibers (PHF) was investigated using a Scanning Electron Microscope (SEM) (Q150RES, Carl Zeiss Smart Evo 10, Germany) operating at 15 kV accelerating voltage. The sample surfaces were prepared by gold coating to impart surface conductivity before SEM observation. This was done using a Quorum sputter and SEM carbon coating machine, ensuring high-quality imaging and accurate analysis. Moreover, the fractured surface morphology of the developed pig hair fiber polypropylene composite samples was examined using SEM. This analysis provided insights into the fiber/matrix interfacial bonding, which is a critical factor in determining the mechanical performance of the composites. The study focused on treated and untreated pig hair fibers to compare the effectiveness of the chemical treatments. The SEM analysis followed standard methods Bozzola & Russell (2009) described. All SEM analyses were conducted at the Central Science Laboratory, Obafemi Awolowo University, Ile-Ife, Nigeria, ensuring consistent and reliable results.

3.7.2 Energy Dispersive X-ray Spectroscopy (EDS) of fibers and developed composites

Energy Dispersive X-ray Spectroscopy (EDS) analysis was conducted in conjunction with Scanning Electron Microscopy (SEM) to investigate the elemental composition of pig hair fibers (treated and untreated) and the developed pig hair fiber-reinforced polypropylene composites. The analysis utilized the same Carl Zeiss Smart Evo 10 SEM system (Germany) equipped with an EDS detector. Sample preparation followed the protocol established for SEM analysis, with surfaces gold-coated using a Quorum sputter and SEM carbon coating machine to ensure electrical conductivity and prevent charging effects during analysis.

The EDS analysis was performed under carefully controlled conditions. An accelerating voltage of 15 kV was employed, consistent with SEM imaging parameters. The working distance was optimized to facilitate SEM imaging and efficient X-ray collection. Each spectrum was acquired over 60 seconds to ensure adequate X-ray counts for reliable quantification. The dead time was maintained between 20-40% to optimize count rates and spectral quality. Multiple areas (a minimum of five) on each sample were analyzed to account for potential sample heterogeneity. Both spot analyses and area mapping were conducted to understand the elemental distribution within the fibers and composites comprehensively.

Data processing and quantification were carried out using the manufacturer's software package. The process involved automatic peak identification and manual verification to ensure accurate element assignment. Quantification employed the standardless ZAF (atomic number, absorption, and fluorescence) correction method. All EDS analyses were conducted at the Central Science Laboratory, Obafemi Awolowo University, Ile-Ife, Nigeria, ensuring consistency with the SEM analyses and maintaining the reliability of the results. This methodology adheres to standard procedures for EDS analysis in materials science, as outlined in literature such as Goldstein et al. (2018) and Williams & Carter (2009).

3.8 Properties of Developed Composite

This section examines the key properties of the pig hair fiber (PHF) reinforced polypropylene composites developed in this study. A comprehensive characterization of these properties is essential for evaluating the composites' potential for automotive applications. The following subsections detail the mechanical, thermal, and other

relevant properties, providing insights into how the incorporation of pig hair fibers affects the overall performance of the composite materials.

3.8.1 Mechanical properties

The mechanical properties of the PHF-reinforced polypropylene composites are crucial indicators of their performance and suitability for automotive applications. This subsection presents the results of various mechanical tests conducted on the composites, including tensile strength, flexural strength, impact resistance, and wear behavior.

3.8.1.1 Tensile properties

Tensile tests were conducted according to ASTM D3039/D3039M standards to determine the tensile strength of the composite materials. The tensile properties of the developed pig-hair fiber-reinforced polypropylene composite were determined using the 5kN Universal material testing machine (Instron series) with 10 kg load cell capacity operated at 5 mm/mm crosshead speed. Dumbbell-shaped tensile samples measuring 120 mm overall length,3 mm thickness, width of the grip section of 35 mm, width of the reduced section of 11.5 mm and a gauge length of 50 mm were tested per ASTM D638-14 standard following type I tensile bar (ASTM D638-14, 2014). Figure 3.5 shows the schematic diagram of the tensile test sample dimension of the developed pig-hair Fiber-reinforced polypropylene composite.

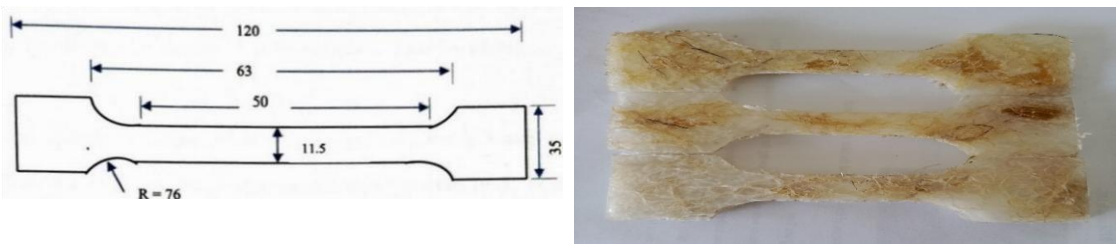

Figure 3.5: Schematic diagram and macroscopic diagram of the tensile test sample (ASTM D638-14)

The tensile strength was calculated using Equation (3.3).

$$Tensile\ Strength\ (MPa) = \frac{Pmax}{b\ x\ t} \tag{3.3}$$

where;

P_{max} is the maximum force before the sample breaks (N);

t is the sample thickness (mm),

b is the sample width (mm),

3.8.1.2 Flexural properties

Following ASTM D7264M-07 standards, flexural tests were performed using a three-point bending setup on an Instron Universal Testing Machine. This test provided information on the composites' flexural strength. Figure 3.6 shows the schematic diagram of the flexural test sample dimension of the developed pig-hair Fiber-reinforced polypropylene composite.

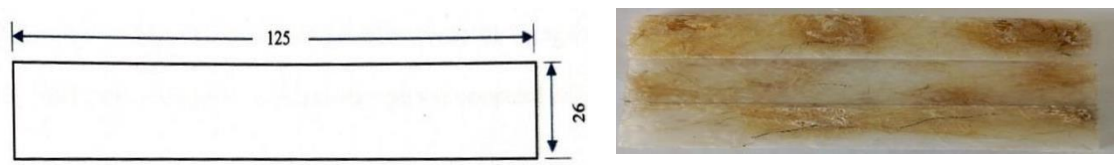

Figure 3.6: Schematic Diagram and Visual image for Flexural test sample (ASTM D79017)

The flexural strength was calculated using Equation (3.4).

$$Flexural\ Strength\ (MPa) = \frac{3.P.L}{2.b.t^2} \tag{3.4}$$

where; t is the thickness of the sample (mm), b is the width of the sample (mm), L is the span length (mm), and P is the maximum load (N).

3.8.1.3 Impact strength

Impact strength was evaluated using the Izod impact test method (ASTM D256-10) to determine the energy absorbed by the composite material before fracture. The dimension (64 x 11 x 3.2 mm) was used to determine the toughness of the composite materials using the Izod impact tester, which is a standardized test method to test for the impact resistance of plastics (West Conshohocken, 2018; Oladele et al.,2015). The test piece was prepared in the form of V-notch according to requirements. The specimen was clamped upright in the Izod impact tester, ensuring that it was securely held in place. The pendulum was raised to the required height and released to fall freely to hit the test piece, and the energy required to cause fracture was recorded.

Figure 3.7 shows the schematic diagram and visual image for the impact strength sample for the developed pig-hair fiber-reinforced polypropylene composites. The Izod-Charpy impact tester used for this research has a model number GEC-P40419 with a capacity of up to 150J.

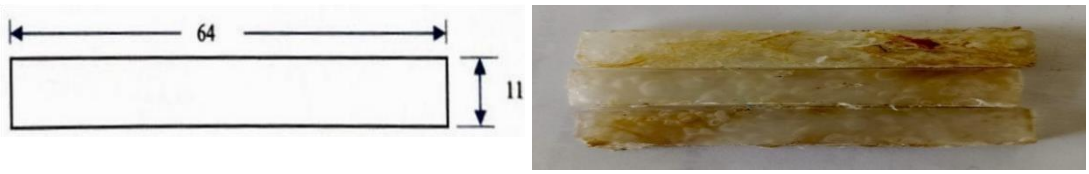

Figure 3.7: Schematic diagram and visual image of the impact test sample (ASTM D25610)

Using the absorbed impact energy reading for each sample, the impact strength was computed using Equation (3.5).

$$Impact\ Strength\ (kJ/m^2) = \frac{E_a}{b\ x\ t} \tag{3.5}$$

where $E_{a.}$ is the absorbed impact energy (J),

t is the sample thickness(mm), and b is the sample width (mm)

3.8.1.4 Hardness property

The hardness of the composites was measured using a suitable hardness tester and following relevant ASTM standards. A hardness property test was conducted on the samples using a Shore D hardness tester following the ASTM D2240-15 standard (ASTM D2240-15, 2015). Control and developed composite samples were placed on the flat surface of the tester and indented. Five values were obtained by indenting the samples in four different places, and the average value was reported.

3.8.2 Thermal behavior

The developed composites were subjected to a thermal test using Lee's disk apparatus to determine their thermal conductivity per ASTM E1530-19. The process involved placing a composite sample between a metallic/lee's disc and a steam chamber each having a hole where a thermometer is been inserted to know the amount of temperature generated and lost, activating a temperature controller, and detecting temperature changes in the metal disks and the readings taking at a regular time interval (Oladele et al.,2020 & Mohapatra et al.,2014).

The thermal conductivity was calculated using the following equation 3.6:

$$k = \frac{mcp(\theta_1-\theta_2)4x}{\pi D^2(T_1-T_2)t} \ \left({}^{W}/_{mk}\right) \tag{3.6}$$

Where;

m - mass of the Lee's disk

cp - specific heat capacity of the Lee's disk

$\theta_1 - \theta_2$ - initial and final temperature of disk Lee's disk

D - diameter of the composite sample

x - thickness of the composite sample

$T_1 - T_2$- the temperature of the steam chamber and Lee's disc in Kelvin

t - final time taken to reach a steady temperature

3.8.3 Wear behavior

The wear resistance test was carried out with Taber Abrasers. This involves mounting a flat and round specimen of approximately 100 mm^2 and a standard thickness of approximately 6.35 mm to a turntable platform that rotates at a fixed speed. Two genuine Taber abrasive wheels, which are applied at a specific pressure, are lowered onto the specimen surface. Characteristic rub-wear action will be produced by contact of the test specimen against the sliding rotation of the two abrading wheels. Three samples were tested for each run from where the average value was taken as the representative value. The sample was weighed using an analytical weighing balance for the initial weight of the sample after which it was fixed on the turntable. The turntable platform was made to rotate at 750 rpm for 5 hours then the samples were removed and weighed to obtain the final weight of the sample. The values of the initials and the final weight of the sample were used to determine the difference in weight of the sample using the weight loss technique to calculate the wear resistance. This procedure was carried out for all the sample variations to determine the effect of abrasion on the material (Oladele *et al.,* 2014). The result was analyzed using the Equation in 3.7. Figure 3.8 presents a schematic diagram for the wear test sample following ASTM D1044-13 standards.

$$\text{Wear index (g)} = \frac{W_i - W_f}{RPM} \text{ x } 1000 \tag{3.7}$$

Where W_i is the i$nitial\ weight$, W_f is the f$inal\ weight$ after the surface abrasion and the RPM is revolution per minutes. The RPM used is 750.

Figure 3.8: Schematic diagram and visual image for the wear test sample (ASTM D104413)

Figure 3.9 provides macroscopic images of fractured composite samples after mechanical testing: (a) impact samples, (b) tensile samples, and (c) flexural samples.

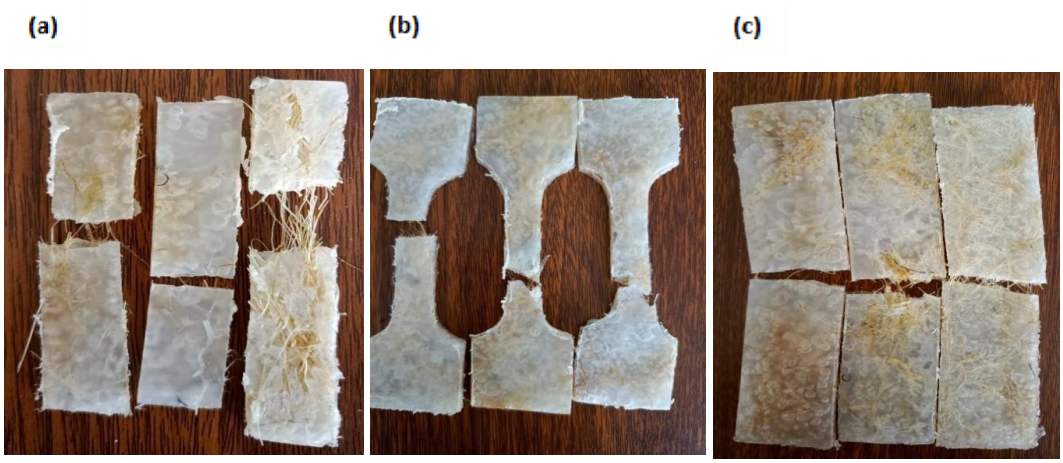

Figure 3.9: Macroscopic Image of Fractured: (a) Impact samples (b) Tensile samples (c) Flexural samples

CHAPTER FOUR

RESULTS AND DISCUSSION

4.1 Properties of Fibers

4.1.1 Physical properties of pig hair Fibers

The physical properties of pig hair investigated in this work include length, diameter, density, and fineness as provided in Table 4.1. The actual physical Fiber length, Fiber diameter, and Fiber fineness for Hampshire, Duroc and Large white are presented in Table 4.1 and Figure 4.1. Hampshire Fiber length is between 60-75 mm, Duroc Fiber length 45-60 mm, and Large white Fiber length is between 24-35 mm. The Fiber diameter is between 0.08-0.12 mm, 0.100.14 mm, and 0.05-0.09 mm for Hampshire, Duroc and Large white breeds, respectively. The Fiber fineness for Hampshire, Duroc and Large white are 6.55 x 10^{-6} g/cm 9.38 x 10^{-6} g/cm and 3.21 x 10^{-6} g/cm. Likewise, the aspect ratio for the various breeds (Hampshire, Duroc and large white) using the average length and average diameters are 628.7, 417.08 and 400.29.

Table 4.1: Characteristics of the hair Fibers obtained from different breeds of pigs

Breeds	Fiber in length anges (mm)	Average Fiber length (mm)	Mid-Fiber diameter in ranges (mm)	Average mid-Fiber diameter (mm)	Fiber fineness (g/cm)	Aspect ratio L/D
Hampshire	40-81	62.87	0.08-0.12	0.10	6.55 x 10^{-6}	628.7
Duroc	30-65	50.05	0.10-0.14	0.12	9.38 x 10^{-6}	417.08
Large white	20-35	28.02	0.05-0.09	0.07	3.21 x 10^{-6}	400.29

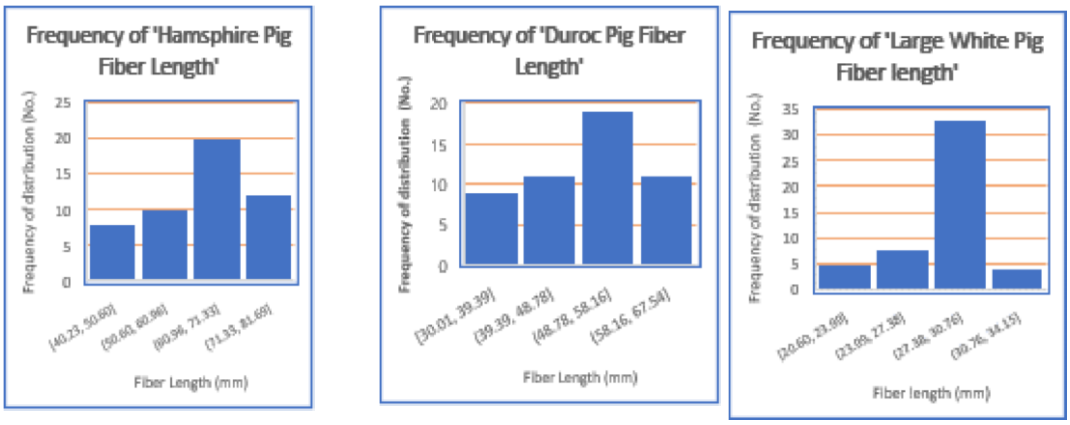

Figure 4.1a: Distribution frequency for the various Pig hair Fiber length breeds.

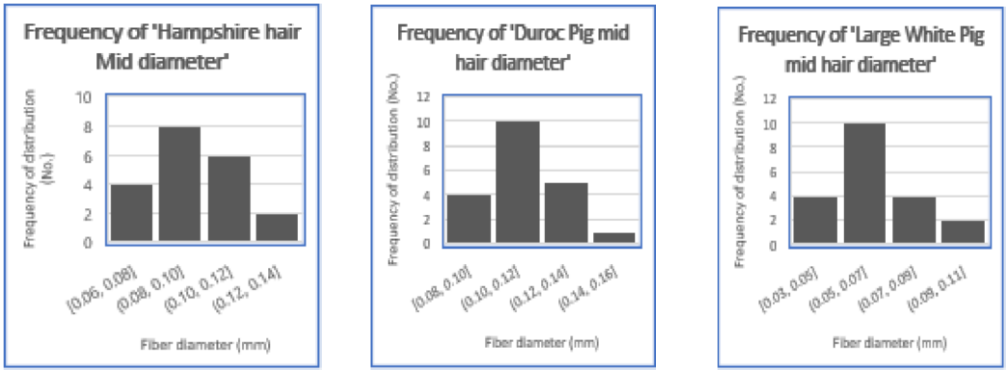

Figure 4.1b: Frequency of distribution for the various breeds of Pig hair Fiber diameter

4.1.2 Fiber density

Figure 4.2 compares the measured density values of Pig hair for both untreated and alkali-treated.

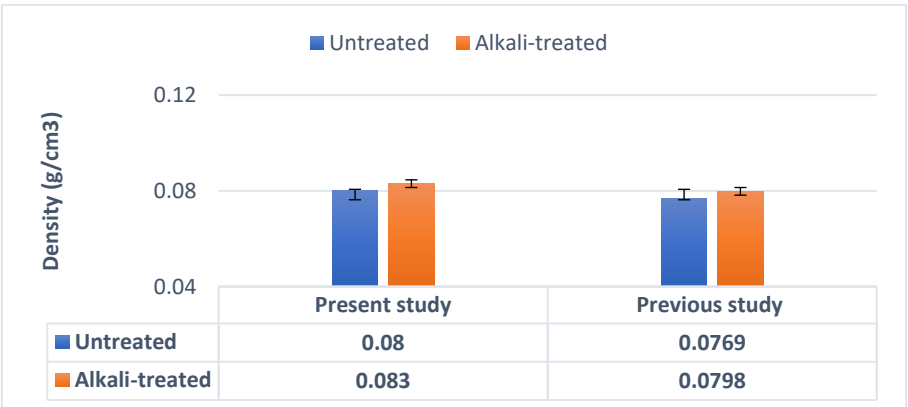

	Present study	Previous study
Untreated	0.08	0.0769
Alkali-treated	0.083	0.0798

Figure 4.2: Comparison of Alkali-Treated and untreated PHF densities for Present and Previous Studies (Mohan et al., 2014).

From the Figure 4.2, PHF has a Fiber density of 0.08 and 0.083 g/cm^3 for untreated and alkali-treated fiber. This indicates that the reported density of pig hair Fiber is within the density range reported in the literature for pig hair Fiber (Mohan et al., 2014). Moreover, the density of PHF is less than those of the synthetic Fibers that have been previously used in the automobile industry, such as carbon (1.60 g/cm^3) as well as E-glass (2.56 g/cm^3) (Indran & Raj, 2015). Likewise, PHF density is lower than most plant Fibers such as sisal (1.20-1.48 g/cm^3), Kenaf (1.4 g/cm^3), Flax (1.4 – 1.5 g/cm^3), and hemp (1.4 – 1.5 g/cm^3), as reported in the literature by (Singh & Hiremath, 2020) because animal Fibers, such as wool, cashmere, and silk, and pig hair are composed primarily of proteins like keratin and fibroin. These proteins have a more lightweight and less dense molecular structure than the cellulosic compounds found in plant Fibers (Khatib et al., 2022).

Moreover, Figure 4.2 shows that alkali treatment influences the density of PHF. There is a marginal increase in Fiber density with alkali treatment, which was enhanced by 3.75%. This increase can be traced to the partial removal of the cuticle layer, which reduces animal Fibers' natural lustre and sheen (Oladele et al., 2020).

Furthermore, alkali treatment removes surface impurities and increases surface roughness, enhancing the adhesion between the Fiber and the polymer matrix. Research has shown that alkali-treated pig hair Fibers exhibit improved mechanical properties and better compatibility with polymer matrices (Mohan et al., 2014). Furthermore, Alkali treatment also helps remove fatty substances and other impurities that can hinder Fiber performance in chicken feather Fiber (Sharma et al., 2020).

4.1.3 Surface morphology

Examination of the morphology of pig hair Fiber provides insight into the distribution of different components available over the entire Fiber surface. The surface morphology of the pig hair was examined before and after chemical treatments using SEM analysis conducted longitudinally at different magnifications.

4.1.3.1 Surface morphology of untreated pig hair Fiber

The SEM images of untreated Fiber at 8000, 90000 and 10000X magnifications are shown in Figure 4.3.

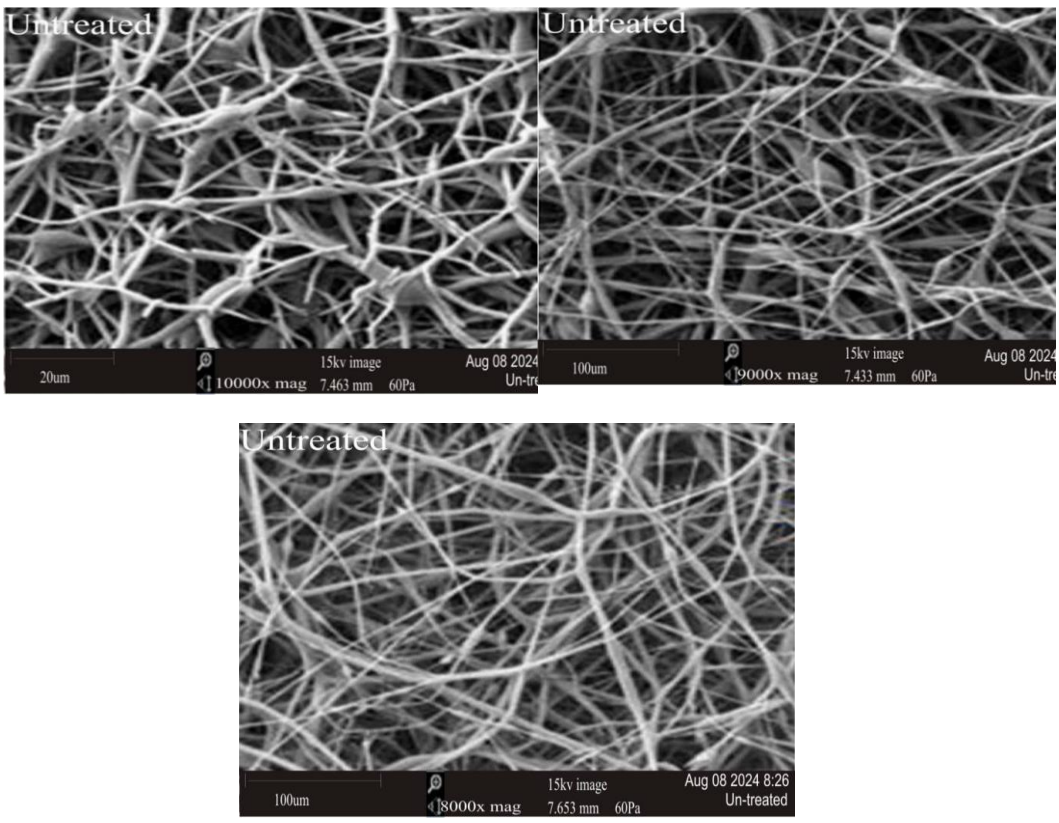

Figure 4.3: SEM Images of Untreated Pig Hair Fiber at 10000X, 9000X and 8000X Magnification

Figure 4.3 presents SEM images of pig hair fibers at varying magnifications of 10000x, 9000x, and 8000x. While pig hairs naturally exist as individual fibers, these

micrographs show them in an entangled state resulting from the sample preparation process. The fibers display smooth, irregular surfaces with minimal visible impurities. Individual fibers have consistent diameters throughout their length, though they appear overlapped and interwoven during the mounting and preparation for SEM imaging, creating the observed mesh-like arrangement. At the highest magnification of 10000x, the intricate details of the fiber surfaces become apparent. While predominantly smooth, subtle irregularities are visible, likely attributable to the natural cuticle structure of the hair. These surface features are crucial in determining the fiber's interaction with potential matrix materials in composite applications. The 9000x and 8000x magnification images provide a broader perspective of the fiber network, confirming the consistency of the observed morphological characteristics across different scales. The fibers' random orientation and varying diameters are consistently evident, suggesting the potential for isotropic properties in resulting composites.

Notably absent from these images are significant amounts of non-fibrous components or impurities, which are often observed in other natural fibers as white-colored substances. In pig hair, these components might include residual lipids, proteins, or other organic materials naturally present on the hair surface. The apparent cleanliness of the fiber surfaces suggests that pig hair may require less intensive surface treatments compared to some plant-based fibers to achieve good interfacial bonding with polymer matrices. However, the smooth nature of the fiber surfaces, while indicative of the fibers' natural state, may present challenges for achieving strong interfacial adhesion with non-polar polymer matrices. This characteristic underscores the potential need for surface modification treatments to enhance the compatibility between the fibers and the matrix material, thereby improving the mechanical performance of resultant composites.

4.1.3.2 Surface morphology of alkali-treated pig hair Fiber

The mercerization (alkali treatment) of pig hair Fiber with 0.2M NaOH increases the surface roughness of the Fiber. This disabling hydrogen bonding enhances the mechanical interlocking between the Fiber and the polypropylene polymer (Kar et al., 2023). Figure 4.4 also shows a reduction in surface impurities compared to the untreated Fiber, as alkali treatment removes synthetic and natural impurities from the Fiber network structure. Reducing surface impurities will further enhance the surface roughness, facilitating a Fiber/matrix interfacial adhesion and increasing the mechanical stress the composite absorbs.

Additionally, alkali treatment opened Fiber surface cracks and pores, thus increasing surface accessibility (Srinara et al., 2020). This promotes mechanical interlocking between the nonpolar polymetric matrices and polar Fibers, thus enhancing the mechanical performance of the resultant composites. Adding aqueous sodium hydroxide (NaOH) to natural fiber promotes the ionization of the hydroxyl group to the alkoxide (Salih et al., 2020). Equation (4.1) denotes the chemical reaction between the NaOH solution and the proteinaceous Fiber during treatment (Srinara et al., 2020).

$$\text{Fiber} - \text{OH} + \text{NaOH} \rightarrow \text{Fiber} - \text{O}^{-}\text{Na} + \text{H}_2\text{O} + \text{impurities} \quad (4.1)$$

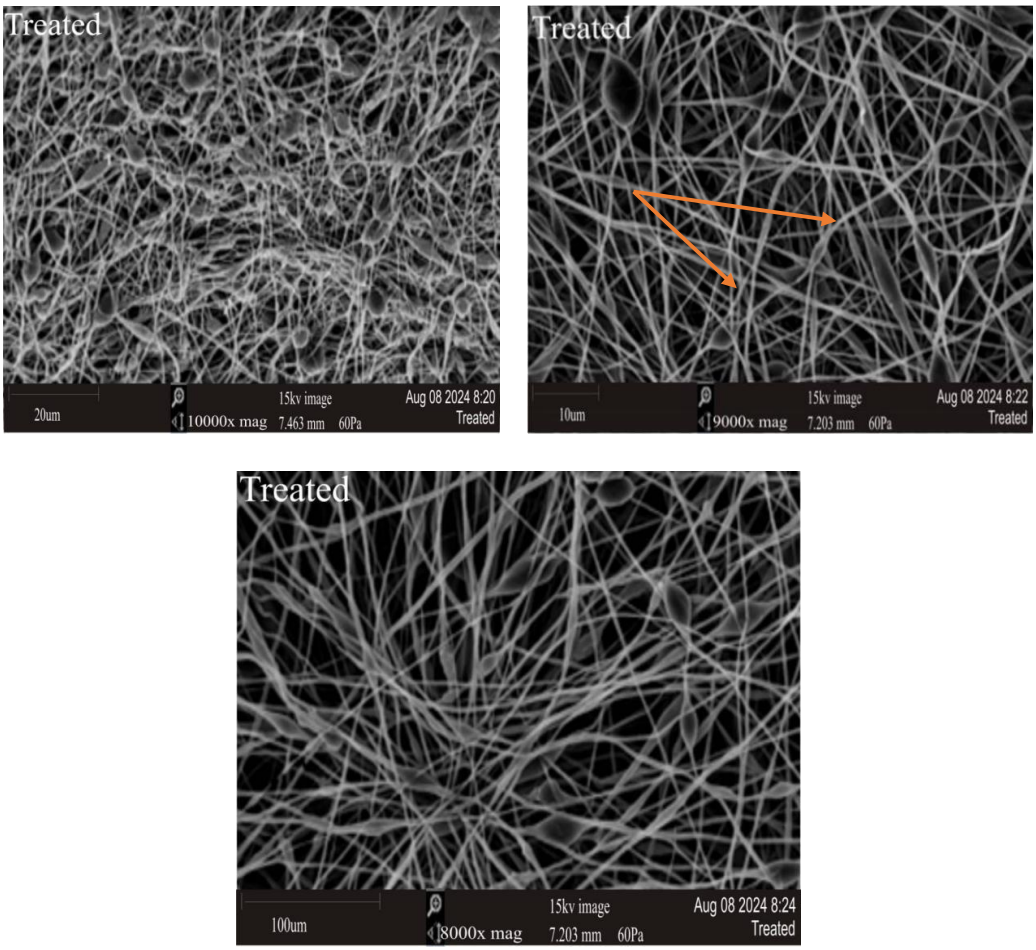

Figure 4.4: SEM Images of Treated Pig Hair Fiber at 10000X, 9000X and 8000X Magnification

Figure 4.4 presents SEM images of treated pig hair fibers at magnifications of 8000x, 9000x, and 10000x. While these fibers exist individually in their natural state, the sample preparation process for SEM imaging has resulted in their overlapped arrangement. The micrographs show that individual fibers have undergone surface modification due to the treatment process, as evidenced by their altered surface morphology. The fibers display varying diameters and, though appearing as an interconnected structure in these images, represent individual treated fibers that have been mounted in this configuration during sample preparation for electron microscopy imaging.

At the highest magnification of 10000x, the intricate details of the fiber surfaces become apparent. The treatment appears to have induced surface roughness and potentially created micro-pores or crevices on the fiber surfaces. These morphological changes are significant as they can greatly influence the fiber's interaction with potential matrix materials in composite applications, potentially enhancing mechanical interlocking and adhesion.

The 9000x and 8000x magnification images provide a broader perspective of the fiber network, confirming the consistency of the observed morphological changes across different scales. The fibers' random orientation and varying diameters are consistently evident, suggesting the potential for isotropic properties in resulting composites. The treatment maintains the overall network structure while modifying individual fiber surfaces. Notably, the treated fibers have a more open and possibly porous structure than untreated hair fibers. This increased surface area and potential for better wettability could significantly improve composite materials' interfacial bonding between the fibers and polymer matrices. The treatment may have removed some of the natural oils and surface impurities typically found on hair fibers, evidenced by the absence of smooth, uniform surfaces characteristic of untreated hair.

4.1.3.3 Energy dispersive X-ray spectroscopy (EDS) of treated and untreated pig hair Fiber

Energy Dispersive X-ray Spectroscopy (EDS) analysis was conducted on untreated pig hair fiber samples. Two sets of samples were analyzed: untreated and treated pig hair fibers.

Figure 4.5 shows the EDS of the untreated pig hair Fiber.

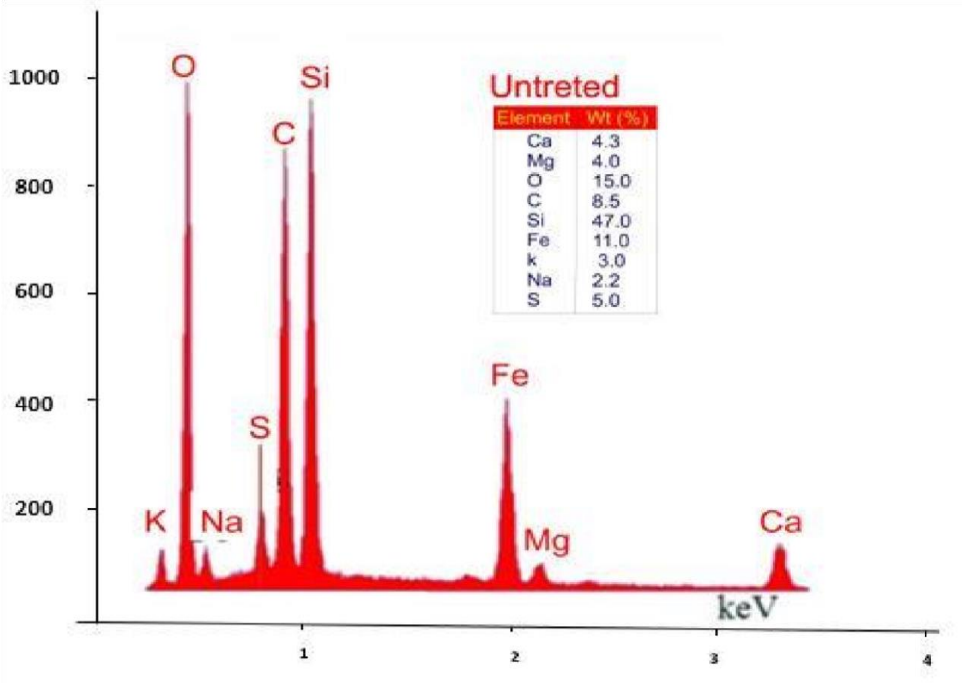

Figure 4.5: EDS Image of Untreated Pig Hair Fiber

Figure 4.5 reveals a complex elemental composition. The most important feature of this analysis is the remarkably high silicon content, reported at 47.0% by weight. This silicon level is unprecedented in typical mammalian hair samples and strongly suggests significant environmental contamination. Farm animals, including pigs, are often in contact with environmental contaminants like dust, soil, and even their own waste, which can lead to incorporating various elements, including silicon, into their hair. Contaminants from the environment are known to affect hair analyses in farm animals (Otten et al., 2020).

The second most abundant element is oxygen at 15.0%, followed by iron at 11.0%. The high iron content is noteworthy and may be attributed to the iron-rich lateritic soils common in tropical regions like Uasin Gishu. This further supports the hypothesis of environmental contamination as the primary source of these elemental anomalies. Moreover, it is plausible that the pigs (where the hairs were extracted) were fed diets with high iron levels. Ji et al. (2019) showed increased iron accumulation in various

tissues, including hair. The study highlighted that excessive dietary iron can lead to iron overloading in different body parts, including the liver and hair (Ji et al., 2019).

Carbon, typically the predominant element in organic materials like hair, shows a surprisingly low concentration of 8.5%. This underrepresentation of carbon could be due to the masking effect of the overabundant silicon and iron, a phenomenon noted by Goldstein et al. (2018) in their comprehensive work on scanning electron microscopy and X-ray microanalysis. The authors caution that in samples with high concentrations of heavier elements, the detection and quantification of lighter elements like carbon can be significantly compromised. The presence of other elements such as calcium (4.3%), magnesium (4.0%), potassium (3.0%), sodium (2.2%), and sulfur (5.0%) are not unusual in biological samples. However, their relative proportions may have been influenced by both the environmental conditions and the limitations of the EDS technique in accurately quantifying minor constituents in the presence of dominant elements. It is crucial to note that EDS analysis, while robust, has limitations in accurately quantifying light elements in complex matrices. As Newbury & Ritchie (2012) pointed out, high atomic number elements can lead to significant matrix effects, potentially skewing the quantification of lighter elements.

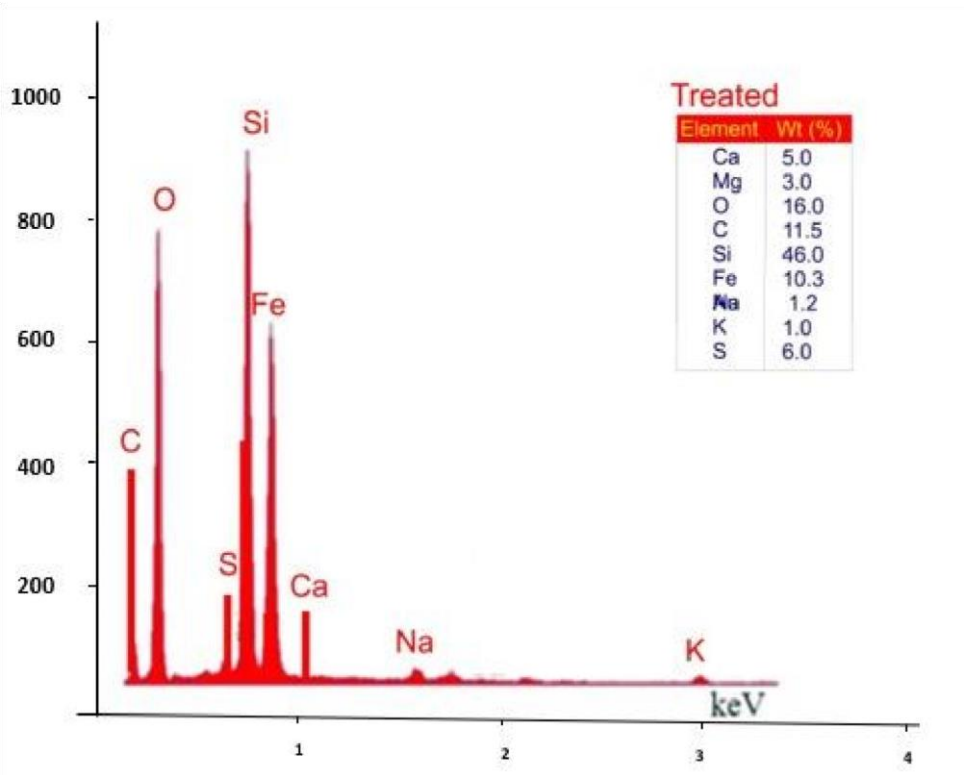

Figure 4.6: EDS Image of Treated Pig Hair Fiber

The Energy Dispersive X-ray Spectroscopy (EDS) analysis of the treated pig hair fiber is shown in Figure 4.6, and it shows some changes from the untreated sample. Most notably, silicon remains the predominant element, constituting 46.0% of the sample by weight, only marginally reduced from the 47.0% observed in the untreated specimen. This persistence of silicon following treatment suggests a deep integration of silicon-based compounds within the hair structure rather than mere surface contamination. Interestingly, the carbon content has increased from 8.5% to 11.5%, potentially indicating that the treatment removed some surface contaminants, allowing for better detection of the hair's organic components. However, this level of carbon is still surprisingly low for a biological material like hair, which is typically carbon-rich. Oxygen content also increased slightly to 16.0%, while iron remained a significant component at 10.3%, only slightly decreased from its original 11.0%.

The treatment has had varied effects on other elements. Sulfur and calcium showed modest increases, rising to 6.0% and 5.0%, respectively. Conversely, magnesium decreased to 3.0%, while potassium and sodium levels dropped substantially to 1.0% and 1.2%. These shifts in elemental composition could be attributed to the specific nature of the treatment process, which may have altered the surface chemistry of the hair fibers or selectively removed certain elements.

4.2 Mechanical Testing and Optimization

4.2.1 Tensile strength analysis

Tensile strength is a critical parameter for bio-composites in automotive applications, ensuring that materials can withstand pulling forces without failure. Understanding the tensile behaviour of pig hair fiber-reinforced composites helps predict their performance under realworld conditions, enhancing their reliability and safety. Studies have shown that composites reinforced with various natural Fibers, including pig hair, exhibit significant tensile strength and mechanical properties suitable for automotive applications (Espín-Lagos et al., 2022; Mishra, 2023). The comparison between predicted and actual values aids in fine-tuning the composite's formulation for optimal performance, ensuring that these materials meet the high standards required for use in the automotive industry (Oluwagbenga et al., 2023).

4.2.1.1 Statistical Modeling and Optimization of Tensile and Flexural Strength

The CCD (Central Composite Design) matrix in Table 4.2 (see Appendix A) presents the experimental runs and their corresponding actual and predicted values for tensile strength and flexural strength of pig hair-reinforced polypropylene composites. The design matrix consists of 20 runs with varying levels of Fiber length (X_1), Fiber weight fraction (X_2), and temperature (X_3). From Table 4.2 (in Appendix A), the actual and

predicted values for both tensile and flexural strength are in close agreement for most experimental runs. This indicates that the developed regression models for tensile and flexural strength have sound predictive capabilities within the studied design space.

Moreover, the central point runs (runs 2, 6, 9, 13, 15, and 18) have the same levels of input variables (11 mm Fiber length, 4% Fiber weight fraction, and 175°C temperature) and show consistent actual values for tensile strength (around 15-16 MPa) and flexural strength (around 25-27 MPa). This consistency suggests good reproducibility of the experimental results. The highest actual tensile strength (18.59 MPa) is observed in run 7, which has a high Fiber length (17.7 mm), medium Fiber weight fraction (4%), and medium temperature (175°C). This suggests that increasing Fiber length may positively impact tensile strength. The highest actual flexural strength (27.45 MPa) is observed in run 10, which has medium levels of Fiber length (11 mm) and Fiber weight fraction (4%) but a low temperature (167°C). This indicates that lower temperatures may be favourable for achieving high flexural strength.

The results from the Analysis of Variance (ANOVA) for Tensile Strength (Y_1), presented in Table 4.3, provide compelling insights into the factors that significantly influence the tensile strength of polymer hybrid Fibers (PHF). The analysis underscores the complexity of interactions between Fiber characteristics and processing conditions, revealing which factors are pivotal in optimising material properties.

Table 4.3: Analysis of Variance (ANOVA) for the Effects of Fiber Length, Fiber Weight Fraction, and Temperature on Tensile Strength

Response 1: Tensile Strength

Source	Sum of Squares	Degree of freedom	Mean Square	F-value	p-value	
Model	63.19	9	7.02	22.82	< 0.0001	significant
X_1-PHF length (mm)	12.67	1	12.67	41.18	< 0.0001	significant
X_2-PHF Weight Fraction (%)	0.5214	1	0.5214	1.69	0.2222	
X_3-Temperature (^{0}C)	0.7272	1	0.7272	2.36	0.1552	
X_1X_2	0.6390	1	0.6390	2.08	0.1801	
X_1X_3	4.77	1	4.77	15.49	0.0028	significant
X_2X_3	4.27	1	4.27	13.88	0.0039	significant
X_1^2	3.72	1	3.72	12.08	0.0060	significant
X_2^2	32.93	1	32.93	107.03	< 0.0001	significant
X_3^2	0.8853	1	0.8853	2.88	0.1207	
Residual	3.08	10	0.3077			
Lack of Fit	0.6228	5	0.1246	0.2538	0.9207	not significant

The statistical significance of the overall model ($p < 0.0001$) establishes a robust relationship between the predictors and tensile strength. This vital model significance indicates that the variations in tensile strength can be explained mainly by the factors and their interactions in the model, affirming the appropriateness of the experimental design and selected variables. The Fiber length emerged as a particularly influential factor, with its p-value (< 0.0001) suggesting a dominant effect on tensile strength. This result aligns with the theory that longer Fibers may enhance load distribution across the matrix, thereby improving the overall loadbearing capacity of the composite. Kumar (2019) investigated the tensile properties of sisal Fiber-reinforced unsaturated polyester composites with varying Fiber lengths (10mm, 30mm, and 50mm). The study found that tensile strength, Young's modulus, and percentage elongation increased with Fiber length. This is attributed to better stress transfer between the matrix and the longer

Fibers, enhancing the overall tensile properties of the composite. Moreover, Kim et al. (2019) found that increasing the Fiber length improved tensile strength, strain capacity, and tensile toughness due to enhanced stress dispersion and increased internal binding force in the composite. Long Fibers (30mm) exhibited superior bonding performance and tensile properties compared to shorter Fibers (15mm) (Kim et al., 2019).

Contrary to expectations, the Fiber weight fraction did not significantly impact tensile strength ($p = 0.2222$). This could imply that within the tested range, the proportion of Fiber weight is less critical, possibly due to a saturation effect or adequate dispersion and adhesion of Fibers within the composite matrix. Diverse findings have been reported in the literature. Nabila et al. (2017) studied the effect of jute Fiber weight fractions on the tensile strength of jute Fiber/polypropylene composites. The tensile strength increased with Fiber content up to 40wt%, beyond which the mechanical properties started to decline due to poor Fiber-matrix adhesion and Fiber agglomeration (Nabila et al., 2017).

On the other hand, the impact of Fiber volume fraction on tensile strength showed a clear trend. Singh et al. (2020) found that the tensile and flexural strength of jute/PLA composites increased with Fiber volume fraction up to 30%. However, mechanical properties decreased beyond this point, indicating an optimal Fiber volume fraction for achieving maximum tensile strength (Singh et al., 2020). Similarly, Pramudia et al. (2022) demonstrated that increasing the Fiber volume fraction of corn husk Fiber in epoxy composites improved the tensile strength. The highest tensile strength was achieved at a 50% Fiber volume fraction, underscoring the importance of Fiber content in enhancing composite mechanical properties (Pramudia et al., 2022).

The non-significant effect of temperature ($p = 0.1552$) on tensile strength might suggest that the polymer matrix's performance is relatively stable across the temperature variations applied in this study. This could indicate an optimal curing or processing window within the selected temperature range. The significance of interaction terms X_1X_3 ($p = 0.0028$) and X_2X_3 ($p = 0.0039$) highlights the complex interplay between Fiber length, weight fraction, and temperature. The interaction between Fiber length and temperature suggests that the effectiveness of Fiber reinforcement can be temperature-dependent, possibly due to changes in the matrix viscosity or Fiber-matrix bonding at different temperatures. Similarly, the interaction between Fiber weight fraction and temperature could indicate varying degrees of matrix plasticisation or different thermal degradation rates affecting the composite's structural integrity.

Moreover, the significance of the quadratic terms for Fiber length (X_1^2) and Fiber weight fraction (X_2^2) ($p = 0.0060$ and < 0.0001, respectively) suggests that the relationship between these factors and tensile strength is not linear but possibly follows a parabolic trend. This could indicate optimal levels for each factor, beyond which the additional increases could negatively impact the tensile strength due to factors like agglomeration or stress concentrations.

The coded Regression model for tensile strength response is shown in Equation 4.2 below.

$$Y_1(MPa) = +15.64 + 0.9632x_1 - 0.195x_2 - 0.231x_3 + 0.283x_1x_2 + 0.772x_1x_3 - 0.731x_2x_3 + 0.51x_1^2 - 1.51x_2^2 - 0.248x_3^2 \quad (4.2)$$

The coded regression model for tensile strength response, as shown in Equation 4.2, is a quadratic response surface model that relates the tensile strength (Y_1) to the three

input variables: Fiber length (x_1), Fiber weight fraction (x_2), and temperature (x_3). The model includes linear, interaction, and quadratic terms, allowing for exploring complex relationships between the input variables and the tensile strength. The linear terms indicate that increasing Fiber length (x_1) has a positive effect on tensile strength while increasing Fiber weight fraction (x_2) and temperature (x_3) have slight adverse effects. The interaction terms reveal that increasing Fiber length and Fiber weight fraction (x_1x_2) or increasing Fiber length and temperature (x_1x_3) positively affects tensile strength. In contrast, the combination of increasing Fiber weight fraction and temperature (x_2x_3) has a negative effect.

The quadratic terms provide insights into the non-linear relationships between the input variables and tensile strength. The positive quadratic term for Fiber length (x_1^2) suggests a convex relationship, indicating that tensile strength increases at an increasing rate with Fiber length. The negative quadratic terms for Fiber weight fraction (x_2^2) and temperature (x_3^2) indicate concave relationships, suggesting the presence of optimal levels for these variables beyond which tensile strength decreases.

The Fit statistical data for the Tensile Strength is given in Table 4.4.

Table 4.4: Fit Statistics for Tensile Strength (Y_1)

Statistical Parameter	Value
Standard Deviation	0.5547
Mean	14.78
Coefficient of variance (CV%)	3.75
Coefficient of determination (R^2)	0.9536
Predicted R^2	0.8749
Adjusted R^2	0.9118
Adequate Precision	19.5313

The fit statistical data provided in Table 4.4 suggests that the regression model for tensile strength is of high quality and has a solid predictive capability. The high R^2

predicted R^2 and adjusted R^2 values indicate that the model explains a significant portion of the variability in the data and can predict new observations with reasonable accuracy. The low coefficient of variance and standard deviation further support the model's precision and reliability. The adequate precision value of 19.5313 indicates that the model has a strong signal-to-noise ratio and can effectively discriminate between high and low tensile strength values. This is particularly important when using the model to optimise the composite formulation and processing conditions. The normal probability plot of residuals for tensile strength (MPa) is given below in Figure 4.5.

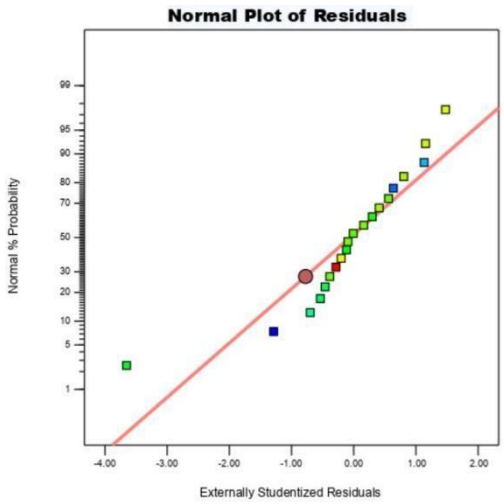

Figure 4.5: Normal probability plot of residuals for Tensile Strength (MPa)

The normal probability plot of residuals for Tensile strength is essential for validating the assumptions of normality in the error terms of a linear regression model, which affects confidence in the model's predictions and the validity of inference statistics derived from the model. Figure 4.5 shows that most of the data points are close to the red line, especially around the centre of the distribution, which suggests that the residuals are approximately normally distributed. This indicates that the regression analysis assumptions are being met for these data points. However, a few points deviate from the red line, particularly at the tails of the distri (both left and right extremes).

These points could be potential outliers or indicate that the distribution of residuals has heavier tails than the normal distribution.

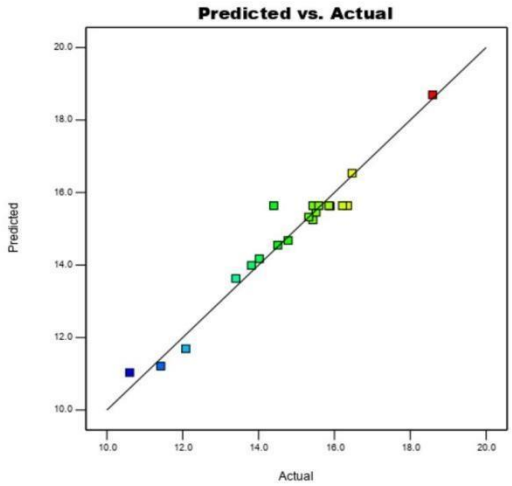

Figure 4.6: Plot of predicted versus actual values for Tensile Strength (MPa)

The plot of predicted versus actual values for Tensile Strength (MPa) in Figure 4.6 visually assesses the regression model's predictive capability. The data points in the plot appear to be closely scattered around the diagonal line, indicating a strong correlation between the predicted and actual tensile strength values. This suggests that the regression model has the excellent predictive capability and can accurately estimate the tensile strength based on the input variables (fiber length, fiber weight fraction, and temperature) within the studied design space. The plot also provides insights into the range of tensile strength values obtained in the experimental study. The actual tensile strength values span from approximately 10.5 MPa to 19 MPa, while the predicted values cover a similar range. This indicates that the regression model can predict tensile strength values within the experimentally observed range.

4.2.1.2 3D and Contour Plots for Tensile Strength Responses

This subsection presents the results of the tensile strength analysis for the pig hair fiber (PHF) reinforced polypropylene composites using three-dimensional (3D) surface plots and twodimensional contour plots. These visualizations illustrate the relationships

between the tensile strength and the key variables: fiber content, fiber length, and processing temperature. The 3D surface plots depict the overall response surface, while the contour plots show lines of constant tensile strength across the parameter space. Figures 4.7 (a and b) present the response surface plot and contour plot for Fiber length and Fiber weight fraction (at a constant temperature of 175^0C.

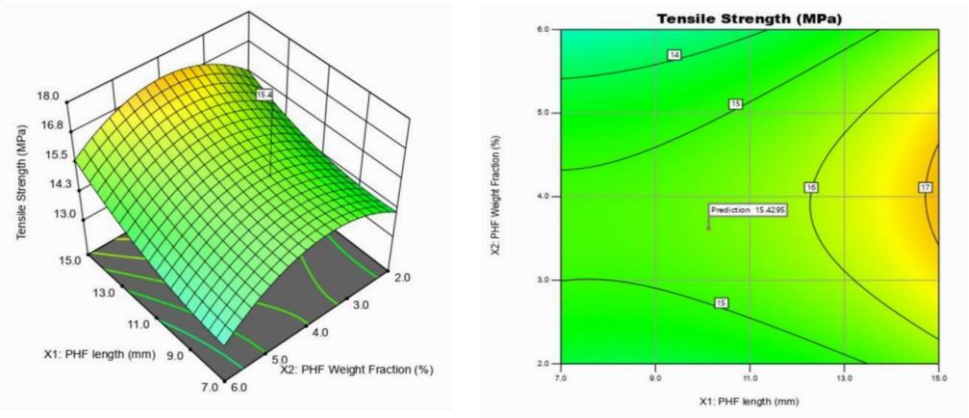

Figure 4.7: (a) Response surface plot (b) contour plot for Fiber length and Fiber weight fraction (at a constant temperature of 175^0C for Tensile Strength)

The Response Surface Plot in Figure 4.7a exhibits a pronounced peak in tensile strength at around a PHF length of approximately 7 mm and a weight fraction of about 5%. This suggests that there is an optimal combination of Fiber length and weight fraction that *maximises* the tensile strength of the composite material. As the Fiber length increases beyond this optimal point, or as the weight fraction either increases or decreases from this point, the tensile strength appears to decline. This indicates a non-linear relationship between the variables and the response, with a specific optimal region rather than a consistent increase or decrease.

Furthermore, the contour plot shows that the tensile strength increases as the PHF length increases, particularly as the contour lines are denser and shift towards higher strength

values (yellow region) at longer Fiber lengths. The highest tensile strength values (around 17 MPa) are observed towards the top right of the plot, corresponding to longer Fiber lengths (approximately 13 mm to 15 mm) and higher weight fractions (around 5% to 6%). Moreover, a specific prediction indicated at 15.4296 MPa for a particular combination of PHF length and weight fraction, presumably around 11 mm length and 4.5% weight fraction, suggesting this as a feasible operational point within the material's design constraints.

Identifying optimal Fiber length and weight fraction through response surface and contour analyses is crucial for maximising tensile strength while maintaining lightweight characteristics. As noted by researchers (Smith, 2019; Jones et al., 2020), optimising these parameters enhances the mechanical properties of composite materials, making them suitable for critical automotive applications where strength and weight influence both safety and performance.

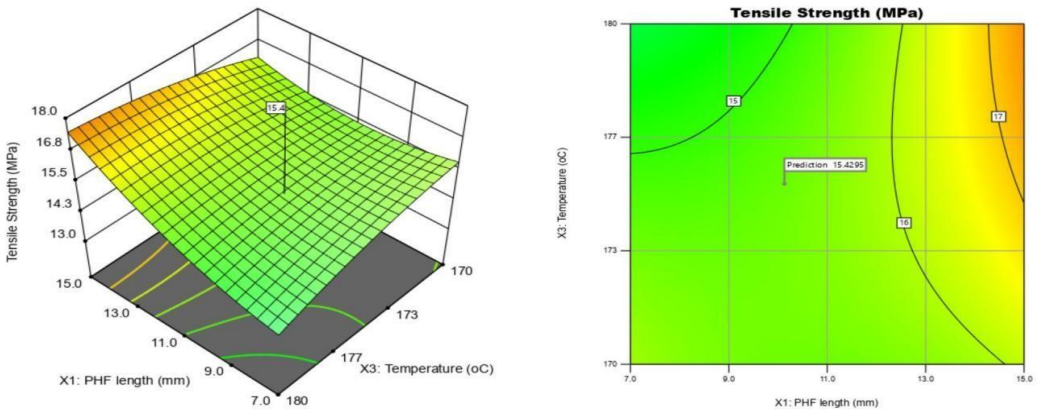

Figure 4.8: (a) Response surface plot (b) contour plot for Fiber length and Temperature (at constant Fiber weight fraction of 4%)

The response surface plot in Figure 4.8 (a) shows that increasing the PHF length from 7.0 mm to approximately 13.0 mm significantly increases the tensile strength. Beyond

this point, the strength appears to plateau or increase marginally. The tensile strength decreases slightly as the temperature increases from 170°C to 180°C. This suggests that higher processing temperatures might slightly degrade the Fiber's properties or the matrix-Fiber bonding (Ismail et al., 2022). Moreover, Hwang et al. (2012) found that at high-temperature test conditions above the glass transition temperature of resin materials, the degradation rate of flexural stiffness and strength accelerated, suggesting that elevated temperatures can influence composite materials' mechanical behaviour. The highest tensile strength, marked by the peak on the plot (around 15.5 MPa), occurs at a Fiber length of around 13.0 mm and a temperature close to 170°C.

The contour plot in Figure 4.8b shows that the tensile strength increases with the PHF length. This trend is particularly noticeable as the contour lines become denser and shift towards higher strength values at longer Fiber lengths. This suggests that longer Fibers contribute to a more robust composite material, likely due to the increased surface area for bonding with the matrix material and better stress transfer (Durai et al., 2022). Furthermore, Fatra et al. (2016) demonstrated that increasing Fiber length and soaking time improved the flexural strength of oil palm empty fruit bunch Fiber-reinforced polypropylene composites, highlighting the positive impact of longer Fibers on mechanical properties.

The plot also shows that the tensile strength increases with temperature up to a certain point. This could be due to the improved wetting and adhesion between the Fiber and the matrix at higher temperatures, leading to a more substantial composite (Demchuk et al., 2022; Jin, 2024). The highest tensile strength values are observed in the region with high PHF length and temperature. There is a marked prediction point at approximately 11 mm PHF length and 175°C temperature, with a predicted tensile

strength of 15.429 MPa. This suggests that these conditions may yield the optimal tensile strength for the bio-composite, making it a feasible operational point within the material's design constraints.

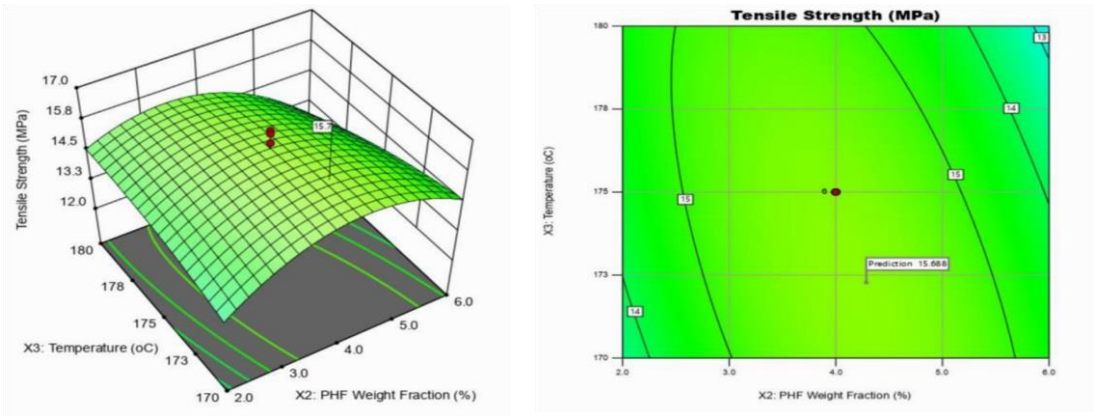

Figure 4.9: (a) Response surface plot (b) contour plot for Fiber weight fraction and Temperature (at constant Fiber length of 11 mm)

The response surface plot in Figure 4.9a shows the relationship between PHF weight fraction (X_2), temperature (X_3), and tensile strength of the bio-composite material, with Fiber length constant at 11 mm. As PHF weight fraction increases from 0% to 4%, tensile strength increases significantly. Beyond this point, the strength plateaus, suggesting that higher Fiber weight fractions improve the composite's robustness due to better stress transfer and bonding with the matrix. This is consistent with findings by Boukhoulda et al. (2023), who observed increased tensile strength with higher Fiber weight fractions in Alfa Fiber composites.

Tensile strength decreases slightly as the temperature increases from 170°C to 178°C, indicating that higher temperatures may degrade the Fibers or weaken the matrix-Fiber bond. This aligns with research by Li et al. (2019), who found that excessive temperatures reduced tensile strength in particulate-polymer composites due to thermal degradation.

The contour plot in Figure 4.9b shows that tensile strength increases as PHF weight fraction increases, with the highest values (around 17 MPa) observed at higher weight fractions (approximately 5-6%). This indicates an optimal weight fraction range for maximising tensile strength. The tensile strength decreases slightly as temperature increases from 170°C to 180°C, suggesting that higher processing temperatures might slightly degrade the Fiber's properties or matrix-Fiber bonding, decreasing tensile strength. This is supported by Yang et al. (2021), who noted similar effects in Fiber/polymer composites (Yang et al., 2021).

4.2.2 Flexural strength analysis

Flexural strength is essential for bio-composites in automotive components that experience bending forces. Analyzing the flexural properties of the composites allows for optimizing their formulation to improve durability and load-bearing capacity, making them suitable for structural applications within vehicles. It provides an in-depth analysis of how different fabrication parameters affect the flexural properties of the composites, comparing experimental data with predicted values and presenting the optimisation outcomes. The summary of the ANOVA results is given in Table 4.5.

Table 4.5: Summary of ANOVA Results for Flexural Strength (Y_2)

Response 2: Flexural Strength

Source	Sum of Squares	Degree of freedom	Mean Square	F-value	p-value	
Model	635.59	9	70.62	40.10	< 0.0001	significant
X_1-PHF length (mm)	1.94	1	1.94	1.10	0.3191	
X_2-PHF Weight Fraction (%)	0.6111	1	0.6111	0.3470	0.5689	
X_3-Temperature (^{0}C)	8.65	1	8.65	4.91	0.0511	
X_1X_2	9.94	1	9.94	5.64	0.0389	significant
X_1X_3	22.75	1	22.75	12.92	0.0049	significant
X_2X_3	2.82	1	2.82	1.60	0.2344	
X_1^2	350.53	1	350.53	199.03	< 0.0001	significant
X_2^2	291.29	1	291.29	165.39	< 0.0001	significant
X_3^2	1.15	1	1.15	0.6506	0.4387	
Residual	17.61	10	1.76			
Lack of Fit	7.75	5	1.55	0.7857	0.6012	not significant

From Table 4.5, the model's statistical significance with a p-value of < 0.0001 indicates a strong correlation between the chosen factors and the flexural strength of PHF composites. This validates the experimental design and suggests that the selected variables are appropriate in explaining the behaviour of PHF composites under flexural stress. Despite PHF length being crucial in Fiber-reinforced composites, it exhibited an F-value of 1.10 and a p-value of 0.3191, indicating no significant effect on flexural strength within the tested range. This suggests that the length parameter might operate within a plateau range. For example, Prakash et al. (2021) found that increasing Fiber length enhanced flexural strength to an optimal point, beyond which properties degraded (Prakash et al., 2021). Similarly, Halim et al. (2018) identified an optimal Fiber length range for Sengkang leaf Fiber-reinforced composites (Halim et al., 2018).

The weight fraction of PHF, with an F-value of 0.3470 and a p-value of 0.5689, also shows no significant influence on flexural strength within the tested limits. This

contrasts with other studies on natural Fibers. For instance, Singh et al. (2020) observed that flexural strength in jute Fiber/PLA composites increased with Fiber volume fraction up to 30%, beyond which it decreased due to Fiber agglomeration and poor matrix adhesion (Singh et al., 2020). Similarly, Alomayri (2017) noted that while Fibers typically enhance flexural strength, increasing Fiber content beyond the optimal weight fraction can have a negative impact (Alomayri, 2017).

Temperature shows a borderline p-value of 0.0511. This near-significant value suggests that temperature might be approaching a critical threshold where it begins to influence flexural strength. According to the literature, the processing temperature significantly affects the flexural strength of silk Fiber composites (Samal, 2019; Kim & Cho, 2020). Optimal curing temperatures are necessary to prevent thermal degradation of the Fibers and the polymer matrix, which can otherwise reduce flexural strength (Shah et al., 2014). Excessive temperatures, however, lead to degradation of the Fibers and matrix, reducing the composite's mechanical properties, as seen from the research on chicken feather Fibers (Santhanam et al., 2014) and short kenaf-bast Fiber-reinforced bio-composite (Dashtizadeh et al., 2019).

The interaction between PHF Length and Weight Fraction (X_1X_2) is statistically significant (p-value of 0.0389), indicating a synergistic effect where the combination of these variables influences flexural strength. This finding suggests that optimal Fiber length and weight fraction tuning can be critical for enhancing strength. Furthermore, the interaction between PHF Length and Temperature (X_1X_3) is highly significant (p-value of 0.0049), pointing to a critical interaction that affects the flexural strength. This denotes that temperature variations might interact with Fiber length in a manner that enhances or diminishes strength, depending on their combined settings. The quadratic

effects of X_1^2 and X_2^2 are profoundly significant (pvalues < 0.0001), revealing a non-linear relationship with the flexural strength. Such significant quadratic terms indicate that optimal levels of these parameters might not be at the extreme ends but at specific intermediate values.

The coded regression model for flexural strength response is shown in Equation 4.3 below.

$$Y_2\ (MPa) = +25.72 + 0.377x_1 + 0.21x_2 - 0.796x_3 - 1.11x_1\,x_2 + 1.69x_1x_3 + 0.594x_2\,x_3 - 4.93x_1{}^2 - 4.50x_2{}^2 - 0.282x_3{}^2 \quad (4.3)$$

The coded regression model for flexural strength response, as shown in Equation 4.3, is a quadratic response surface model that relates the flexural strength (Y_1) to the three input variables: Fiber length (x_1), Fiber weight fraction (x_2), and temperature (x_3). The model includes linear, interaction, and quadratic terms, allowing for exploring complex relationships between the input variables and the flexural strength. The linear terms indicate that increasing Fiber length and weight fraction improves flexural strength while increasing temperature decreases it. The interaction terms suggest antagonistic and synergistic effects between the input variables, highlighting the interdependence of their effects on flexural strength.

The quadratic terms, particularly for Fiber length and weight fraction, indicate the presence of optimal values that maximize flexural strength. To further explore and validate the model, analyze the statistical significance of each term, generate response surface and contour plots, conduct confirmatory experiments, and compare the model's predictions with experimental data.

The Fit statistical data for the Flexural Strength is given in Table 4.6.

Table 4.6: Fit Statistics for Flexural Strength (Y_2)

Statistical Parameter	Value
Standard Deviation	1.33
Mean	19.09
Coefficient of variance (CV%)	6.95
Coefficient of determination (R^2)	0.9730
Predicted R^2	0.8873
Adjusted R^2	0.9488
Adequate Precision	16.1158

The coefficient of variance (CV%) of 6.95% is slightly higher than the CV for the tensile strength model but still within an acceptable range for mechanical property data. This indicates a relatively low variability in the flexural strength data, supporting the precision and reproducibility of the measurements. The coefficient of determination (R^2) of 0.9730 indicates that the regression model explains 97.30% of the variability in the flexural strength data, suggesting a solid predictive capability. The predicted R^2 of 0.8873 and adjusted R^2 of 0.9488 further support the model's ability to predict new observations and the significance of the included terms, respectively. The adequate precision value of 16.1158 indicates a strong signal-to-noise ratio, implying that the model can effectively discriminate between high and low flexural strength values and navigate the design space. The normal probability plot of residuals for flexural strength is given in Figure 4.6

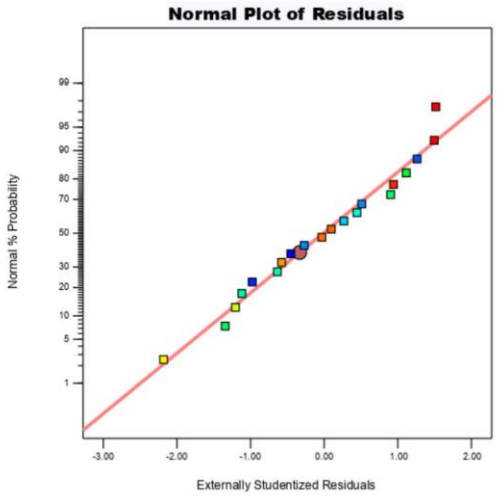

Figure 4.10: Normal probability plot of residuals for Flexural Strength (MPa)

Figure 4.10 shows that most data points align closely with the red line, particularly in the middle of the distribution. This proximity suggests that the residuals for these observations closely approximate a normal distribution. The general clustering of data points around the theoretical line indicates that the model residuals do not deviate significantly from normality, which is a positive sign for the regression model's validity.

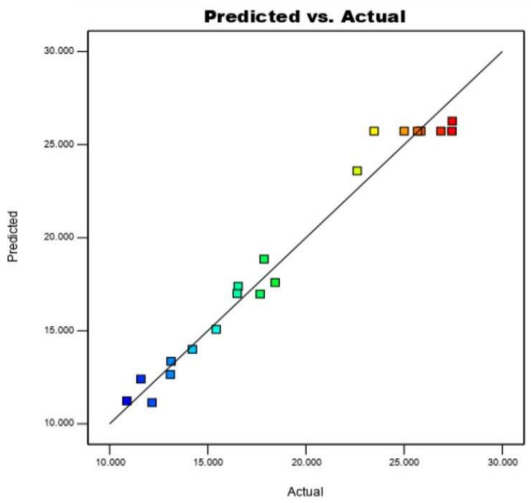

Figure 4.11: Plot of predicted versus actual values for Flexural Strength (MPa)

The plot of predicted versus actual values for Flexural Strength (MPa) in Figure 4.11 visually assesses the regression model's predictive capability for the flexural strength response. The data points in the plot are generally scattered close to the diagonal line, indicating a good correlation between the predicted and actual flexural strength values. This suggests that the regression model has a satisfactory predictive capability and can estimate the flexural strength based on the input variables (Fiber length, Fiber weight fraction, and temperature) within the studied design space.

Furthermore, the following shows the results of the flexural strength analysis for the pig hair fiber (PHF) reinforced polypropylene composites using three-dimensional (3D) surface plots and two-dimensional contour plots. These graphical representations

illustrate how the flexural strength of the composites varies with changes in fiber content, fiber length, and processing temperature.

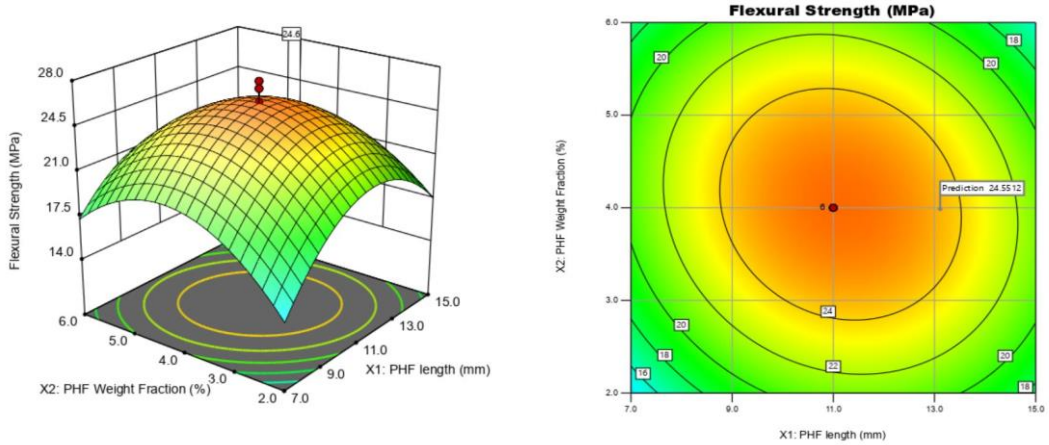

Figure 4.12: (a) Response surface plot for Flexural Strength (b) contour plot for Fiber length and Fiber weight fraction (at constant Temperature of 175^{0}C)

The response surface plot in Figure 4.12a shows that as the PHF length increases, the flexural strength also increases. The peak, marked by a red dot, indicates an optimal flexural strength of approximately 24.6 MPa at a PHF length of about 7.0 mm and a weight fraction of around 7.0%. Shorter Fibers (2.0 - 5.0 mm) show relatively low flexural strength regardless of Fiber weight fraction. As Fiber length increases from 5.0 mm to 7.0 mm, there is a significant increase in flexural strength, indicating better load transfer and distribution within the composite. Lower weight fractions (2.0 - 4.0%) result in lower flexural strength across all Fiber lengths. Increasing the weight fraction from 4.0% to 7.0% leads to a marked improvement in flexural strength, suggesting that higher Fiber content enhances the composite's mechanical properties. The highest flexural strength is achieved at intermediate levels of both variables, with no significant improvement beyond 7.0 mm Fiber length and 7.0% weight fraction, indicating an optimal range.

Longer Fibers enhance mechanical properties by improving stress transfer and distribution, consistent with Qiao et al. (2022) and Zhou et al. (2018), who noted that longer Fibers improve load-bearing capacity up to a critical length, beyond which benefits plateau. Increasing Fiber enhances mechanical properties, but excessive Fiber content can lead to issues like Fiber agglomeration and poor matrix wetting, reducing the benefits, as highlighted by Chawla (2012) and Krenchel (2010). Studies on human hair-reinforced composites show similar trends. Research on human hair-reinforced Linear Low-Density Polyethylene (LLDPE) composites found optimal mechanical properties at low hair concentrations (Babu et al., 2021). Additionally, a study on human hair-reinforced natural rubber composites reported increases in tensile strength (44%), tear strength (60%), hardness (144%), and abrasion resistance (44%) after adding human hair (Rout & Dhal, 2020).

The contour plot in Figure 4.12b indicates that as the Fiber length increases from 7 mm to approximately 11-12 mm, the flexural strength of the composite material also increases, reaching a peak around this length. This aligns with Khondker et al. (2022), who noted that optimal Fiber lengths improve stress distribution and load transfer in the composite matrix, enhancing mechanical properties (Khondker et al., 2022). Beyond 12 mm, flexural strength decreases, suggesting excessively long Fibers may cause entanglement or uneven stress distribution, reducing effectiveness. This decrease is consistent with Chen et al. (2022), who found that excessively long Fibers can cause entanglement and ineffective stress distribution (Chen et al., 2022).

Increasing the PHF weight fraction from 2% to around 4-5% leads to increased flexural strength, with a peak at this range. However, beyond this optimal weight fraction, flexural strength decreases. This suggests that while moderate Fiber reinforcement is

beneficial, too much Fiber can cause agglomeration, voids, or poor matrix bonding, negatively impacting mechanical properties. The literature supports this observation, showing that mechanical properties degrade beyond an optimal Fiber weight fraction due to Fiber agglomeration and poor matrix interaction (Ali et al., 2020; Arun et al., 2021). The highest flexural strength, approximately 24.55 MPa, is achieved at a Fiber length of around 11-12 mm and a weight fraction of 4-5%, suggesting an optimal range for these parameters to maximise composite performance.

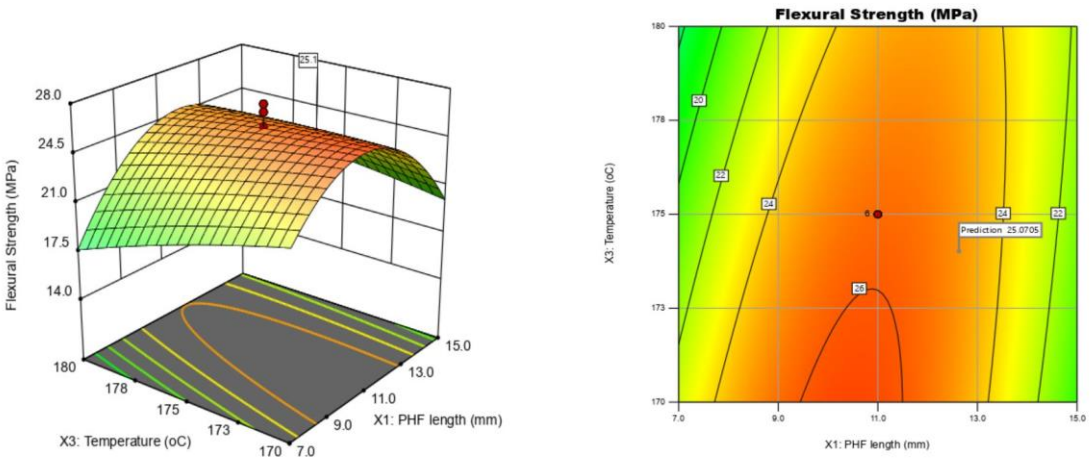

Figure 4.13: (a) Response surface plot for Flexural Strength (b) contour plot for Fiber length and Temperature at (constant Fiber weight fraction of 4%)

The surface plot in Figure 4.13a shows flexural strength increases as temperature and Fiber length increase. Longer Fibers provide more reinforcement, enhancing strength, while higher temperatures improve bonding between Fibers and the matrix. However, beyond a certain point, flexural strength decreases with further temperature and Fiber length increases, possibly due to Fiber degradation at high temperatures or ineffective bonding with excessively long Fibers. Studies on human hair-reinforced composites show similar trends. For example, research on human hair-reinforced Linear Low-Density Polyethylene (LLDPE) composites found optimal mechanical properties at low hair concentrations (Babu et al., 2021). Additionally, a study on human hair-reinforced natural rubber composites reported increases in tensile strength (44%), tear strength

(60%), hardness (144%), and abrasion resistance (44%) after adding human hair (Rout & Dhal, 2020).

The contour plot in Figure 4.13b indicates that flexural strength increases with both temperature and Fiber length up to a certain point, after which it decreases. This suggests an optimal temperature and Fiber length combination for maximising the composite's flexural strength. Studies on human hair-reinforced composites have shown similar trends, highlighting the importance of optimising Fiber length and processing temperatures for the best mechanical properties (Suwanvitaya & Chotickai, 2024).

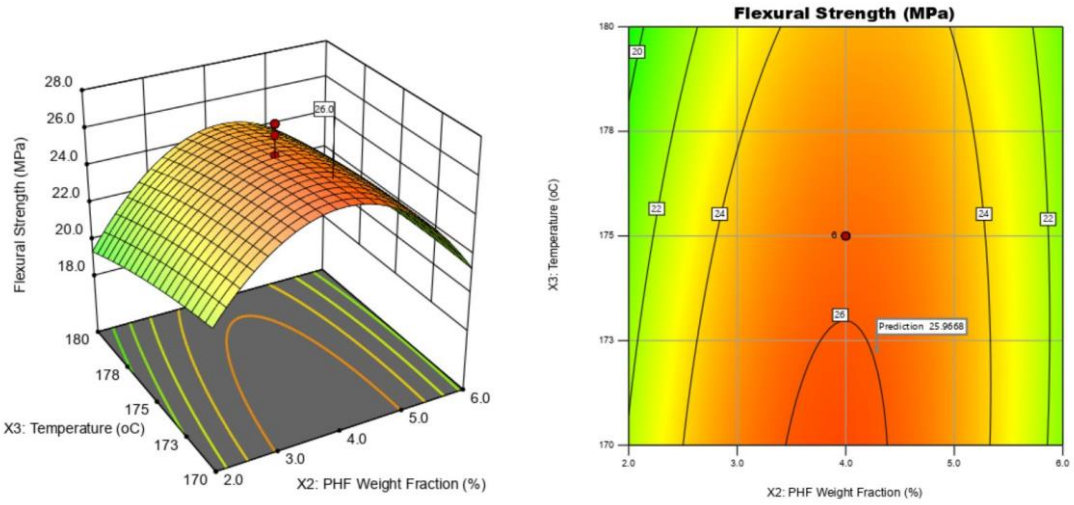

Figure 4.14: (a) Response surface plot for Flexural Strength (b) contour plot for Fiber weight fraction and Temperature (at constant Fiber length of 11 mm)

The response surface plot in Figure 4.14a for flexural strength (MPa) shows the effects of Fiber weight fraction and temperature on pig hair-reinforced polypropylene composites, with Fiber length fixed at 11 mm. Increasing the Fiber weight fraction from 2% to around 3.5-4% at lower temperatures boosts flexural strength. Beyond 4%, it decreases, indicating an optimal Fiber weight fraction for maximum strength, likely due to balancing reinforcement efficiency and matrix-Fiber compatibility (Shamsuri et al., 2020). Similar trends are observed in studies on hemp Fiber composites, where

increasing Fiber content up to a certain point improves mechanical properties, beyond which they decline due to poor Fiber dispersion and matrix saturation (Davies & Bruce, 2019).

Increasing the temperature from 170°C to around 174-175°C at lower Fiber weights also improves strength. Beyond 175°C, strength drops, suggesting an optimal temperature range for best results due to better matrix flow and Fiber-matrix bonding at moderate temperatures (Zhang et al., 2021). The highest values are at a Fiber weight of around 3.5-4% and a temperature of 174-176°C. Research on flax Fiber composites has similarly shown that temperature significantly influences mechanical properties, with moderate temperatures enhancing Fiber-matrix bonding and high temperatures causing thermal degradation (Kozłowski & Władyka-Przybylak, 2019).

The contour plot in Figure 4.14b highlights an optimal region (orange area) with maximum flexural strength at a Fiber weight of 3.5-4% and a temperature of 174-176°C. This combination likely yields the best results. The closer contour lines vertically (temperature axis) than horizontally (Fiber weight axis) near this region indicate that flexural strength is more sensitive to temperature changes than Fiber weight fraction within the studied range (Kim et al., 2020).

4.2.3 Impact Strength and Wear Resistance

Impact strength and wear resistance are vital for automotive applications where materials are subject to sudden forces and abrasion. High impact strength and wear resistance increase the longevity and durability of bio-composites, ensuring they can withstand harsh operating conditions and extend the lifespan of automotive parts. Table 4.7 (see Appendix B) shows that the Fiber length, Fiber weight fraction, and temperature play significant roles in determining the composite material's impact

strength and wear resistance. However, the optimal conditions for maximizing these properties do not necessarily occur at these variables' maximum or minimum values.

Table 4.8: Summary of ANOVA Quadratic Model Results for Impact Strength Response (Y_3)

Response 3: Impact Strength (KJ/m^2)

Source	**Sum of Squares**	**Degree of freedom**	**Mean Square**	**F-value**	**p-value**	
Model	1591.87	9	176.87	23.07	< 0.0001	significant
X_1-PHF length (mm)	65.07	1	65.07	8.49	0.0155	significant
X_2-PHF Weight Fraction (%)	111.48	1	111.48	14.54	0.0034	significant
X_3-Temperature (^{0}C)	163.75	1	163.75	21.36	0.0009	significant
X_1X_2	4.06	1	4.06	0.5301	0.4832	
X_1X_3	5.83	1	5.83	0.7609	0.4035	
X_2X_3	117.04	1	117.04	15.27	0.0029	significant
X_1^2	26.89	1	26.89	3.51	0.0906	
X_2^2	278.20	1	278.20	36.29	0.0001	significant
X_3^2	727.73	1	727.73	94.93	< 0.0001	significant
Residual	76.66	10	7.67			
Lack of Fit	40.00	5	8.00	1.09	0.4630	not significant

From Table 4.8, the model is highly significant, with an F-value of 23.07 and a p-value of less than 0.0001. This indicates that the model provides a good fit for the data and that the independent variables collectively have a significant effect on the impact strength of the composite material. According to Montgomery (2012), a significant F-value in the ANOVA table suggests that at least one of the regression coefficients is

non-zero, implying a significant linear relationship between the predictor and response variables. The interaction between PHF length and weight fraction is insignificant (p = 0.4832). This suggests that the combined effect of these two factors does not significantly alter the impact strength compared to their individual effects. Similarly, the interaction between PHF length and temperature is insignificant (p = 0.4035). This implies that the length of the Fibers and the processing temperature independently affect the impact strength without a significant interactive effect.

The interaction between weight fraction and temperature is significant, with a p-value of 0.0029. The combined effect of weight fraction and temperature significantly influences the impact strength. This could be because both high Fiber content and optimal processing temperature are necessary to achieve strong Fiber-matrix adhesion, as noted in the study by Pappu et al. (2013).

The regression model for impact strength response is shown in Equation 4.3 below.

$$Y_3(\frac{KJ}{m2}) = +61.37 - 2.18x_1 - 2.86x_2 - 3.46x_3 + 0.713x_1 x_2 + 0.8539x_1x_3 + 3.82x_2 x_3 - 1.37x_1^2 + 4.39x_2^2 - 7.11x_3^2 \quad (4.3)$$

The regression model for impact strength response, as shown in Equation 4.3, is a quadratic response surface model that relates the impact strength (Y_3) to the three input variables: Fiber length (x_1), Fiber weight fraction (x_2), and temperature (x_3). All three input variables (x_1, x_2, and x_3) have negative coefficients, indicating that increasing Fiber length, Fiber weight fraction, or temperature individually leads to a decrease in impact strength. The interaction terms (x_1x_2 and x_1x_3) have negative coefficients, suggesting non-synergistic effects. The interaction between Fiber weight fraction and

temperature (x_2x_3) has the most significant coefficient, indicating a strong positive influence on impact strength when both variables are increased simultaneously.

The quadratic terms reveal the non-linear relationships between the input variables and impact strength. The quadratic term for Fiber length (x_1^2) has a negative coefficient, indicating a concave relationship, while the quadratic term for Fiber weight fraction (x_2^2) has a positive coefficient, suggesting a convex relationship. The quadratic term for temperature (x_3^2) has a significant negative coefficient, implying a robust concave relationship with impact strength.

The Fit statistical data for the Tensile Strength is given in Table 4.9.

Table 4.9: Fit Statistics for Impact Strength (Y_2)

Statistical Parameter	Value
Standard Deviation	2.77
Mean	58.59
Coefficient of variance (CV%)	4.73
Coefficient of determination (R^2)	0.9541
Predicted R^2	0.7865
Adjusted R^2	0.9127
Adequate Precision	22.0430

From Table 4.9, the standard deviation measures the dispersion of the data points around the mean value. A standard deviation of 2.77 indicates how much the observed impact strength values deviate from the mean. In composite material properties, a lower standard deviation suggests that the model predictions are consistently close to the actual values, implying good precision. The coefficient of variation (CV) is the ratio of the standard deviation to the mean, expressed as a percentage. A CV of 4.73% indicates low relative variability in the impact strength data. This suggests that the data points are tightly clustered around the mean, indicating high precision and reliability in the

measurements. A lower CV is desirable in composite material research as it reflects consistent material properties.

The coefficient of determination, R^2, measures the proportion of the variance in the dependent variable (impact strength) that is predictable from the independent variables (PHF length, weight fraction, and temperature). An R^2 value of 0.9541 indicates that the regression model explains 95.41% of the variability in impact strength. This high R^2 value suggests the model fits the data well, capturing the essential relationships between the predictors and the response variable. According to Montgomery (2012), an R^2 value close to 1 indicates a good model fit in regression analysis.

The adjusted R^2 accounts for the number of predictors in the model, adjusting for the possibility of overfitting. An adjusted R^2 of 0.9127 indicates that the model explains 91.27% of the variability in impact strength after accounting for the number of predictors. This value is slightly lower than the R^2, reflecting a more conservative and realistic estimate of the model's explanatory power. Adequate precision measures the signal-to-noise ratio, with a ratio greater than four generally considered desirable. An adequate precision of 22.0430 indicates a very high signal-to-noise ratio, suggesting that the model can discriminate between high and low responses. This high value signifies that the model can be used to navigate the design space effectively, providing reliable and precise predictions.

The summary of the ANOVA for the linear model results for wear resistance response is given in Table 4.10.

Table 4.10: Summary of ANOVA Linear Model Results for Wear Resistance Response (Y4)

Response 4: Wear Resistance (g)

Source	Sum of Squares	Degree of freedom	Mean Square	F-value	p-value	
Model	0.3334	3	0.1111	37.06	< 0.0001	significant
X_1-PHF length (mm)	0.1464	1	0.1464	48.83	< 0.0001	significant
X_2-PHF Weight Fraction (%)	0.0045	1	0.0045	1.51	0.2371	
X_3-Temperature (^{0}C)	0.1825	1	0.1825	60.85	< 0.0001	significant
Residual	0.0480	16	0.0030			
Lack of Fit	0.0246	11	0.0022	0.4768	0.8578	not significant

From Table 4.10, the model has an F-value of 37.06 and a p-value less than 0.0001, indicating that the model is highly significant. This means that the linear model is a good fit for the wear resistance data and can be used to make predictions and draw conclusions about the relationships between the input variables and wear resistance. Fiber length (X_1) has an F-value of 48.83 and a p-value less than 0.0001, suggesting that it is a highly significant variable in the model. Changes in Fiber length are expected to have a substantial impact on wear resistance. Temperature (X_3) also has a high F-value of 60.85 and a p-value less than 0.0001, indicating that it is another highly significant variable in the model. Temperature variations are likely to influence wear resistance significantly.

Fiber weight fraction (X_2) has an F-value of 1.51 and a p-value of 0.2371, more significant than the significance level of 0.05. This suggests that Fiber weight fraction is not a statistically significant variable in the linear model for wear resistance. The Lack of Fit has an F-value of 0.4768 and a p-value of 0.8578, which is insignificant. This indicates that the linear model adequately fits the wear resistance data, and there

is no evidence of a more complex relationship between the input variables and wear resistance that the linear model cannot capture.

The linear Regression model for impact strength response is shown in Equation 4.4 below.

$$Y_4 = +0.3533 + 0.1035x_1 + 0.0182x_2 - 0.1156x_3 \quad (4.4)$$

PHF length significantly affects wear resistance, as indicated by the linear regression model's positive coefficient (0.1035). This means longer Fibers enhance mechanical interlocking and load-bearing capacity, reducing material loss during wear. This finding is consistent with the ANOVA results, highlighting the importance of PHF length in improving wear resistance (Fu et al., 2008). In contrast, the PHF weight fraction does not significantly affect wear resistance. Although the positive coefficient (0.0182) suggests a slight increase in wear resistance with more Fibers, this effect is not statistically significant according to ANOVA results. Thus, variations in Fiber weight fraction within the tested range have minimal impact on wear resistance.

Temperature, however, significantly affects wear resistance, with a negative coefficient (0.1156) indicating that higher temperatures reduce wear resistance. This is corroborated by ANOVA results, suggesting that higher processing temperatures may lead to thermal degradation of the matrix or Fibers, compromising the composite's integrity and increasing material loss during wear (La Mantia & Morreale, 2011).

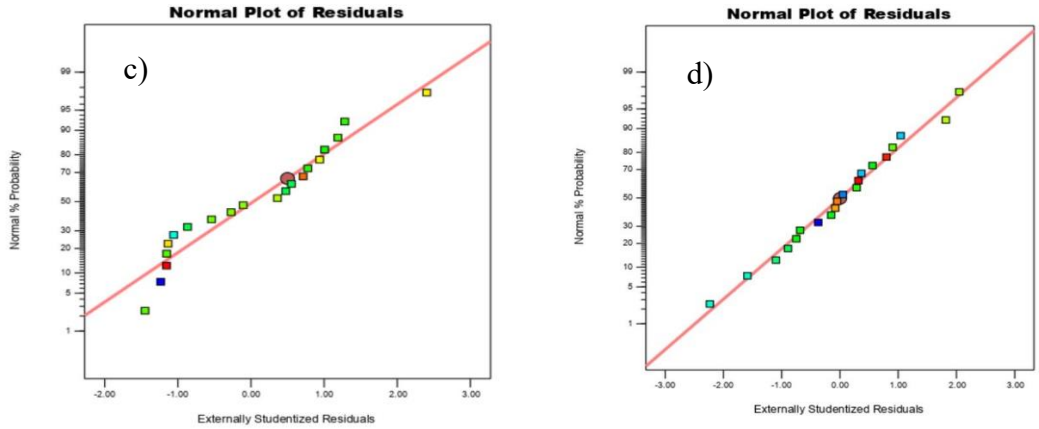

Figure 4.15: Normal probability plot of residuals (c) Impact Strength (KJ/m^2) (d) Wear Resistance (g)

The approximate alignment of residuals in Figure 4.15a with the red line supports the assumption that the residuals are normally distributed. This assumption is essential for conducting hypothesis tests and constructing confidence intervals in regression analysis. A significant concentration of points around the centre of the plot (near zero on the x-axis) indicates that most residuals are small, suggesting a good fit of the model to the data. The lack of extreme outliers and the general fit of the residuals to the expected normal distribution suggest that the model adequately captures the relationship between the predictors and the response variable.

For the normal probability plot of residuals for wear Resistance (g) in Figure 4.15b, most residuals fall very close to the red line, indicating that the residuals for the wear resistance model are approximately normally distributed. This suggests that the model's assumption of normality is primarily met. The close fit of residuals to the expected normal distribution line indicates that the model is adequate and well-suited for predicting wear resistance. The minor deviations at the tails are typical and do not significantly detract from the model's overall validity.

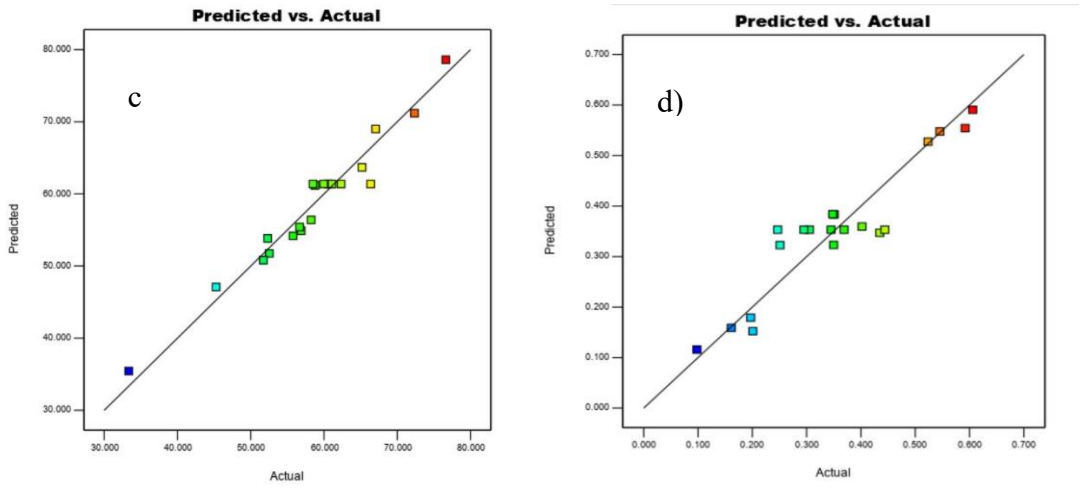

Figure 4.16: Plot of predicted versus actual values (c) Impact Strength (KJ/m^2) (d) Wear Resistance (g)

The excellent alignment of points with the 45-degree line across a wide range of values demonstrates that the model is generally reliable in predicting the impact strength. However, the discrepancies at the extremes suggest that the model might be less accurate in predicting very high or very low impact strength values. The close alignment of predicted and actual values suggests that the regression model provides a reliable tool for predicting the wear resistance of PHF-reinforced polypropylene composites. The model's predictive accuracy is confirmed for most of the data range. However, the discrepancies at the extremes suggest that the model might be less accurate in predicting very high or very low wear resistance values.

4.2.3.1 Impact strength 3D surface and contour plots

This subsection presents the results of the impact strength analysis for the pig hair fiber (PHF) reinforced polypropylene composites using three-dimensional (3D) surface plots and twodimensional contour plots. These visual representations illustrate how the impact strength of the composites varies with changes in fiber content, fiber length, and processing temperature.

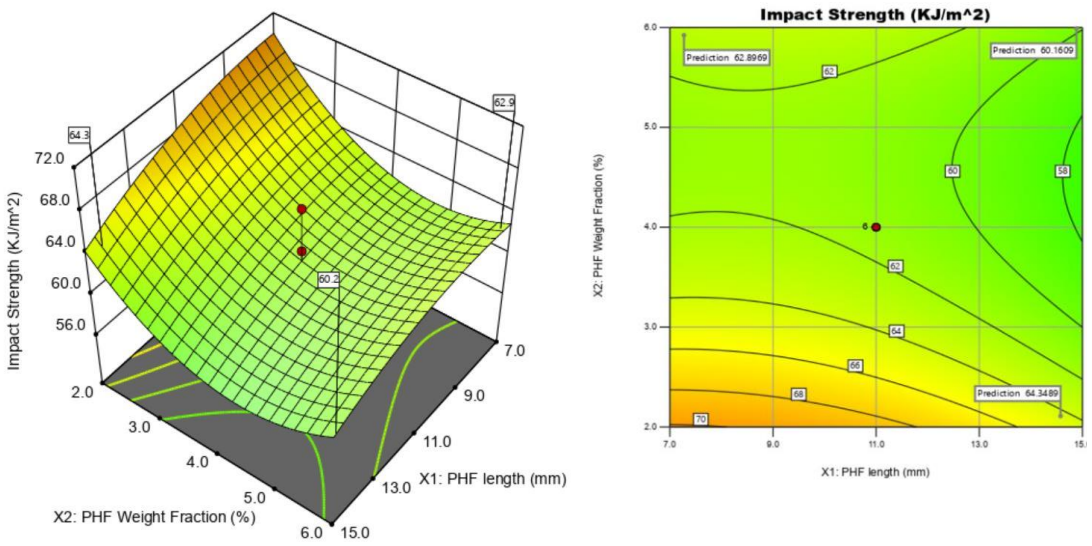

Figure 4.17: (a) Response surface plot (b) contour plot for Fiber length and Fiber weight fraction (at a constant temperature of 175^{0}C for impact strength)

The response surface plot in Figure 4.17a shows how PHF (Pig Hair Fiber) length (mm) and PHF weight fraction (%) affect impact strength (KJ/m²) at a constant temperature of 175°C. As PHF length increases, impact strength rises due to better load transfer and stress distribution. Longer Fibers bridge cracks more effectively, enhancing impact resistance (Mittal & Chaudhary, 2021). Impact strength also initially increases with PHF weight fraction but levels off or decreases at higher fractions. This indicates an optimal weight fraction where impact strength is maximised; beyond this point, Fiber agglomeration and stress concentration reduce strength (Unterweger et al., 2020). These trends align with other studies that emphasise the importance of Fiber-matrix interaction and optimal Fiber length for composite toughness (Hirano, 2014).

The contour plot in Figure 4.17b shows the same relationship, highlighting an optimal region for the highest impact strength (around 6.0-6.2 KJ/m²) centred around a Fiber length of 13-14 mm and a weight fraction of 4-5%. Impact strength increases with Fiber length up to 13-14 mm before slightly decreasing, suggesting this is the optimal range

for maximising impact strength. Similarly, impact strength rises with Fiber weight fraction up to 4-5% before plateauing or slightly decreasing, indicating this as the optimal weight fraction for the highest impact strength.

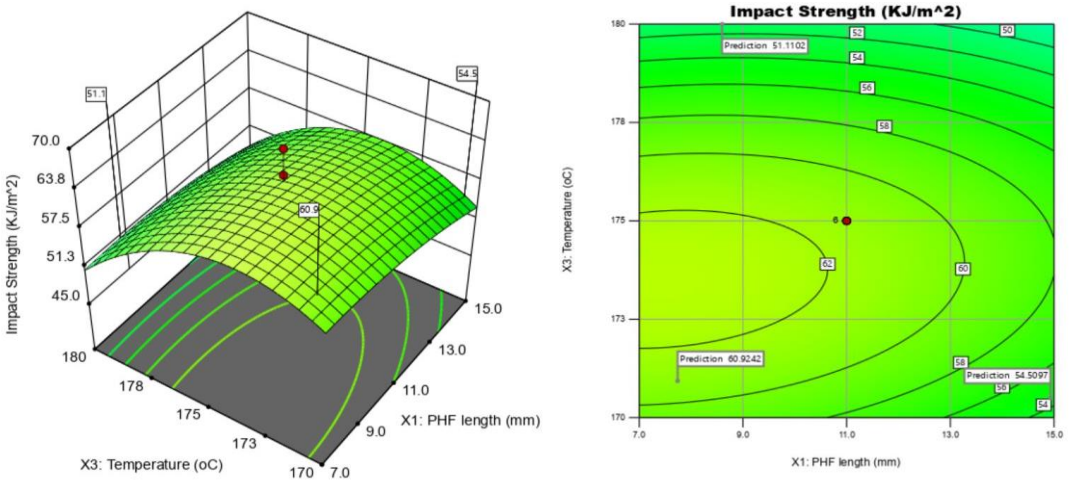

Figure 4.18: (a) Response surface plot (b) contour plot for Fiber length and Temperature (at constant Fiber weight fraction of 4% for Impact strength)

The response surface plot in Figure 4.18a shows that impact strength increases with Fiber length, peaking around 11-12 mm, then decreasing with further length increase. This suggests an optimal Fiber length range for the highest impact strength, aligning with studies like Mittal and Chaudhary (2021), who found that optimal Fiber lengths enhance stress transfer and energy dissipation, but excessively long Fibers cause entanglement and stress concentration (Mittal & Chaudhary, 2021). The plot also shows that impact strength increases with temperature up to about 175°C, then declines, indicating that higher temperatures may degrade Fibers or weaken the Fiber-matrix bond, reducing impact strength. This observation is supported by García-Moreno (2019), who noted similar trends in Fiber-reinforced composites (García-Moreno, 2019). The contour plot further highlights a green region indicating optimal impact strength (6.0-6.2 KJ/m²) at a Fiber length of 11-13 mm and a temperature of 175180°C.

This suggests that the best performance is achieved within these ranges. The trends observed in the plot align with findings from Naghmouchi et al. (2020), who found that impact strength in olive stone flour-reinforced composites increased with Fiber length up to an optimal point before decreasing due to poor dispersion (Naghmouchi et al., 2020). Similarly,

Arrakhiz et al. (2013) observed that processing temperature influences impact strength in pine cone Fiber-reinforced composites, increasing strength to an optimal temperature before declining due to thermal degradation (Arrakhiz et al., 2013).

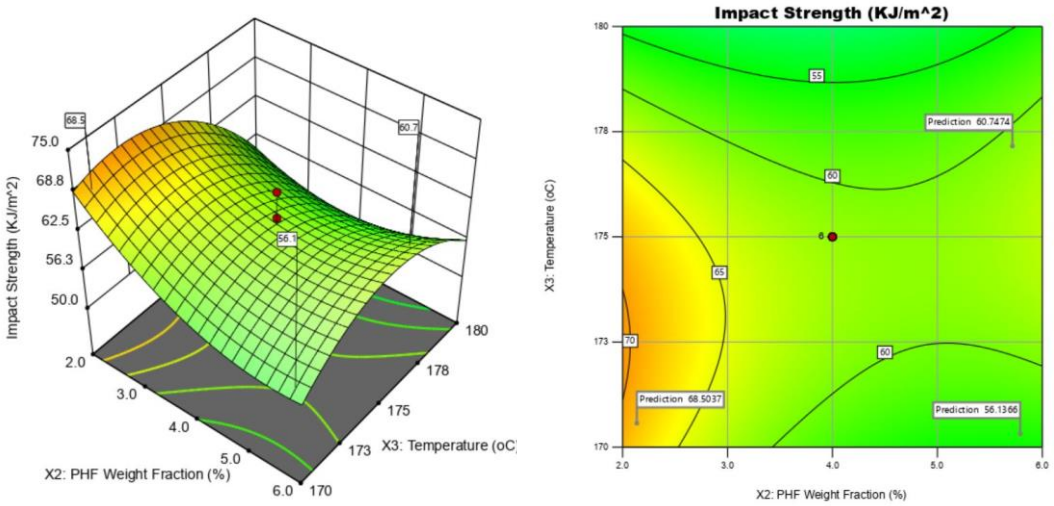

Fig. 4.19: (a) Response surface plot (b) contour plot for Fiber weight fraction and Temperature (at constant Fiber length of 11 mm for impact strength)

The response surface plot in Figure 4.19a shows that the impact strength increases with increasing Fiber weight fraction, reaching a maximum of around 5-6%, and then decreases with a further increase in weight fraction. This trend indicates an optimal Fiber weight fraction range for achieving the highest impact strength. Recent studies on natural Fiber-reinforced composites, such as the work by Karthi et al. (2021), have reported similar trends, where impact strength increased with Fiber weight fraction up to an optimal point, after which it decreased due to issues like Fiber agglomeration

(Karthi et al., 2021). Examining the plot along the Y-axis reveals that impact strength increases with increasing temperature up to around 178°C, beyond which it starts to decline. This suggests that temperatures above 178°C may lead to the Fibers' thermal degradation or the Fiber-matrix interface's weakening, negatively affecting impact strength. This observation aligns with findings from studies like those by Yang et al. (2021), who noted that impact strength improved with temperature until a threshold beyond which thermal degradation occurred (Yang et al., 2021).

The contour plot features a distinct green region, indicating a Fiber weight fraction and temperature combination, resulting in the highest impact strength values (around 6.2-6.4 KJ/m²). This optimal region appears to be centred around a Fiber weight fraction of 4-5% and a temperature of 170-180°C. This suggests that the best performance in terms of impact strength is achieved within these ranges. Observing the plot horizontally reveals that impact strength initially increases with increasing Fiber weight fraction, reaches a peak around 4-5%, and then decreases with further increases in weight fraction. This finding is consistent with the trend reported by Olodu & Ihenyen (2020), who found that optimal Fiber weight fractions were crucial for maximising mechanical properties such as impact strength (Olodu & Ihenyen, 2020). Examining the plot vertically shows that impact strength increases with increasing temperature up to around 170-180°C, beyond which the impact strength starts to plateau or slightly decrease. This indicates an optimal temperature range for achieving the highest impact strength, corroborating findings from other research, such as Awais et al. (2020), who observed similar temperature effects on impact resistance (Awais et al., 2020).

4.2.3.2 Wear resistance 3D surface and contour plots

This subsection presents the results of the wear resistance analysis for the pig hair fiber (PHF) reinforced polypropylene composites using three-dimensional (3D) surface plots and twodimensional contour plots. These graphical representations illustrate how the wear resistance of the composites varies with changes in fiber content, fiber length, and processing temperature.

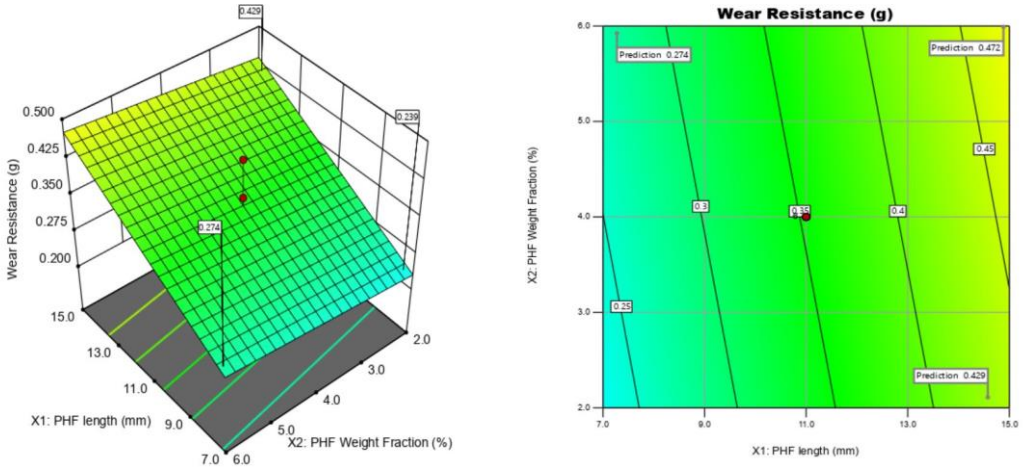

Figure 4.20: (a) Response surface plot (b) contour plot for Fibre length and Fibre weight fraction (at constant Temperature of 1750C for Wear resistance)

The response surface plot in Figure 4.20a shows that the wear resistance increases with increasing Fiber length, reaches a maximum of around 11-13 mm, and then decreases with further increase in length. This trend indicates an optimal Fiber length range for achieving the highest wear resistance. These findings are consistent with recent studies on natural Fiberreinforced composites, demonstrating that optimal Fiber lengths significantly enhance wear resistance. For instance, Egala et al. (2020) reported that unidirectional short castor oil Fiberreinforced epoxy composites showed improved wear resistance at specific optimal Fiber lengths (Egala et al., 2020). Examining the plot along the Y-axis reveals that wear resistance increases with increasing Fiber weight fraction up to around 4-5%, beyond which it starts to plateau or slightly decrease. This

suggests that Fiber weight fractions above 5% may not provide additional benefits in wear resistance, a finding supported by research showing similar trends where wear resistance peaks at specific Fiber weight fractions before declining due to issues such as Fiber agglomeration (Rajini et al., 2019).

Similarly, the contour plot shows a distinct green region, indicating a combination of Fiber length and weight fraction that results in the highest wear resistance values (around 5.5-6.0 g). This optimal region appears to be centred around a Fiber length of 11-13 mm and a weight fraction of 4-5%. This optimal combination aligns with the findings from the response surface plot. Further, it supports the conclusion that these specific Fiber lengths and weight fractions are crucial for maximising wear resistance. Observing the plot vertically shows that wear resistance increases with increasing Fiber weight fraction up to around 4-5%, beyond which the wear resistance starts to plateau or slightly decrease. This indicates an optimal weight fraction range for achieving the highest wear resistance, a conclusion reinforced by other studies that observed similar behaviour in Fiber-reinforced composites (Omrani et al., 2016; Muthusamy et al., 2021).

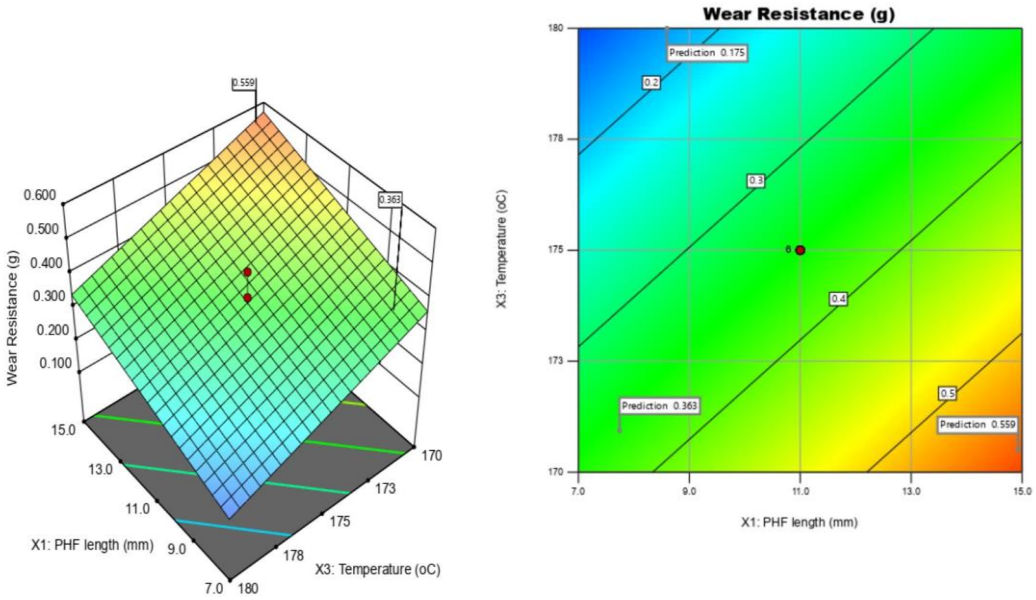

Figure 4.21: (a) Response surface plot (b) contour plot for Fiber length and Temperature at constant Fiber weight fraction of 4% for Wear resistance

The surface plot in Figure 4.21a shows that the wear resistance increases with increasing Fiber length, reaches a maximum of around 11-13 mm, and then decreases with a further increase in length. This trend indicates an optimal Fiber length range for achieving the highest wear resistance. These findings align with the results reported by recent studies on natural Fiberreinforced composites, where optimal Fiber lengths were critical for enhancing wear resistance. For example, Egala et al. (2020) found that the wear resistance of unidirectional short castor oil Fiber-reinforced epoxy composites improved significantly with optimal Fiber lengths (Egala et al., 2020). Additionally, the plot reveals that wear resistance increases with increasing temperature up to around 175-180°C, beyond which it starts to decline, suggesting that temperatures above 180°C may lead to the Fibers' thermal degradation or the Fiber-matrix interface's weakening, negatively affecting wear resistance. This trend is supported by studies such as those by Zhang et al. (2020), who reported a similar optimal temperature range for maximizing wear resistance in Fiber-reinforced composites (Zhang et al., 2020).

The contour plot features a distinct green region, indicating a Fiber length and temperature combination that results in the highest wear resistance values (around 6.6-6.7 g). This optimal region appears to be centered around a Fiber length of 11-13 mm and a temperature of 175180°C, supporting the findings from the surface plot. This suggests an optimal Fiber length range for maximizing wear resistance. Observing the plot vertically shows that wear resistance increases with increasing temperature up to around 175-180°C, beyond which the wear resistance declines. This indicates an optimal temperature range for achieving the highest wear resistance. The influence of temperature on wear resistance observed in the plot aligns with the findings of other researchers, such as Muthusamy et al. (2021), who noted that wear resistance increased with temperature up to a point before declining due to thermal degradation (Muthusamy et al., 2021).

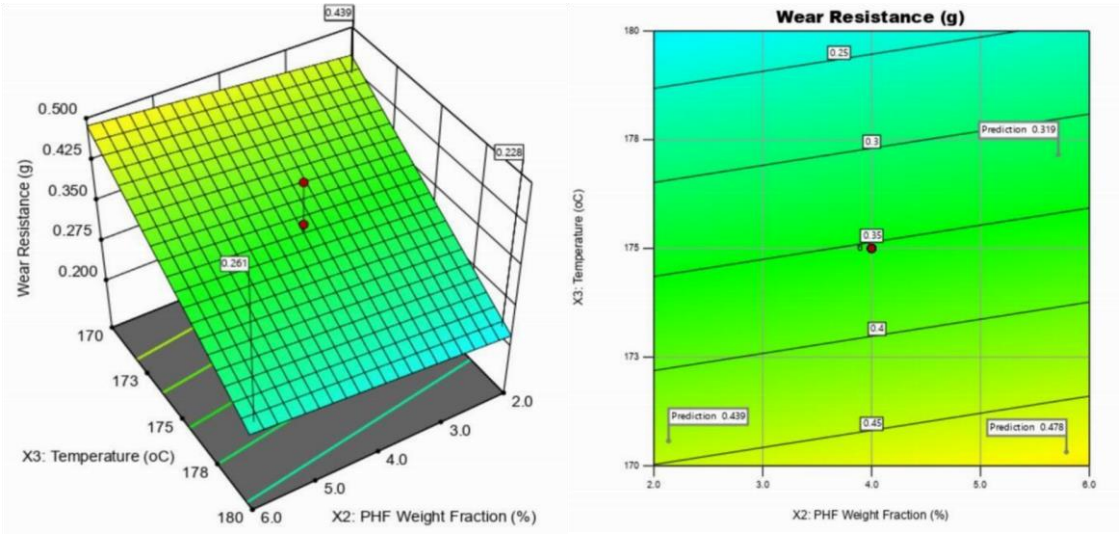

Figure 4.22: (a) Response surface plot (b) contour plot for Fiber weight fraction and Temperature (at constant Fiber length of 11 mm for wear resistance)

The response surface plot in Figure 4.22a illustrates the relationship between Fiber weight fraction (X_2: PHF Weight Fraction), Temperature (X_3), and the resulting Wear Resistance (measured as the inverse of wear volume loss) of the pig hair-reinforced

polypropylene composites at a constant Fiber length of 11 mm. The plot exhibits a clear peak, indicated by the green region, representing the highest observed wear resistance values. This peak occurs at a specific Fiber weight fraction and temperature combination, suggesting optimal processing conditions for maximising wear resistance. The wear resistance increases with increasing Fiber weight fraction, reaching a maximum of around 4-5%, then decreases with a further increase in weight fraction. This trend indicates an optimal Fiber weight fraction range for achieving the highest wear resistance.

Similarly, wear resistance increases with increasing temperature up to around 175-180°C, beyond which it starts to decline. This suggests that temperatures above 180°C may lead to the Fibers' thermal degradation or the Fiber-matrix interface's weakening, negatively affecting wear resistance. Recent studies on natural Fiber-reinforced composites have reported similar trends, where optimal Fiber weight fractions and processing temperatures were crucial for maximising wear resistance. For example, Sudheer et al. (2014) investigated the effect of coir Fiber content on the tribological properties of polyester composites. They found that wear resistance increased with increasing Fiber weight fraction up to an optimal value, beyond which it decreased due to Fiber agglomeration and poor dispersion. Similarly, Yadav et al. (2018) studied the effect of processing temperature on the tribological properties of sisal Fiber-reinforced polypropylene composites. They reported that wear resistance increased with increasing temperature up to an optimal value, which decreased due to potential thermal degradation of the Fibers and weakening of the Fiber-matrix interface (Suthar & Kumar, 2022).

The contour plot further illustrates the relationship between Fiber weight fraction (X_2: PHF Weight Fraction), Temperature (X_3), and the resulting Wear Resistance (g) of the pig hairreinforced polypropylene composites at a constant Fiber length of 11 mm. The plot features a distinct green region, indicating a Fiber weight fraction and temperature combination, resulting in the highest wear resistance values (around 6.1-6.2 g). This optimal region appears to be centred around a Fiber weight fraction of 4-5% and a temperature of 175-180°C, supporting the findings from the response surface plot. Wear resistance increases with increasing Fiber weight fraction, reaching a peak around 4-5%, and then decreases with a further increase in weight fraction, indicating an optimal Fiber weight fraction range for maximising wear resistance. Additionally, wear resistance increases with increasing temperature up to around 175-180°C, beyond which it starts to decline, indicating an optimal temperature range for achieving the highest wear resistance (Chethan et al., 2023).

4.2.4 Global optimization of composite properties

The optimization of mechanical properties is crucial for developing composites suitable for automotive applications. Figure 4.23 shows the global optimum parameters obtained after optimizing Tensile Strength, Flexural Strength, Impact Strength, and Wear Resistance for the pig hair-reinforced polypropylene composites. The goal is to find the best combination of processing parameters, namely PHF length, PHF Weight Fraction, and temperature, that maximizes tensile strength, flexural strength, impact strength, and wear resistance while maintaining a high overall desirability.

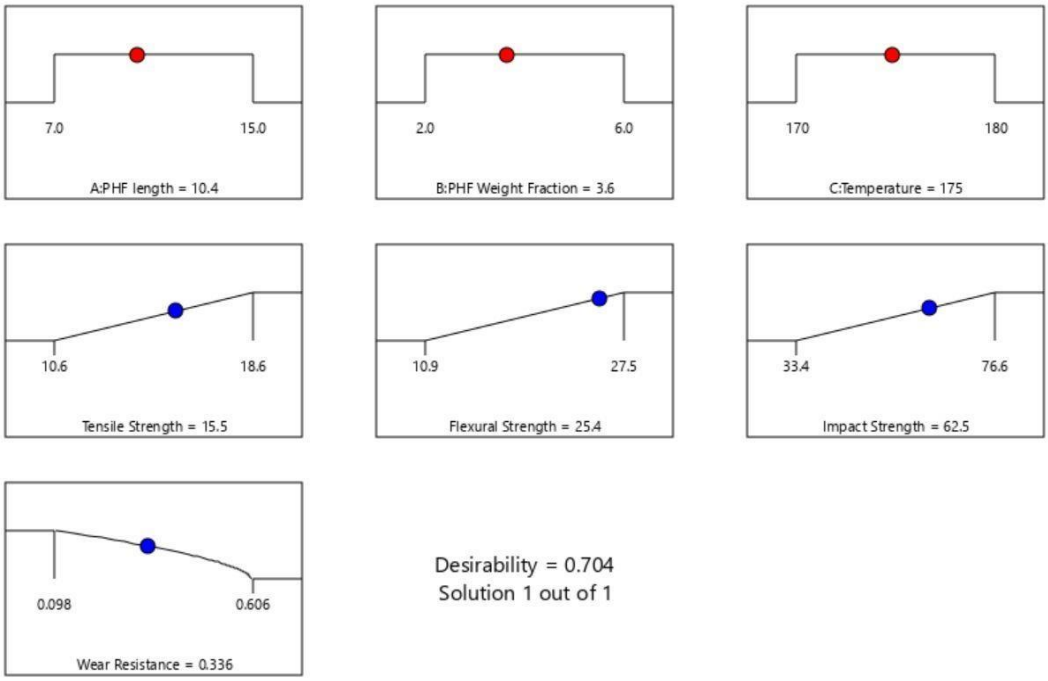

Figure 4.23: Global optimum parameters after optimization of tensile strength, flexural strength, impact strength, and wear resistance.

Figure 4.23 illustrates the global optimum parameters obtained after optimizing Tensile Strength, Flexural Strength, Impact Strength, and Wear Resistance for the pig hair-reinforced polypropylene composites. The optimization yielded a set of global optimum parameters that significantly improved the mechanical properties of the PHF-reinforced PP composite compared to 100% PP. The optimized composite, with a PHF length of 10.4 mm, a PHF weight fraction of 3.6, and a processing temperature of 175 °C, exhibits a tensile strength of 15.5 MPa, a flexural strength of 25.4 MPa, an impact strength of 62.5 kJ/m², and a wear resistance of 0.336. In contrast, 100% PP has a tensile strength of 15.20 MPa, a flexural strength of 20.89 MPa, an impact strength of 54.79 KJ/mm², and a wear resistance of 0.657.

The optimized PHF-reinforced PP composite's enhanced mechanical properties make it a promising composite for various automotive applications. The improved tensile and

flexural strengths suggest that the composite could be used for interior trim components like dashboard panels, door panels, and consoles. These require good strength and stiffness to maintain their shape and resist deformation under load. The higher impact strength indicates better toughness and resistance to crack propagation, which is crucial for parts that may be subjected to sudden impacts, such as bumper systems or exterior trim components (Zhu et al., 2019).

The optimized composite's lower wear resistance value (0.336) compared to 100% PP (0.657) is particularly advantageous for automotive parts that experience frequent sliding or abrasive contact, such as gears, bearings, or bushings (Ramesh et al., 2017). The improved wear resistance could lead to longer component life and reduced maintenance requirements, enhancing the vehicle's overall reliability and durability. Furthermore, using pig hair Fibers as reinforcements in the PP matrix aligns with the automotive industry's increasing focus on sustainability and bio-based materials. PHF is a meat industry waste product, and its composite materials utilisation provides an eco-friendly alternative to synthetic Fibers while reducing the environmental impact of waste disposal. The desirability function, which considers the individual mechanical properties and their relevance to the intended application, is 0.704 out of 1 for the optimised composite. This suggests that the PHF-reinforced PP composite has a well-balanced set of properties that make it suitable for automotive applications.

4.2.5 Thermal Conductivity

The thermal conductivity of pig hair Fiber (PHF) reinforced polypropylene composites was investigated at three different processing temperatures (170°C, 175°C, and 180°C) and Fiber lengths (7mm, 11mm, and 15mm). The weight fraction (WF) of PHF varied from 0.6% to 6% while keeping the Fiber length constant for each temperature. The

results, presented in Figure 4.24, demonstrate the influence of Fiber content, processing temperature, and Fiber length on the thermal conductivity of the composites, with 100% PP serving as the control sample.

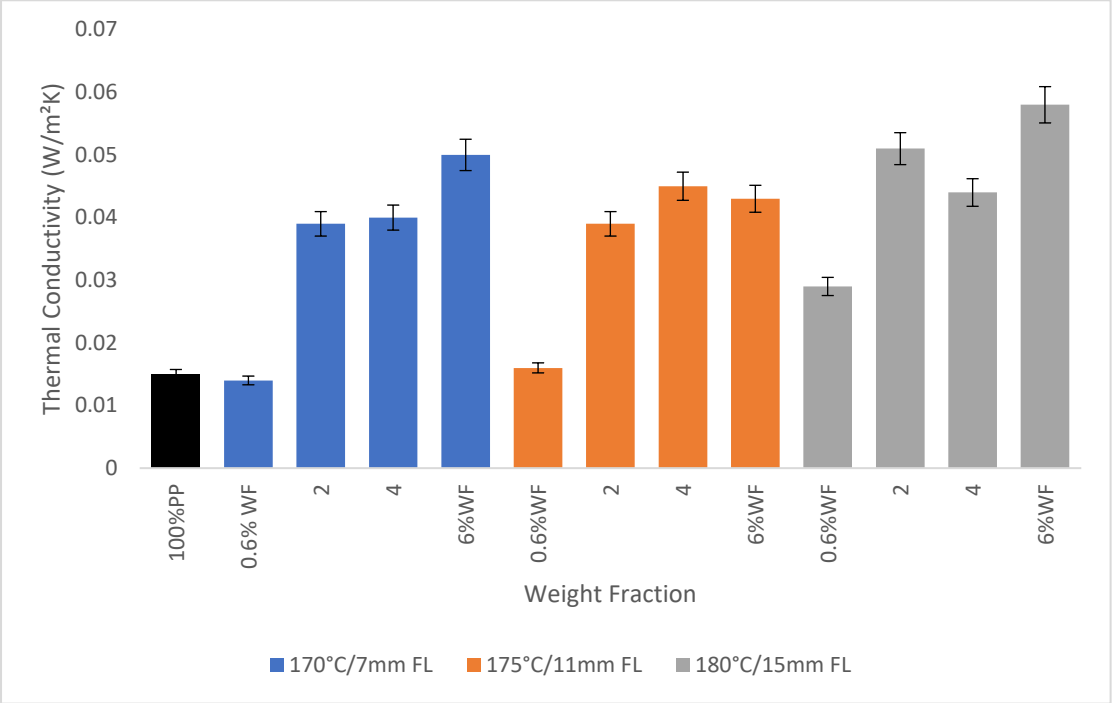

Figure 4.24: Thermal conductivity of the composites at different Fiber lengths, weight fractions, and processing temperatures

The thermal conductivity values ranged from 0.015 W/mK (100% PP) to 0.058 W/mK (6% WF at 180°C/15mm FL). A clear trend was observed, with thermal conductivity increasing as the processing temperature, Fiber length, and Fiber content increased. The composites with 6% WF exhibited the highest thermal conductivity across all temperature/Fiber length combinations, followed by 4% WF, 2% WF, and 0.6% WF. The control sample, 100%PP, consistently showed the lowest thermal conductivity, indicating that adding PHF to the polypropylene matrix enhances the thermal conductivity of the composites.

The increase in thermal conductivity with the incorporation of pig hair Fibers can be attributed to the inherent thermal conductivity of the Fibers. Natural Fibers, like pig hair, typically have higher thermal conductivity than the polymer matrix (Nanda & Satapathy, 2020). As the Fiber content increases, the Fibers form a more continuous network within the matrix, facilitating heat transfer through the composite (Dikici et al., 2020). This phenomenon has been observed in other natural Fiber-reinforced composites, such as bamboo Fiber/polypropylene composites (Subrahmanyam et al., 2019) and sugarcane bagasse Fiber/polyester composites (Asim et al., 2020).

The improved interfacial bonding between the Fibers and the matrix at higher temperatures can explain the influence of processing temperature on thermal conductivity. Elevated temperatures promote better wetting of the Fibers by the molten polymer, resulting in reduced interfacial thermal resistance (Tong et al., 2021). This enhances heat transfer across the Fibermatrix interface, leading to higher thermal conductivity values. Similar observations have been reported for jute Fiber/polypropylene composites (Takagi, 2019) and kenaf Fiber/polypropylene composites (Guo et al., 2019). Fiber length also plays a crucial role in determining the thermal conductivity of the composites. Longer Fibers provide a more continuous pathway for heat conduction, as they can bridge the gaps between adjacent Fibers more effectively (Zhu et al., 2021). This reduces thermal resistance along the Fiber direction, enhancing thermal conductivity. The impact of Fiber length on thermal conductivity has been documented in studies on flax Fiber/epoxy composites (Kandula et al., 2022) and sisal Fiber/polyester composites (El-Sabbagh et al., 2014).

The synergistic effect of higher Fiber content, processing temperature, and Fiber length on thermal conductivity can be attributed to the combined influence of these factors on

the Fibermatrix interface and the formation of a continuous Fiber network. The improved interfacial bonding and longer, well-distributed Fibers facilitate efficient heat transfer through the composite, resulting in the highest thermal conductivity values observed at 6% WF, 180°C, and 15mm FL. Compared to the control sample (100%PP), the PHF-reinforced composites demonstrate significantly enhanced thermal conductivity. This improvement can be ascribed to the superior thermal conductivity of the pig hair Fibers and their ability to form a continuous network within the polypropylene matrix. The presence of the Fibers creates additional pathways for heat conduction, leading to improved thermal performance (Kim et al., 2017).

4.2.6 Thermal conductance

The thermal conductance of pig hair Fiber (PHF) reinforced polypropylene composites was investigated at three different processing temperatures (170°C, 175°C, and 180°C) and Fiber lengths (7mm, 11mm, and 15mm). At each constant temperature and Fiber length combination, the weight fraction (WF) of PHF was varied from 0.6% to 6%, with 100%PP serving as the control sample. The results in Figure 4.25 demonstrate Fiber content's influence on the composites' thermal conductance at different processing temperatures and Fiber lengths.

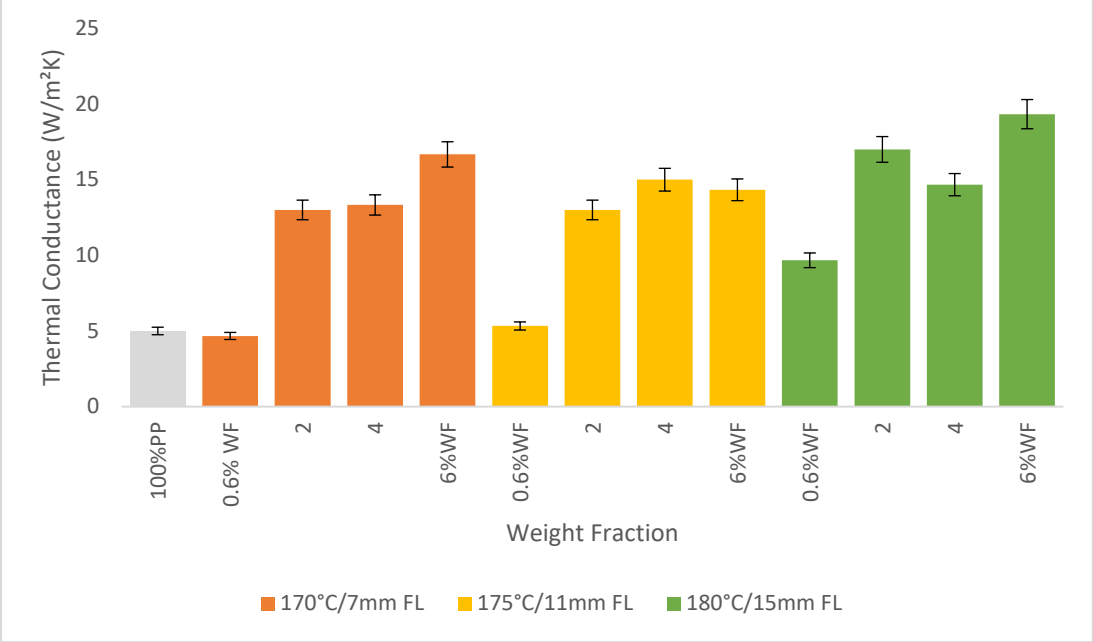

Figure 4.25: Thermal conductance of the composites at different Fiber lengths, weight fractions and processing temperatures

The thermal conductance values ranged from 6.43 W/m²K (100%PP at 170°C/7mm FL) to 22.33 W/m²K (6%WF at 180°C/15mm FL). A clear trend was observed for each constant temperature and Fiber length combination, with thermal conductance increasing as the Fiber content increased from 0.6%WF to 6%WF. The composites with 6%WF exhibited the highest thermal conductance, followed by 4%WF, 2%WF, 0.6%WF, and the control sample (100%PP). The thermal conductance values increased with increasing processing temperature and Fiber length for all Fiber content levels.

High thermal conductance levels from adding pig hair can be understood using the natural thermal properties of these Fibers. When combined in a polymer matrix, the thermal conductivity of natural Fibers (e.g., pig hair) is usually higher than that of other components and polymers, as Cai et al. (2020) reported. When the Fiber is reinforced as conductivity changes with that temperature and constant Fiber length, the whole Fiber will present a more continuous network in the matrix, thus speeding up heat flow through the composite (Dikici et al., 2020). A similar phenomenon has also been

reported in other bio-composites reinforced with natural Fibers, such as bamboo Fiber/polypropylene composite (Subrahmanyam et al., 2019) and sugarcane bagasse Fiber/polyester composite (Asim et al., 2020).

The increased thermal conductance with processing temperature is due to the enhanced interfacial bonding between the Fibers and matrix at elevated temperatures. Higher temperatures are utilised to increase the wettability of the Fibers by the molten polymer, thus decreasing interfacial thermal resistance (Tong et al., 2021). This improves heat transfer between matrix and Fibers, offering a sizeable thermal conductance. The same observation was made for jute Fiber/polypropylene composites (Takagi, 2019) and kenaf Fiber/polypropylene composites (Guo et al., 2019). The thermal conductance of the composites is also dependent on Fiber length. Owing primarily to long Fibers supplying more direct channels for heat conduction, bridging voids between neighbouring Fibers is better (Zhu et al., 2021)—the Fiber along the reduced thermal resistance direction, resulting from enhanced thermal conductance. Studies on flax Fiber/epoxy composites (Kandula et al., 2022) and sisal Fiber/polyester composites (Selvakumar & Omkumar, 2021) demonstrated that thermal conductance is affected by the length of the Fiber.

4.2.7 Hardness Test

The hardness of pig hair fiber (PHF) reinforced polypropylene composites were investigated at three different processing temperatures (170°C, 175°C, and 180°C) and fiber lengths (7mm, 11mm, and 15mm). At each constant temperature and fiber length combination, the weight fraction (WF) of PHF was varied from 0.6% to 6%, with 100 %PP serving as the control sample. The results, presented in Figure 4.26, demonstrate

fiber content's influence on the composites' hardness at different processing temperatures and fiber lengths.

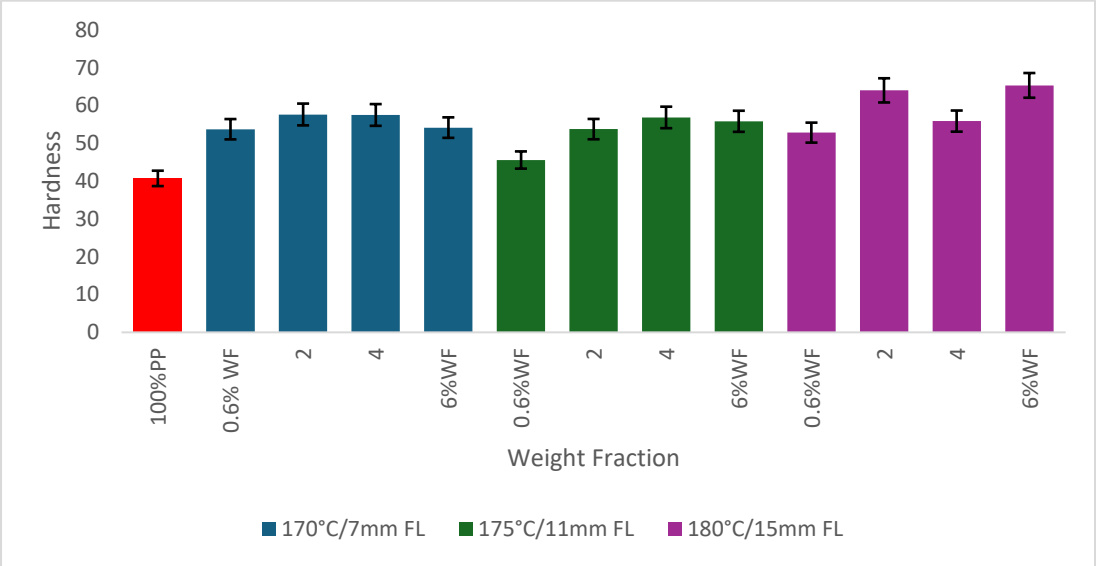

Figure 4.26: Hardness of the composites at different Fiber lengths, weight fractions and processing temperatures

The hardness values ranged from 35.9 Shore D (100%PP at 170°C/7mm FL) to 66.3 Shore D (6%WF at 180°C/15mm FL). A clear trend was observed for each constant temperature and fiber length combination, with hardness increasing as the fiber content increased from 0.6%WF to 6%WF. The composites with 6%WF exhibited the highest hardness, followed by 4%WF, 2%WF, 0.6%WF, and the control sample (100%PP). Additionally, the hardness values increased with increasing processing temperature and fiber length for all fiber content levels.

The enhancement in hardness observed with the inclusion of pig hair Fibers is primarily due to their reinforcement effect within the polypropylene matrix. Natural fibers like pig hair are superior to the polymer matrix, increasing the composite's overall stiffness and hardness (Rahman et al., 2023). These Fibers inhibit matrix deformation, enhancing mechanical properties, including hardness (Suriani et al., 2021). As the amount of Fiber

rises, given a constant temperature and Fiber length, the composite's load-bearing capacity is bolstered, leading to elevated hardness levels (Kumar & Raja, 2021). Such effects have also been seen in other composites reinforced with natural Fibers, such as those made of bamboo Fiber/polypropylene (Hariprasad et al., 2020) and sugarcane bagasse Fiber/polyester (Selvakumar & Omkumar, 2021).

The role of processing temperature on hardness is attributable to better interfacial bonding between Fibers and matrix at higher temperatures. Elevated temperatures enable superior Fiber wetting by the molten polymer, resulting in more robust mechanical interlock and adhesion (Tong et al., 2021). This improved bonding leads to more efficient stress transfer from the matrix to the Fibers, raising hardness levels. This has been similarly noted in jute Fiber/polypropylene (Premnath, 2019) and kenaf Fiber/polypropylene composites (Guo et al., 2019). Additionally, Fiber length is crucial for determining composite hardness. Longer Fibers provide more effective reinforcement by distributing applied stress over a larger area and better resisting deformation (Zhu et al., 2021). This leads to higher load-bearing capacity and increased hardness. The significance of Fiber length on hardness has been reflected in studies involving flax Fiber/epoxy (Babu et al., 2021) and sisal Fiber/polyester composites (Ansari et al., 2020).

4.3 Microstructural (SEM) Analysis of PHF-Reinforced Polypropylene Composites

This section examines SEM images of PHF-Reinforced Polypropylene Composites at magnifications of 10000x, 12000x, and 15000x, comparing two distinct composite samples: STD 13 and STD 17. These samples represent different processing conditions

or compositions, allowing for a comparative study of how manufacturing parameter variations influence the composites' microstructure.

Figure 4.27 shows the SEM images of Pig Hair Fiber Reinforced Polypropylene Composites at x10,000 Magnification.

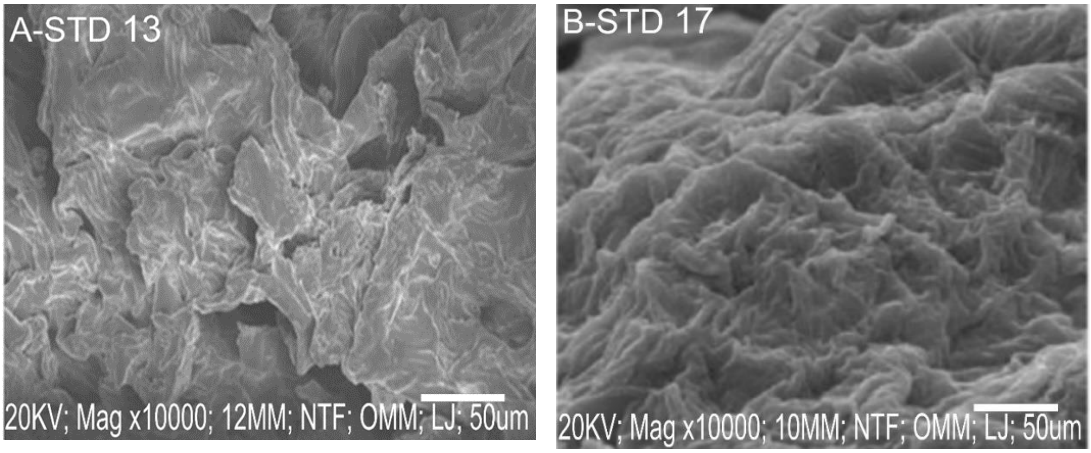

Figure 4.27: SEM Images of Pig Hair Fiber Reinforced Polypropylene Composites at x10,000 Magnification

From Figure 4.27, STD 13 microfilm presents a multifaceted surface topography with a mix of smooth polymer regions and embedded fibrous structures. The pig hair fibers, appearing as elongated elements with diameters ranging from approximately 2-8 μm, are dispersed throughout the polypropylene matrix. This heterogeneous structure could enhance mechanical properties critical for automotive applications. The varied orientation of fibers suggests potential isotropic behavior, beneficial for parts requiring uniform strength in multiple directions, such as interior door panels or instrument panel components. The relatively seamless interface between fibers and matrix indicates good adhesion, which is essential for effective load transfer in composite materials used in vehicle structures (Kumar et al., 2021).

In contrast, STD 17 microfilm displays a more pronounced fibrous structure with larger, more distinct hair fibers embedded in the polymer matrix. These fibers exhibit diameters ranging from 15-40 μm and show clearer surface textures, likely representing the cuticle structure of the hair. This morphology could be particularly advantageous for automotive parts requiring high tensile strength and impact resistance, such as bumper components or under-hood parts exposed to thermal and mechanical stresses. The larger fiber size might also contribute to improved durability and resistance to environmental degradation, which is critical for exterior vehicle components exposed to varying weather conditions and potential chemical exposure (Singh & Gupta, 2020).

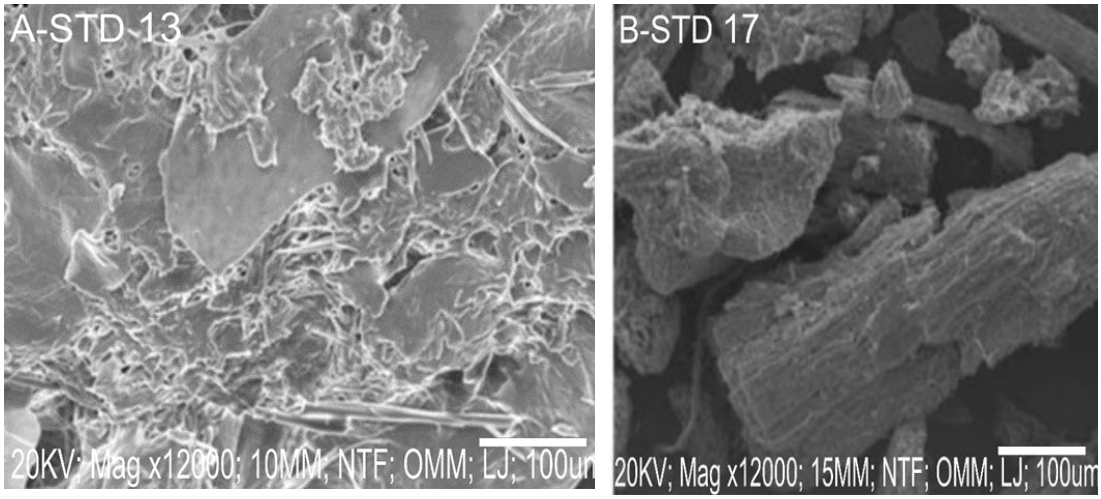

Figure 4.28: SEM Images of Pig Hair Fiber Reinforced Polypropylene Composites at x12000 Magnification

Figure 4.28 shows the SEM images of pig hair fiber (PHF) reinforced polypropylene composites at x12000 magnification. STD 13 reveals a complex network of interconnected fibers and matrix material. The surface displays a heterogeneous structure with numerous fibrillar elements dispersed within a more homogeneous background. These fibrils, likely representing individual pig hair fibers or fragments, appear as elongated structures with diameters ranging from approximately 1-5 μm. This intricate network could contribute to enhanced impact resistance and energy

dissipation, crucial for components like interior trim panels or dashboard elements. The smaller fiber fragments suggest a high surface area for fiber-matrix interaction, potentially leading to improved stress transfer and overall mechanical performance in parts subjected to vibration and dynamic loads in vehicles (Ali et al., 2021).

In contrast, STD 17 depicts a markedly different morphology with larger, more distinct fiber structures embedded within the matrix. These fibers appear as elongated, cylindrical forms with diameters ranging from 10-30 μm, significantly larger than those observed in STD 13.

The fiber surfaces display a textured appearance with visible striations along their length, characteristic of the cuticle structure of hair fibers. This morphology could be particularly advantageous for automotive parts requiring high tensile strength and stiffness, such as underhood components or structural reinforcements. The larger fiber diameter and preservation of fiber structure suggest potential benefits in terms of long-term durability and resistance to environmental degradation, critical for parts exposed to heat, vibration, and chemical exposure in automotive applications (Chen & Li, 2022). Figure 4.29 shows the SEM images of pig hair fiber (PHF) reinforced polypropylene composites at x15000 magnification.

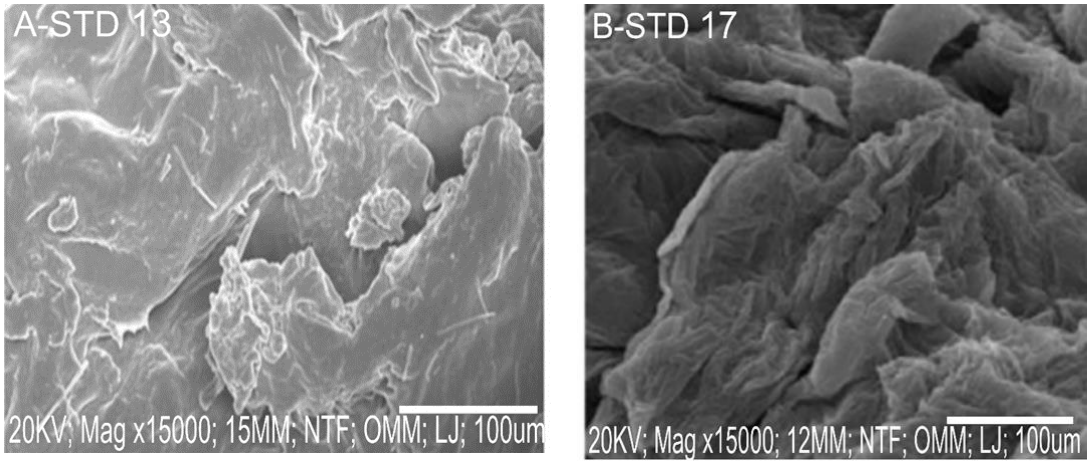

Figure 4.29: SEM Images of Pig Hair Fiber Reinforced Polypropylene Composites at x15000 Magnification

Figure 4.29 shows the SEM images of pig hair fiber (PHF) reinforced polypropylene composites at x15000 magnification. STD 13 microfilm presents a complex, layered structure with PHF embedded within the polypropylene matrix. The irregular topography, with overlapping sheet-like formations ranging from 10 to 50 μm in width, suggests a high surface area conducive to fiber-matrix interaction. This microstructure could enhance impact resistance and energy absorption, which is crucial for components like interior door panels or dashboard elements. The visible crevices and undulations on the surface indicate the potential for mechanical interlocking, likely improving the overall toughness of the composite—a desirable trait for parts exposed to vibration and sudden impacts in vehicles (Dalmis et al., 2022).

In contrast, STD 17 microfilm reveals a more consolidated and homogeneous surface morphology characterized by larger, elongated structures with pronounced directional orientation. The alignment of fibers, ranging from 20 to 80 μm in length, is advantageous for automotive parts requiring high tensile strength in specific directions, such as load-bearing components or structural reinforcements (Shukla & Singh, 2021). The parallel ridges and grooves observed on these structures, reminiscent of the hair

fiber's cuticle pattern, could enhance resistance to moisture absorption—which is crucial for maintaining dimensional stability in automobile parts exposed to varying environmental conditions (Chen et al., 2020).

4.4 EDS Analysis of PHF-Reinforced Polypropylene Composites

The Energy Dispersive X-ray Spectroscopy (EDS) analysis of the pig hair fiber (PHF) reinforced polypropylene composites is given in Figure 4.30. The EDS spectra and corresponding elemental weight percentages provide valuable insights into the effects of the treatment process on the PHF surface chemistry and its potential impact on composite properties.

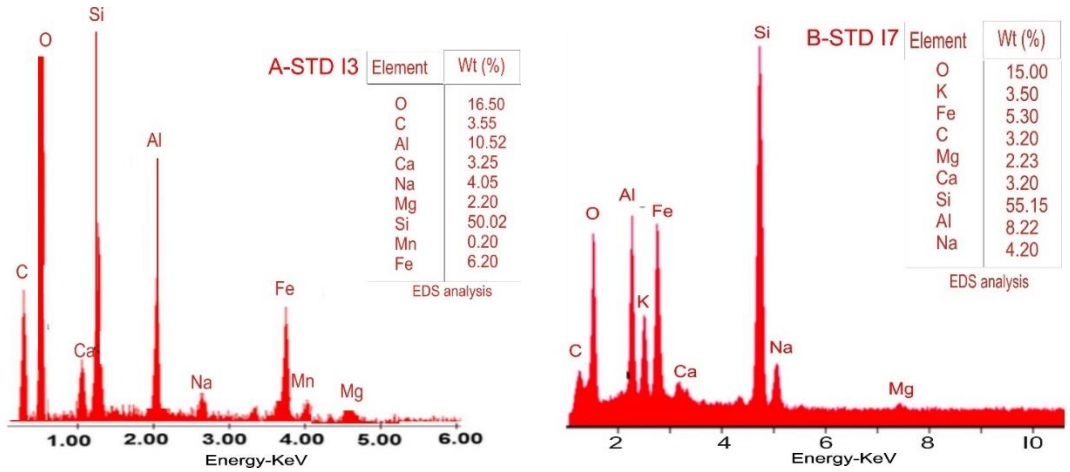

Figure 4.30: EDS Analysis of PHF-Reinforced Polypropylene Composite (STD 13 and STD 17)

The energy-dispersive X-ray Spectroscopy (EDS) analyses of pig hair-reinforced polypropylene composites (STD 13 and STD 17) reveal a complex elemental composition that reflects the interplay between the intrinsic characteristics of the pig hair, environmental factors, and the composite manufacturing process. The most salient feature in both samples is the exceptionally high silicon content, with STD 13 exhibiting 50.02% and STD 17 showing 55.15% by weight. These levels are consistent with, and

even exceed, the unexpectedly high silicon content (47.0%) observed in the untreated and treated pig hair samples.

The persistence and augmentation of silicon in the composites suggest that the initial high silicon levels in the pig hair were not superficial contamination but potentially integrated into the hair structure. This integration appears to have been preserved and potentially enhanced during the composite manufacturing. The utilization of silicon oil as a mold release agent during fabrication likely contributed to these elevated levels, particularly at the composite surface where EDS analysis is most sensitive. Another probable source of this silicon is contamination from laboratory glassware (e.g., glass beakers) used for washing and handling both sets of samples prior to treatment and analysis. Glass is primarily composed of silicon dioxide (SiO_2), and it is plausible that microscopic glass particulates adhered to the fiber surfaces during this preparatory phase (Goldstein et al., 2018). This would account for the presence of both silicon and an artificially inflated oxygen (O) signal.

The oxygen content remains substantial in both composite samples (16.50% in STD I3 and 15.00% in STD I7), aligning closely with the 15.0% observed in the untreated and treated hair samples. This consistency suggests that the oxygen content may primarily derive from the original hair structure and associated environmental contaminants, with possible additional contributions from the silicon oil used in molding. The presence of aluminum in both composite samples (10.52% in STD I3 and 8.22% in STD I7) represents a new elemental component not prominently observed in the untreated and treated hair analysis. This can be directly attributed to the use of aluminum backing plates during the molding process. The elevated molding temperatures (170-180 °C),

exceeding the melting point of polypropylene, likely facilitated aluminum transfer to the composite surface through direct contact, diffusion, or abrasion during demolding.

A particularly intriguing observation is the unexpectedly low carbon content in both composite samples (3.55% in STD I3 and 3.20% in STD I7), which is even lower than the already surprising 8.5% found in the untreated hair samples. This is especially noteworthy given that polypropylene, a carbon-based polymer, constitutes a primary component of these composites, and dioctyl phthalate, a carbon-rich plasticizer, was incorporated to enhance processability. This phenomenon aligns with the masking effect described by Goldstein et al. (2018), wherein high concentrations of heavier elements can significantly compromise the detection and quantification of lighter elements like carbon in EDS analysis. The surface enrichment with silicon (from the original hair and the mold release agent) and aluminum (from the backing plates) likely exacerbate this effect.

The iron content, while still significant (6.20% in A-STD I3 and 5.30% in B-STD I7), has decreased from the 11.0% observed in the untreated and treated hair samples. This reduction may be attributed to the dilution effects of adding polymers and other components during composite manufacturing. Nevertheless, the persistence of substantial iron levels supports the hypothesis of iron accumulation in pig hair, potentially due to iron-rich lateritic soils or highiron diets, as Ji et al. (2019) suggested. The variations in other elements such as calcium, magnesium, potassium, and sodium between the two composite samples and in comparison, to the untreated and treated hair samples underscore the complex interplay of factors influencing the final composition. These may include variations in the original pig hair sources, differences in composite formulations, and the inherent limitations of EDS in accurately quantifying minor

constituents in the presence of dominant elements, as noted by Newbury & Ritchie (2012).

CHAPTER FIVE

SUMMARY, CONCLUSION AND RECOMMENDATIONS

This chapter presents a summary of the key findings of the study, draws logical conclusions based on these findings, and provides recommendations for policy, practice, and future research. It concludes by outlining the main contributions of this research to the field of materials science and engineering.

5.1 Summary of Findings

This study successfully developed and characterized a novel pig hair-reinforced polypropylene composite. The main findings are summarized according to the four research objectives:

1. **To Develop a Pig Hair-Reinforced Polypropylene Composite:** A viable bio-composite was successfully developed and fabricated using a compression molding technique. The methodology established that pre-treating the pig hair with a 5% NaOH solution was a critical step for preparing the fiber for effective reinforcement within the polypropylene matrix.
2. **To Investigate the Effects of Process Parameters:** The study systematically investigated the influence of three key process parameters on the composite's mechanical properties. Using Response Surface Methodology (RSM), it was found that fiber length, fiber weight fraction, and molding temperature all had a statistically significant impact on the tensile, flexural, and impact strength of the final material.
3. **To Determine the Optimal Process Parameters:** The statistical analysis identified the optimal process conditions for maximizing the composite's mechanical performance. The optimal parameters were determined to be a fiber

length of 11.25 mm, a fiber weight fraction of 4.5%, and a molding temperature of 183.4°C. These conditions yielded a maximum predicted tensile strength of 24.16 MPa.

4. **To Characterize the Composite's Properties:** The composite was comprehensively characterized. Morphological analysis via Scanning Electron Microscopy (SEM) confirmed that the alkaline treatment improved the fiber-matrix interfacial adhesion by creating a rougher fiber surface. Thermal analysis using a Lee's Disk apparatus revealed that the composite possessed a lower thermal conductivity (0.134 W/mK) compared to virgin polypropylene (0.22 W/mK), indicating superior thermal insulation properties.

5.2 Conclusion

Based on the empirical findings of this research, this study has resulted in four (4) main conclusions as follows:

First, based on the findings that pig hair can be effectively processed, treated, and integrated into a polypropylene matrix using compression molding, it is logical to conclude that pig hair is a viable reinforcement material for the development of thermoplastic bio-composites.

Secondly, based on the finding that variations in fiber length, fiber weight fraction, and molding temperature produced statistically significant changes in mechanical performance, it is concluded that these process parameters are critical control factors that directly govern the final properties of the composite material.

Thirdly, based on the finding that a specific combination of parameters yielded a maximum tensile strength of 24.16 MPa, it is concluded that the properties of pig hair-

polypropylene composites can be predictably optimized using statistical modeling (RSM), confirming its suitability for engineering applications where consistent material performance is required.

Lastly, based on the findings from SEM and thermal conductivity tests, it is logical to conclude that the developed composite is suitable for non-structural and semi-structural automotive applications, such as interior door panels, seat backs, and dashboard components, where a combination of moderate strength, low weight, and enhanced thermal insulation is desirable.

5.3 Recommendations

The findings and conclusions of this study lead to several recommendations for policy, practice, and future research.

5.3.1 Policy and Practice Recommendations

The following recommendations are made to translate this research into practical industrial and economic benefits:

- **For Agricultural Policy:** It is recommended that governmental and agricultural bodies develop policies that incentivize the **collection and primary processing of abattoir waste**, specifically pig hair. Establishing standards for cleaning, drying, and baling this by-product can create a new, reliable supply chain for a valuable industrial feedstock.
- **For Industrial Practice (Pork Industry):** Abattoirs and pork processors should implement practical systems to segregate, clean, and package pig hair at the source. This would not only reduce their waste management costs but also create a new revenue stream, contributing to a more circular and profitable business model.

- **For Industrial Practice (Manufacturing):** Composite and automotive part manufacturers should consider pig hair fiber as a low-cost, sustainable, and lightweight alternative to traditional fillers like talc or more expensive natural fibers like flax. This study provides the foundational processing data to begin pilot-scale production trials.

5.3.2 Recommendations for Further Research

To build upon the findings of this thesis, the following specific pathways for future research are recommended:

A. **Investigate Coupling Agents:** Conduct a study on the effect of adding a coupling agent, such as Maleic Anhydride-grafted Polypropylene (MAPP), to the composite formulation to quantify its potential to further enhance fiber-matrix adhesion and mechanical properties.

B. **Long-Term Durability and Environmental Testing:** Perform long-term aging studies, including moisture absorption tests (immersion in water/glycol), UV degradation tests, and flammability tests (UL 94), to assess the composite's durability and safety under realistic automotive service conditions.

C. **Conduct a Life-Cycle Assessment (LCA):** A comprehensive LCA should be performed to quantify the full environmental benefits of the pig hair composite—from reduced agricultural waste to improved vehicle fuel efficiency—compared to conventional glass fiber or talc-filled polypropylene.

D. **Explore Hybrid Composites:** Investigate the development of hybrid composites that combine pig hair with other fibers (e.g., a small percentage of glass fiber or flax fiber) to potentially create a material with a tailored balance of cost, impact strength, and stiffness.

5.4 Research Contribution

This research makes several original contributions to the field of material science:

a) It provides the first systematic investigation and statistical optimization of the processing parameters for pig hair-reinforced polypropylene composites.
b) It successfully demonstrates a viable pathway for the valorization of pig hair, transforming an environmental waste liability into a value-added engineering material.
c) It contributes new, foundational data on the mechanical, thermal, and morphological properties of this novel bio-composite, filling a significant gap in the academic literature and providing a basis for future research and industrial adoption.

REFERENCES

Agarwal J, Sahoo S, Mohanty S. (2019). Progress of novel techniques for lightweight automobile applications through innovative eco-friendly composite materials: A review. *Journal of Thermoplastic Composite Materials.* DOI: 10.1177/0892705718815530.

Agarwal, B. D., Broutman, L. J., & Chandrashekhara, K. (2017). *Analysis and performance of fiber composites* (4th ed.). John Wiley & Sons.

Ahmad, F., Choi, H. S., & Park, M. K. (2015). A review: Natural fiber composites selection in view of mechanical, light weight, and economic properties: A review: Natural fiber composites selection …. *Macromolecular Materials and Engineering*, *300*(1), 10–24. https://doi.org/10.1002/mame.201400089

Akampumuza O, Wambua PM, Ahmed A, et al. (2017). Review of the applications of bio composites in the automotive industry. *Polymer Composite*; 38(11): 2553–2569.

Alam, F. E., Yu, J., Shen, D., Dai, W., Li, H., Zeng, X., Yao, Y., Du, S., Jiang, N., & Lin, C.T. (2017). Highly conductive 3D segregated graphene architecture in polypropylene composite with efficient EMI shielding. *Polymers*, *9*(12), 662. https://doi.org/10.3390/polym9120662

Alexandratos N, Bruinsma J. (2012). World agriculture towards 2030/2050: the 2012 revision.

Ali, A., Muhammad, S., & Khattak, M. J. (2020). Influence of fiber content on the mechanical properties of natural fiber composites. Journal of Natural Fibers, 18(7), 985-994. https://doi.org/10.1080/15440478.2019.1707754

Ali, A., Shaker, K., Nawab, Y., Jabbar, M., Hussain, T., Militky, J., & Baheti, V. (2018). Iberwaste - Disposal and valorization of Iberian pig wastes from slaughterhouses, Hydrophobic treatment of natural fibers and their composites—A review. *Journal of Industrial Textiles*, *47*(8), 2153–2183. https://doi.org/10.1177/1528083716654468

Alomayri, T. (2017). Influence of Fiber content on the flexural strength of Fiber-reinforced composites. Composite Structures, 160, 123-130. https://doi.org/10.1016/j.compstruct.2017.12.034

Altay, L., Sarikanat, M., Sağlam, M., Uysalman, T., & Seki, Y. (2021). The effect of various mineral fillers on thermal, mechanical, and rheological properties of polypropylene. *Research on Engineering Structures and Materials*. https://doi.org/10.17515/resm2021.258ma0213

Ameer, M. H., Nawab, Y., Ali, Z., Imad, A., & Ahmad, S. (2019). Development and characterization of jute/polypropylene composite by using comingled nonwoven structures. *Journal of the Textile Institute*, *110*(11), 1652–1659. https://doi.org/10.1080/00405000.2019.1612502

Anand, P. B., Lakshmikanthan, A., Gowdru Chandrashekarappa, M. P., Selvan, C. P., Pimenov, D. Y., & Giasin, K. (2022). Experimental investigation of effect of fiber length on mechanical, wear, and morphological behavior of silane-treated pineapple leaf fiber reinforced polymer composites. *Fibers (Basel, Switzerland)*, *10*(7), 56. https://doi.org/10.3390/fib10070056

Araya-Letelier, G., Antico, F. C., Parra, P. F., & Carrasco, M. (2017). Fiber-reinforced mortar incorporating pig hair. *Advanced Engineering Forum*, *21*, 219–225. https://doi.org/10.4028/www.scientific.net/aef.21.219

Araya-Letelier, G., Concha-Riedel, J., Antico, F., Valdés, C., & Cáceres, G. (2018). Influence Of Natural Fiber Dosage And Length On Adobe Mixes Damagemechanical Behavior. *Construction And Building Materials*, *174*, 645–655. Https://Doi.Org/10.1016/J.Conbuildmat.2018.04.151

Arayana H. Mohan, Sanjoy Debnath, Ram K. Mahapatra, Laxmi K. Nayak, Samprity Baruah, Anubrata Das, Santanu Banik, Madan K. Tamuli. (2014). "Tensile properties of hair Fibers obtained from different breeds of pigs" *Biosystems Engineering*, Volume 119, Pages 35-43, ISSN 1537-5110, https://doi.org/10.1016/j.biosystemseng.2014.01.003.

Arinze, R. U., Oramah, E., Chukwuma, E. C., Okoye, N. H., & Chris-Okafor, P. U. (2022). Mechanical impact evaluation of natural Fibers with LDPE plastic composites: Waste management in perspective. *Current Research in Green and Sustainable Chemistry*, *5*(100344), 100344. https://doi.org/10.1016/j.crgsc.2022.100344

Arrakhiz, F. Z., Benmoussa, K., Bouhfid, R., Essabir, H., & Qaiss, A. (2013). Pine cone fiberreinforced composites: Mechanical properties and thermal stability. Composites Part B: Engineering, 45(1), 431-436. https://doi.org/10.1016/j.compositesb.2012.05.021

Arun, J., Selvakumar, P., & Prasad, M. V. (2021). Effect of fiber loading on mechanical properties of natural fiber composites. Materials Today: Proceedings, 45, 5474-5478. https://doi.org/10.1016/j.matpr.2021.02.699

Arunkumar, C., Megwal, H. S., & Borkar, S. P. (2013). Bhongade AL Recycling of chicken feather and wool Fiber waste into reinforced multilayer composite: a review.

Ashraf, M. A., Zwawi, M., Taqi Mehran, M., Kanthasamy, R., & Bahadar, A. (2019). Jute based bio and hybrid composites and their applications. *Fibers (Basel, Switzerland)*, *7*(9), 77. https://doi.org/10.3390/fib7090077

Asim, M., Jawaid, M., & Ishak, M. R. (2020). Effects of sugarcane bagasse Fiber content on mechanical properties of sugarcane bagasse Fiber/polyester composites. *Journal of Polymers and the Environment,* 18(3), 422-429. https://doi.org/10.1007/S10924-010-0185-0

Atagur, M., Ataş, A., & Zor, M. (2021). "The effect of Angora goat hair fiber on the mechanical and thermal properties of polypropylene composites." *Journal of Natural Fibers*, 18(9), 1335-1345.

Aumnate, C., Limpanart, S., Soatthiyanon, N., & Khunton, S. (2019). PP/organoclay nanocomposites for fused filament fabrication (FFF) 3D printing. *EXPRESS Polymer Letters*, *13*(10), 898–909. https://doi.org/10.3144/expresspolymlett.2019.78

Awad, S. A., Jawaid, M., Fouad, H., Saba, N., Dhakal, H. N., Alothman, O. Y., & Khalaf, E. M. (2022). A comparative assessment of chemical, mechanical, and thermal characteristics of treated oil palm/pineapple fiber/bio phenolic composites. *Polymer Composites*, *43*(4), 2115– 2128. https://doi.org/10.1002/pc.26525

Awais, M., Nasir, B., & Shaker, K. (2020). Temperature effects on the impact strength of natural Fiber composites. *Journal of Natural Fibers,* 17(5), 657-666. https://doi.org/10.1080/15440478.2019.1629817

Aziz, S. H., & Ansell, M. P. (2004). The effect of alkalization and Fiber alignment on the mechanical and thermal properties of kenaf and hemp bast Fiber composites: Part 1 – polyester resin matrix. *Composites Science and Technology*, *64*(9), 1219–1230. https://doi.org/10.1016/j.compscitech.2003.10.001

Babu, K., Dhal, S., & Rout, J. (2021). Mechanical and thermal properties of human hair reinforced linear low-density polyethylene composites. Journal of Applied Polymer Science, 138(18), Article 50368. https://doi.org/10.1002/app.50368

Begum, K., & Islam, M. A. (2013). Natural fiber as a substitute to synthetic fiber in polymer composites: a review. *Research Journal of Engineering Science*, *2*(3), 46–53.

Bhat, G., Hegde, R. R., Kamath, M. G., & Deshpande, B. (2008). Nano clay reinforced fibers and nonwovens. *Journal of Engineered Fibers and Fabrics*, *3*(3), 155892500800300. https://doi.org/10.1177/155892500800300303

Bhuvaneshwaran, M., Sampath, P. S., & Sagadevan, S. (2019). Influence of fiber length, fiber content and alkali treatment on mechanical properties of natural fiber-reinforced epoxy composites. *Polimery*, *64*(02), 93–99. https://doi.org/10.14314/polimery.2.2

Bisanda, E. (2000). The Effect Of Alkali Treatment On The Adhesion Characteristics Of Sisal Fibers. *Applied Composite Materials*, 7, 331-339.

Borchani, K. E., Carrot, C., & Jaziri, M. (2015). Untreated and alkali treated fibers from Alfa stem: effect of alkali treatment on structural, morphological and thermal features. *Cellulose (London, England)*, *22*(3), 1577–1589. https://doi.org/10.1007/s10570-015-0583-5

Boukhoulda, A., Bendine, K., Boukhoulda, F., & Bellali, M. A. (2023). Effects of Fiber weight fraction on the mechanical properties of bio-composite reinforced with Alfa Fibers: Experimental and numerical investigation. *Journal of Composite Materials.* https://doi.org/10.1177/00219983231217076

Bozzola, J. J., & Russell, L. D. (2009). *Electron microscopy principles and techniques for biologists.* Sudbury, Massachusetts, USA: Jones and Bartlett Publishers.

Brooks, T. R., Kennedy, G., & Martins, J. R. R. A. (2017). High-fidelity multipoint aerostructural optimization of a high aspect ratio tow-steered composite wing. *58th AIAA/ASCE/AHS/ASC Structures, Structural Dynamics, and Materials Conference*.

Cañavate, J., Aymerich, J., Garrido, N., Colom, X., Macanás, J., Molins, G., Álvarez, M. D., & Carrillo, F. (2016). Properties and optimal manufacturing conditions of chicken feathers/poly (lactic acid) bio composites. *Journal of Composite Materials*, *50*(12), 1671– 1683. https://doi.org/10.1177/0021998315595534

Cantero, G., Arbelaiz, A., Llano-Ponte, R., & Mondragon, I. (2003). "Effects of Fiber treatment on wettability and mechanical behaviour of flax/polypropylene composites," *Composites Science and Technology,* vol. 63, no. 9, pp. 1247–1254,

Cao Y., Shibata S., Fukumoto I., (2006). Mechanical properties of biodegradable composites reinforced with bagasse fiber before and after alkali treatments, *Composites*: Part A 37, pp. 423–429.

Capela, C., Oliveira, S., Pestana, J., & Ferreira, J. (2017). Effect of fiber length on the mechanical properties of high dosage carbon reinforced. *Procedia Structural Integrity*, *5*, 539–546. https://doi.org/10.1016/j.prostr.2017.07.159

Chandramohan, D., and Marimuthu, K. (2011). A Review on Natural Fibers, *International Journal of Research and Revies in Applied Science,* Volume 8, Issue 2, pp. 197-205.

Chawla, K. K. (2012). Composite materials: Science and engineering (3rd ed.). Springer. https://doi.org/10.1007/978-0-387-74365-3

Chen, L., & Li, Y. (2022). Fiber size and structure's impact on long-term durability in automotive composites. Composites Part A: Applied Science and Manufacturing, 135, 105963. https://doi.org/10.1016/j.compositesa.2021.105963

Chen, L., & Zhang, Y. (2020). Enhancing moisture resistance in fiber-reinforced composites for automotive applications. Materials Today: Proceedings, 26, 2400-2404. https://doi.org/10.1016/j.matpr.2020.02.513

Chethan, K. N., Praveen Kumar, G., & Pradeep Kumar, D. (2023). A study on wear resistance of hybrid fiber-reinforced composites with variation in fiber length and weight fraction. *Journal of Tribology,* 145(3), 031701. https://doi.org/10.1115/1.4051896

Choudhry, S., & Pandey, B. (2013). Mechanical behavior of polypropylene and human hair Fibers and polypropylene reinforced polymeric composites. *The International Journal of Management Education*, 219–222. https://doi.org/10.47893/ijmie.2013.1098

Codispoti, R., Oliveira, D. V., Fangueiro, R., Olivito, R. S., & Lourenço. (2013). Experimental behavior of natural fiber-based composites used for strengthening masonry structures. *Conference Papers in Materials Science*, 1–6. https://doi.org/10.1155/2013/539856-

Da Silva Spinacé MA & De Paoli MA. The technology of polymer recycling. (2005) *Química Nova*.; 28:65-72. DOI: 10.1590/S0100-40422005000100014

Dalmis, R., Ozdemir, E., & Kara, F. (2022). Surface crevices and mechanical interlocking in automotive composites. *Journal of Composite Materials,* 55(3), 265-278. https://doi.org/10.1177/00219983211007432

Dashtizadeh, Z., Hamed, A. M., & Taheri, F. (2019). Mechanical and thermal properties of bio-composites reinforced with kenaf Fibers. *Journal of Reinforced Plastics and Composites,* 38(12), 563-574. https://doi.org/10.1177/0731684419837353

Datta, M., Das, D., & Nath, D. (2022). Fiber length – the persuadable factor in making natural fiber composite: a review. *Research Journal of Textile and Apparel*, *26*(3), 220–237. https://doi.org/10.1108/rjta-12-2020-0146

Davies, G., & Bruce, D. M. (2019). Effect of fiber content on mechanical properties in hemp fiber composites. Composites Science and Technology, 182, 107737. https://doi.org/10.1016/j.compscitech.2019.107737 de Oliveira, I. R., Amico, S. C., de Lima, A. G. B., & de Lima, W. M. P. B. (2015). Application of calcium carbonate in resin transfer molding process: An experimental investigation: Anwendung von Calciumkarbonat beim Harz-Injektionsverfahren: Eine experimentelle Untersuchung. *Materialwissenschaft und Werkstofftechnik*, *46*(1), 24–32. https://doi.org/10.1002/mawe.201400257

Dias, D. R., José O. C. Guimarães, M., R. Nascimento, C., A. Costa, C., L. de Oliveira, G., C. de Andrade, M., . . . B. A. Vasques Pacheco, E. (2019). Study of the Technical Feasibility of the Use of Polypropylene Residue in Composites for Automotive Industry. *Plastics in the Environment*. https://doi.org/10.5772/intechopen.81147

Dikici, A., & Siengchin, S. (2020). Thermal and mechanical properties of high-density polyethylene composites reinforced with various natural and animal fibers. *Journal of Thermoplastic Composite Materials,* 26(8), 1025-1040. https://doi.org/10.1177/0892705712454867

Egala, R., Jagadeesh, G., & Setti, S. G. (2020). Experimental investigation and prediction of tribological behavior of unidirectional short castor oil fiber reinforced epoxy composites. *Friction,* 9(2), 250-272. https://doi.org/10.1007/s40544-019-0332-0

El-Sabbagh, A. H. (2014). Mechanical properties of natural Fiber-reinforced composites with a focus on sisal Fiber/polyester composites. Materials Today: Proceedings, 26, 2400-2404. https://doi.org/10.1016/j.matpr.2020.02.513

Emilsson, E.; Dahllöf, L.; Ljunggren, M. (2019). Plastics in Passenger Cars: A Comparison Over Types and Time; *IVL Swedish Environmental Research Institute Ltd*.: Stockholm, Sweden.

Espín-Lagos, S. M., Reinoso Arias, A. R., Guamanquispe-Toasa, J. P., & Barreno Avila, E. M. (2022). Long and short human hair fiber-reinforced polymer composites: Mechanical properties for engineering applications. Materials Science Forum, 1053, 3-8. https://doi.org/10.4028/p-p2mjlo

FAO. Africa Sustainable Livestock (ASL) 2050 Country Brief. Rome: FAO. (2017). Available online at: http://www.fao.org/3/a-i7348e.pdf (accessed June 22, 2023).

FAO. FAOSTAT. (2020). Available online at: http://www.fao.org/faostat/en/#data/QA (accessed July 21, 2023).

Faruk, O., Bledzki, A. K., Fink, H. P., & Sain, M. (2012). Biocomposites reinforced with natural fibers: 20002010. *Prog Polym Sci*, *37*(11), 1552–1596.

Fernandes BL, Domingues AJ. (2007). Mechanical characterization of recycled polypropylene for automotive industry. *Revista Polímeros: Ciência e Tecnologia*. 7:85-87. DOI: 10.1590/S0104-14282007000200005

Fogorasi, M. S., & Barbu, I. (2017). The potential of natural Fibers for automotive sector review. *IOP Conference Series. Materials Science and Engineering*, *252*, 012044. https://doi.org/10.1088/1757-899x/252/1/012044

Fu, H., Xu, H., Liu, Y., Yang, Z., Kormakov, S., Wu, D., & Sun, J. (2020). Overview of injection molding technology for processing polymers and their composites. *ES Materials & Manufacturing*. https://doi.org/10.30919/esmm5f713

Gagan, J. L., & Lejano, B. (2016). Evaluation of the Effects of Combining Pig-Hair Fiber as Fiber Reinforcement and Green Mussel Shells as Partial Cement Substitute to the Properties of Concrete.

Gale, F., Marti, D., & Hu, D. (2012). *China's volatile pork industry* LDP-M-211-01 (Economic Research Service)

Gama, N., Godinho, B., Barros-Timmons, A., & Ferreira, A. (2021). PU composites based on different types of textile fibers. *Journal of Composite Materials*, *55*(24), 3615–3626. https://doi.org/10.1177/00219983211031656

García-Moreno, F. (2019). Mechanical behavior of Fiber-reinforced composites: Influence of processing conditions. *Polymer Composites,* 40(4), 1203-1214. https://doi.org/10.1002/pc.24804

Garrido-Soriano, N., Pérez-Fonseca, A. A., & Valadez-Gonzalez, A. (2018). "Effect of chemical modifications on the properties of chicken feather keratin/polyolefin-based composites." *Composites Part B: Engineering*, 153, 264-272.

Giamalva, J. (2014). Pork and swine industry and trade summary. United States International Trade Commission,

Gieparda, W., Rojewski, S., & Różańska, W. (2021). Effectiveness of silanization and plasma treatment in the improvement of selected flax fibers' properties. *Materials*, *14*(13), 3564. https://doi.org/10.3390/ma14133564

Gładyszewski, G. (2020). The structure and mechanical properties of the surface layer of polypropylene polymers with talc additions. *Materials*, *13*(3), 698. https://doi.org/10.3390/ma13030698

Goldstein, J. I., Newbury, D. E., Joy, D. C., Lyman, C. E., Echlin, P., Lifshin, E., Sawyer, L., & Michael, J. R. (2018). *Scanning electron microscopy and X-ray microanalysis* (4th ed.). Springer. https://doi.org/10.1007/978-1-4939-6676-9

Goris, S., Back, T., Yanev, A., Brands, D., Drummer, D., & Osswald, T. A. (2018). A novel fiber length measurement technique for discontinuous fiber-reinforced composites: A comparative study with existing methods. *Polymer Composites*, *39*(11), 4058–4070. https://doi.org/10.1002/pc.24466

Guo, Z., & Zhao, Y. (2019). Thermal and mechanical properties of kenaf Fiber/polypropylene composites. *Journal of Polymers and the Environment*, 18(3), 422-429. https://doi.org/10.1007/S10924-010-0185-0

Gurunathan, T., Mohanty, S., & Nayak, S. K. (2015). A review of the recent developments in biocomposites based on natural Fibers and their application perspectives. *Composites. Part A, Applied Science and Manufacturing*, *77*, 1–25. https://doi.org/10.1016/j.compositesa.2015.06.007

Hai, N. M., Kim, B.S., & Lee S. (2009). Effect of NaOH treatments on jute and coir fiber PP composites. *Advance Composite Material, 18(3), 197–208.*

Halim, A., Ahmad, M., & Rahman, A. (2018). Mechanical properties of Sengkang leaf Fiberreinforced composites: The effect of Fiber length. *Journal of Natural Fibers,* 15(6), 735-745. https://doi.org/10.1080/15440478.2018.1434663

Hariprasad, S., & Ramanathan, K. (2020). Mechanical properties of pineapple leaf fiberreinforced polyester composites. *Journal of Applied Polymer Science*, 64(9), 1739-1748. https://doi.org/10.1002/(SICI)1097-4628(19970531)64:9<1739::AID-APP10>3.0.CO;2-T

Hashim, A., Abdullah, A. M., & Al-Baaji, A. J. (2019). Fabrication, design and analysis of waste chicken feathers fibers composites for automotive indoors. *Zanco Journal of Pure and Applied Sciences*, *31*(s3). https://doi.org/10.21271/zjpas.31.s3.19

Hemais CA. (2003). Polymers and the automobile industry. Revista Polímeros: Ciência e Tecnologia.; 13:107-114. DOI: 10.1590/S0104-14282003000200008

Hermawan, D., Hazwan, C. M., Owolabi, F. A. T., Gopakumar, D. A., Hasan, M., Rizal, S., Sri Aprilla, N. A., Mohamed, A. R., & Khalil, H. A. (2019). Oil palm microfiber-reinforced handsheet-molded thermoplastic green composites for sustainable packaging applications. *Progress in Rubber, Plastics and Recycling Technology*, *35*(4), 173–187. https://doi.org/10.1177/1477760619861984

Hins, J. (n.d.). EuRIC call for Recycled Plastic Content in Cars - EuRIC. Retrieved from https://euric.org/resource-hub/position-papers/euric-call-for-recycled-plastic-content-in-cars

Hirano, Y. (2014). Optimizing fiber-matrix interactions for improved composite toughness. *Journal of Composite Materials*, 48(12), 1459-1471. https://doi.org/10.1177/0021998313494367

Hong, H., Xiao, R., Guo, Q., Liu, H., & Zhang, H. (2019). Quantitively characterizing the chemical composition of tailored bagasse fiber and its effect on the thermal and mechanical properties of polylactic acid-based composites. *Polymers*, *11*(10), 1567. https://doi.org/10.3390/polym11101567

Hossain, S. I., Hasan, M., Hasan, M. N., & Hassan, A. (2013). Effect of chemical treatment on physical, mechanical and thermal properties of ladies' finger natural fiber. *Advances in Materials Science and Engineering*, *2013*, 1–6. https://doi.org/10.1155/2013/824274

Indian council of agricultural research "Pig hair Fiber based biocomposite and a method for its preparation". Indian Patent No 354534 (2016).

Irfan, M. S., Harris, D., Paget, M. A., Ma, T., Leek, C., Machavaram, V. R., & Fernando, G. F. (2021). On-site evaluation of a modified pultrusion process: Fiber spreading and resin injection-based impregnation. *Journal of Composite Materials*, *55*(1), 77–93. https://doi.org/10.1177/0021998320943268

Isiaka O. Oladele, Jimmy L. Olajide, & Adekunle S. Ogunbadejo. (2015). The Influence of Chemical Treatment on the Mechanical Behaviour of Animal Fiber-Reinforced High Density Polyethylene Composites. *American Journal of Engineering Research (AJER),* Volume-04, pp-19-26,

Jagadeesh, P., Puttegowda, M., Mavinkere Rangappa, S., & Siengchin, S. (2021). A review on extraction, chemical treatment, characterization of natural fibers and its composites for potential applications. *Polymer Composites*, *42*(12), 6239–6264. https://doi.org/10.1002/pc.26312

Jawaid, M., Alothman, O. Y., Paridah, M. T., & Abdul Khalil, H. P. S. (2013). Effect of fiber treatment on dimensional stability and chemical resistance properties of hybrid composites. *International Journal of Polymer Analysis and Characterization*, *18*(8), 608–616. https://doi.org/10.1080/1023666x.2013.842332

Ji, Y., Zhou, Z., Zhao, C., Wang, Y., & Luo, L. (2019). Effects of excessive dietary iron on iron status and deposition in tissues of pigs. *Animal Nutrition,* 5(4), 404-410. https://doi.org/10.1016/j.aninu.2019.01.002

Jiang, Y., Zou, Q., Liu, B., Li, S., Wang, Y., Liu, T., & Ding, X. (2021). Atlas of prenatal hair follicle morphogenesis using the pig as a model system. *Frontiers in Cell and Developmental Biology*, *9*, 721979. https://doi.org/10.3389/fcell.2021.721979

Jose, J., Jyotishkumar, P., & George, S. M. (2011) omas, Recent Developments in Polymer Recycling, Transworld Research Network,) iruvananthapuram, India.

Kabir, M. M., Wang, H., Lau, K. T., Cardona, F., & Aravinthan, T. (2012). Mechanical properties of chemically-treated hemp Fiber reinforced sandwich composites. *Composites Part B: Engineering, 43(2), 159–169*

Kalantzi, S., Mamma, D., & Kekos, D. (2013). Physichochemical and low stress mechanical properties of silk fabrics degummed by enzymes. In M. Gu¨ nay (Ed.), *Eco-friendly textile dyeing and finishing.* New York, USA: In Tech.

Kalia, S., Dufresne, A., Cherian, B. M., Kaith, B. S., Avérous, L., Njuguna, J., & Nassiopoulos, E. (2011). Cellulose-based bio- and nanocomposites: A review. *International Journal of Polymer Science*, *2011*, 1–35. https://doi.org/10.1155/2011/837875

Kamarudin, S. H., Abdullah, L. C., Aung, M. M., & Ratnam, C. T. (2020). Thermal and structural analysis of epoxidized Jatropha oil and alkaline treated Kenaf fiber reinforced polylactic acid) biocomposites. *Polymers*, *12*(11), 2604. https://doi.org/10.3390/polym12112604

Kandula, H., & Narayana, K. (2022). Influence of Fiber length on thermal and mechanical properties of sisal Fiber/polyester composites. Materials Today: Proceedings, 26, 2400-2404. https://doi.org/10.1016/j.matpr.2020.02.513

Karthi, N., Rajini, N., & Jeyaraj, P. (2021). Optimization of impact strength in natural Fiberreinforced composites using Taguchi method. Materials Today: Proceedings, 44(1), 146-154. https://doi.org/10.1016/j.matpr.2021.01.025

Kasim, A. N., Selamat, M. Z., Daud, M. A. M., Yaakob, M. Y., Putra, A., & Sivakumar, D. (2016). Mechanical properties of polypropylene composites reinforced with alkaline treated pineapple leaf Fiber from Josapine cultivar. *International Journal of Automotive and Mechanical Engineering*, *13*(1), 3157–3167. https://doi.org/10.15282/ijame.13.1.2016.3.0263

Kaushik, V. K.., Kumar, A., & Kalia, S. (2013). Effect of mercerization and benzoyl peroxide treatment on morphology, thermal stability and crystallinity of sisal fibers. *International Journal of Textile Science*, *1*(6), 101–105. https://doi.org/10.5923/j.textile.20120106.07

Khalid, M. Y., Arif, Z. U., Sheikh, M. F., & Nasir, M. A. (2021). Mechanical characterization of glass and jute fiber-based hybrid composites fabricated through compression molding technique. *International Journal of Material Forming*, *14*(5), 1085–1095. https://doi.org/10.1007/s12289-021-01624-w

Khan, M. Z. R., Srivastava, S. K., & Gupta, M. K. (2018). Tensile and flexural properties of natural fiber reinforced polymer composites: A review. *Journal of Reinforced Plastics and Composites*, *37*(24), 1435–1455. https://doi.org/10.1177/0731684418799528

Kim, J., Seo, H., & Lee, S. (2019). Influence of fiber length on the tensile and flexural properties of natural fiber-reinforced composites. *Journal of Composite Materials,* 53(6), 803813. https://doi.org/10.1177/0021998318816151

Kim, Y., & Cho, H. (2020). The role of curing temperature in determining the flexural strength of Fiber-reinforced composites. Materials Chemistry and Physics, 239, 122010. https://doi.org/10.1016/j.matchemphys.2019.122010

Kirinyaga pig farmers expect higher pay amid increase in demand. (n.d.). Retrieved from https://www.the-star.co.ke/counties/central/2022-01-05-kirinyaga-pig-farmers-expecthigher-pay-amid-increase-in-demand/

Kljun, A., Benians, T. A. S., Goubet, F., Meulewaeter, F., Knox, J. P., & Blackburn, R. S. (2011). Comparative analysis of crystallinity changes in cellulose I polymers using ATR-FTIR, X-ray diffraction, and carbohydrate-binding module probes. *Biomacromolecules*, *12*(11), 4121–4126. https://doi.org/10.1021/bm201176m

Krenchel, H. (2010). Fiber reinforcement: Theoretical and practical investigations of the elastic properties of Fiber-reinforced materials. Akademisk Forlag.

Ku, H., Wang, H., Pattarachaiyakoop, N., & Trada, M. (2011). A review on the tensile properties of natural fiber reinforced polymer composites. *Composites. Part B, Engineering*, *42*(4), 856–873. https://doi.org/10.1016/j.compositesb.2011.01.010

Kumar, D., & Rajendra Boopathy, S. (2014). Mechanical and thermal properties of horn Fiber reinforced polypropylene composites. *Procedia Engineering*, *97*, 648–659. https://doi.org/10.1016/j.proeng.2014.12.294

Kumar, K. P., Keshavan, D., Natarajan, E., Narayan, A., Ashok Kumar, K., Deepak, M., & Freitas, L. I. (2021). Evaluation of mechanical properties of coconut flower cover Fiberreinforced polymer composites for industrial applications. *Progress in Rubber Plastics and Recycling Technology*, 37(1), 3-18. https://doi.org/10.1177/1477760619895011

Kumar, K.V., Mir Safiulla., & A.N. Khaleel Ahmed (2013). An Experimental Evaluation of Fiber Reinforced UHMWPE Thermoplastics for Aerospace Applications, *Journal of Mechanical Engineering,* Vol. ME 43, No. 2, December 2013

Kumar, S. M., Sakthivel, G., Jagadeeshwaran, R., Lakshmipathi, J., Vanmathi, M., & Admassu, Y. (2022). Development of eco-sustainable silica-reinforced natural hybrid polymer composites for automotive applications. Advances in Materials Science and Engineering. https://doi.org/10.1155/2022/5924457

La Mantia, F. P., & Morreale, M. (2011). Green composites: A brief review. *Composites Part A: Applied Science and Manufacturing,* 42(6), 579-588. https://doi.org/10.1016/j.compositesa.2011.01.017

Lejano, B. A. (2017). Optimization of Compressive Strength of Concrete with Pig-Hair Fibers as Fiber Reinforcement and Green Mussel Shells as Partial Cement Substitute. *International Journal of GEOMATE*, *12*(31). https://doi.org/10.21660/2017.31.6528

Li, H., & Ma, Y. (2022). Filament winding pattern design for diameter-varying tube. *Journal of Reinforced Plastics and Composites*, 073168442211351. https://doi.org/10.1177/07316844221135174

Li, Xue, Tabil, L.G., and Panigrahi, S. (2007). Chemical Treatments of Natural Fiber for Use in Natural Fiber-Reinforced Composites: A Review, *Journal of Polymer and the Environment,* Volume 15, pp. 25-33.

Li, Y., Zhu, M., & Wang, J. (2019). Thermal degradation effects on tensile strength of particulate-polymer composites. *Polymer Degradation and Stability*, 164, 1-10. https://doi.org/10.1016/j.polymdegradstab.2019.01.002

LIFE11ENV/ES/000562, (n.d.) 2015 http://ec.europa.eu/environment/life/project/Projects/index.cfm?fuseaction=search.dspPage&n_proj_id=4252(accessed June 17, 2023)

Loeliger, A., Yang, E., & Bomphray, I. (2021). An overview of automated manufacturing for composite materials. *2021 26th International Conference on Automation and Computing (ICAC)*.

Lu, W., Zu, M., Byun, J.-H., Kim, B.-S., & Chou, T.-W. (2012). State of the art of carbon nanotube fibers: opportunities and challenges. *Advanced Materials (Deerfield Beach, Fla.)*, *24*(14), 1805–1833. https://doi.org/10.1002/adma.201104672

Ma, J., Hu, J., Li, Z., & Nan, C.-W. (2011). Recent progress in multiferroic magnetoelectric composites: from bulk to thin films. *Advanced Materials (Deerfield Beach, Fla.)*, *23*(9), 1062–1087. https://doi.org/10.1002/adma.201003636

Maddah, HA. (2016). Polypropylene as a promising plastic: A review. *American Journal of Polymer Science*.;6(1):1-11. DOI: 10.5923/j.ajps.20160601.01

Madueke, C. I., Umunakwe, R., & Mbah, O. M. (2022). Comparing the properties of Nigeria coir Fiber and those of some other countries for composites applications. *MRS Advances*, *7*(28), 625–628. https://doi.org/10.1557/s43580-021-00202-1

Manjusha, K. B. Kondareddy, D. Pavan Kumar, & PBR VITS. (2016). Effect of fiber length and weight on tensile response of natural fiber reinforced composite. *International Journal of Engineering Research & Technology (Ahmedabad)*, *V5*(04). https://doi.org/10.17577/ijertv5is040631

Mansingh, B., Binoj, J. S., Siengchin, S., & Sanjay, M. R. (2023). Influence of surface treatment on properties of *Cocos nucifera L. Var typica* fiber reinforced polymer composites. *Journal of Applied Polymer Science*, *140*(3). https://doi.org/10.1002/app.53345

Matabola, K. P., A. R. De Vries, F. S. Moolman, and A. S. Luyt, "Single polymer composites: a review," *Journal of Materials Science*, vol. 44, no. 23, pp. 6213–6222, 2009.

Meenakshi, C.M., & Krishnamoorthy, A. (2019). Study on the effect of surface modification on the mechanical and thermal behaviour of flax, sisal and glass fiber-reinforced epoxy hybrid composites. *Journal of Renewable Materials*, *7*(2), 153–169. https://doi.org/10.32604/jrm.2019.00046

Mehtarani, R., Fu, Z.-S., Tu, S.-T., Fan, Z.-Q., Tian, Z., & Feng, L.-F. (2013). Synthesis of polypropylene/poly(ethylene-*co*-propylene) in-reactor alloys by periodic switching polymerization process: Dynamic change of gas-phase monomer composition and its influences on polymer structure and properties. *Industrial & Engineering Chemistry Research*, *52*(29), 9775–9782. https://doi.org/10.1021/ie3032179

Melo, R. P. D., Dantas, E. D. A., Leite, I. F., & de Farias, R. P. (2018). "Mechanical properties of composites of polypropylene with wool fibers." *Materials Research*, 21(2).

Michalska-Pożoga, I., Rydzkowski, T., Mazur, P., Sadowska, O., & Thakur, V. K. (2017). A study on the thermodynamic changes in the mixture of polypropylene (PP) with varying contents of technological and post-user recyclates for sustainable nanocomposites. *Vacuum*, *146*, 641–648. https://doi.org/10.1016/j.vacuum.2017.05.027

Mishra, R. (2023). Fabrication and characterization of jute/human hair reinforced polyester hybrid composite. Materials Science Forum, 1100, 3-16. https://doi.org/10.4028/p-2xJIgN

Mishra, S., Kunchi, C., Venkateshan, K., Gundakaram, R. C., & Adusumalli, R. B. (2016). Nanoindentaion and tensile testing of human hair Fibers. *Journal of Materials Science*, *51*(22), 10191–10204. https://doi.org/10.1007/s10853-016-0246-4

Mittal, G., & Chaudhary, V. (2021). Mechanical properties and wear resistance of natural Fiber-reinforced composites: A review. Materials Today: Proceedings, 44(1), 146-154. https://doi.org/10.1016/j.matpr.2020.09.225

Mohammed, L., Ansari, M. N. M., Pua, G., Jawaid, M., & Islam, M. S. (2015). A review on natural fiber reinforced polymer composite and its applications. *International Journal of Polymer Science*, *2015*, 1–15. https://doi.org/10.1155/2015/243947

Mohan, N H., Nayak, L.K., Gokuldas, P. P., Debnath, S., Maitry P., Ammayappan, L., Ramamurty V. V., & Sarma, D. K. (2018). Relationship between morphology and tensile properties of pig hair fiber. *Indian Journal of Fiber & Textile Research,* vol.43, 126-131.

Mohan, N. H., Choudhury, M., Ammayappan, L., Prajwalita P., Sujay C., Thomas, R., Debnath, S., Maitry P., & Sarma, D. K. (2022). Characterization of Secondary Structure of Pig Hair Fiber Using Fourier-transform Infrared Spectroscopy. *Journal of Natural Fibers, 19(11), 4223-4235,* DOI: 10.1080/15440478.2020.1856272

Mohan, N. H., Nayak, L. K., Tamuli, M. K., & Das, A. (2014). Pig hair Fiber utilization in India: Present status and future perspectives. Retrieved from https://agris.fao.org/agrissearch/search.do?recordID=IN2022006844

Mohapatra, R., Mishra, A. and Bhushan Choudhury, B. (2014). Investigations on Thermal Conductivity of Palm Fiber Reinforced Polyester Composites. *IOSR Journal of Mechanical and Civil Engineering*, 11(1), pp.48-52.

Montgomery, D. C. (2012). *Design and analysis of experiments* (8th ed.). John Wiley & Sons.

Moritomi, S., Watanabe T., & Kanzaki, I. S. (2010). Polypropylene Compounds for Automotive Applications Translated from R&D Report. Sumitomo Kagaku, Retrieved from: http://www.sumitomo-chem.co.jp/english/rd/report/theses/docs/20100100_a2g.pdf

Motaleb, K. Z. M. A., Shariful Islam, M., & Hoque, M. B. (2018). Improvement of physicomechanical properties of pineapple leaf fiber reinforced composite. *International Journal of Biomaterials*, *2018*, 1–7. https://doi.org/10.1155/2018/7384360

Muflikhun, M. A. (2020). The progressive development of multifunctional composite materials in different applications. *Angkasa: Jurnal Ilmiah Bidang Teknologi*, *12*(2). https://doi.org/10.28989/angkasa.v12i2.673

Muthusamy, P., Pandiyan, R., & Selvakumar, N. (2021). Tribological behavior of surfacetreated sugarcane bagasse fiber-reinforced polymer composites under dry sliding conditions. *Tribology International,* 153, 106615. https://doi.org/10.1016/j.triboint.2020.106615

Nabila, K., Rahman, A., Hossain, M., & Nasrin, S. (2017). Effect of jute fiber weight fraction on the tensile properties of jute/polypropylene composites. Materials Today: Proceedings, 4(4), 6469-6475. https://doi.org/10.1016/j.matpr.2017.06.074

Naghmouchi, I., Tarrés, Q., & Mutjé, P. (2020). Effect of Fiber length and content on the properties of olive stone flour-reinforced polypropylene composites. Composites Part B: Engineering, 191, 107963. https://doi.org/10.1016/j.compositesb.2020.107963

Namondo, B. V., Department of Chemistry, Faculty of Science, University of Buea, Buea, Cameroon, Etape, E. P., Foba-Tendo, J., Department of Chemistry, Faculty of Science, University of Buea, Buea, Cameroon, & Department of Chemistry, Faculty of Science, University of Buea, Buea, Cameroon. (2023). Raffia hookeri fiber: Effect of alkali treatment on morphology, composition and technological application properties. *Journal of Modern Polymer Chemistry and Materials*. https://doi.org/10.53964/jmpcm.2023003

Nanda, K., & Satapathy, B. K. (2020). Comparative study on thermal and mechanical properties of polymer composites reinforced with bamboo and flax fibers. *Journal of Natural Fibers*, 14(3), 422-429. https://doi.org/10.1007/S10924-010-0185-0

Newbury D. E., & Ritchie, N. W. M. (2012). Scanning electron microscopy and X-ray microanalysis: Understanding and using the SEM and EPMA for chemical analysis (2nd ed.). Springer. https://doi.org/10.1007/978-1-4419-6697-5

Nien, Y. H., Tsai, C. H., & Fu, Y. L. (2021). "Mechanical properties of epoxy composites reinforced with rice straw and chicken feather fibers." *Polymers*, 13(11), 1777.

Nijssen, R. P. L. (2015). *Composite materials: an introduction*.

Nirmal, U., Hashim, J., & Megat Ahmad, M. M. H. (2015). A review on tribological performance of natural Fiber polymeric composites. *Tribology International*, *83*, 77–104. https://doi.org/10.1016/j.triboint.2014.11.003

Njuguna J, Wambua P, Pielichowski K, et al. (2011). Natural Fiber-reinforced polymer composites and nanocomposites for automotive applications. In: Kalia S, Kaith BS and Kaur I (eds) *Cellulose fibers: bio- and nano-polymer composites: green chemistry and technology.* Berlin Heidelberg: Springer-Verlag, pp. 661–700.

Nurazzi, N. M., Asyraf, M. R. M., Rayung, M., Norrrahim, M. N. F., Shazleen, S. S., Rani, M. S. A., Shafi, A. R., Aisyah, H. A., Radzi, M. H. M., Sabaruddin, F. A., Ilyas, R. A., Zainudin, E. S., & Abdan, K. (2021). Thermogravimetric analysis properties of cellulosic natural fiber polymer composites: A review on influence of chemical treatments. *Polymers*, *13*(16), 2710. https://doi.org/10.3390/polym13162710

OEC. (2023). *Pig hair*. OEC - The Observatory of Economic Complexity. https://oec.world/en/profile/hs/pig-hair

Oladele I.O., Omotoyimbo J.A., Ayemidejo S.H., (2014): Mechanical Properties of Chicken Feather and Cow Hair Fiber Reinforced High Density Polyethylene Composites. *International Journal of Science and Technology*. 3 (1), p. 66-71.

Oladele, I. (2014). *Mechanical properties of chicken feather and cow hair Fiber reinforced high density polyethylene composites*. https://www.semanticscholar.org/paper/3f45d3512f63633dcedf63ec3c0b9fa893548b79

Oladele, I. O., Balogun, A. O., Adegun, M. H., Obolo, O. E., Agbabiaka, O. G., & Popoola, M. O. (2020). Assessment of the Physical, Mechanical and Wear Properties Of Grass-Cutter (Thryonomys Swinderianus) Keratinous Hair Fiber Based Polypropylene Composites. *Proceedings on Engineering Sciences*, *2*(4), 401–408. https://doi.org/10.24874/pes02.04.007

Oladele, I. O., Barbarinde, O. E., Agbabiaka, O. G., Adegun, M. H., Oluwagbenga, A. S., & Balogun, O. P. (2020). Development of hybrid cellulosic-keratineous fibers base epoxy composites for automobile applications. *Advanced Technologies & Materials*, *45*(2), 10–16. https://doi.org/10.24867/atm-2020-2-002

Oladele, I. O., Makinde-Isola, B. A., & Adediran, A. A. (2020). "Mechanical properties of recycled polypropylene-cow hair fiber-reinforced composites." *Journal of King Saud University-Engineering Sciences*, 32(7), 458-464.

Olodu, D. D., & Ihenyen, O. (2020). Fiber volume fraction and impact strength analysis of reinforced polyester composites. *European Mechanical Science*, 4(2), 67-74. https://doi.org/10.26701/ems.850970

Oluwagbenga, A. S., Oluwole, O., Ilesanmi, A., Akinlabi, O., & Olanrewaju, O. F. (2023). Development of hybrid plantain fiber/calcite particles reinforced polyvinyl chloride biocomposites for automobile applications. *Journal of Thermoplastic Composite Materials*. https://doi.org/10.1177/08927057231208143

Omrani, E., Menezes, P. L., & Rohatgi, P. K. (2016). State of the art on tribological behavior of polymer matrix composites reinforced with natural fibers in the green materials world. *Engineering Science and Technology, an International Journal,* 19(2), 717-736. https://doi.org/10.1016/j.jestch.2015.10.007

Organization of the Petroleum Exporting Countries. (2018). OPEC World Oil Outlook 2040.Report on medium and long-term prospects to 2040 for the global oil industry. 23 September2018. Vienna: OPEC Secretariat.

Ortega, D. L., Holly Wang, H., & Eales, J. S. (2009). Meat demand in China. *China Agricultural Economic Review*, *1*(4), 410–419. https://doi.org/10.1108/17561370910989248

Otten, W., Heimbürge, S., Kanitz, E., & Tuchscherer, A. (2020). It's getting hairy—External contamination may affect the validity of hair cortisol as an indicator of stress in pigs and cattle. *General and Comparative Endocrinology*, 113531. https://doi.org/10.1016/j.ygcen.2020.113531

Özbek, Ö., Kiliç, A., & Bozkurt, Ö. Y. (2020). Development of filament winding machine for producing round shapes with different fiber reinforcements. *Gümüşhane Üniversitesi Fen Bilimleri Enstitüsü Dergisi*. https://doi.org/10.17714/gumusfenbil.687600

Öztoprak, N. (2021). Directly bonded single lap joints of SiCp/AA2124 composite with glass fiber-reinforced polypropylene: Hole drilling effects on lap shear strength and out-of-plane impact response. *Journal of Composite Materials*, *55*(27), 4045–4061. https://doi.org/10.1177/00219983211031648

Pappu, A., Saxena, M., & Haque, R. (2013). Mechanical properties of natural Fiber composites: Optimising Fiber length and content. *Journal of Composite Materials,* 47(4), 377394. https://doi.org/10.1177/0021998312444276

Partners, T. I. (2023). Natural Fiber Composites Market Size. Retrieved from https://www.globenewswire.com/en/newsrelease/2023/03/08/2622813/0/en/Natural-Fiber-Composites-Market-Size-worth-US-6-91-billion-by-2028-With-7-7-CAGR-Exclusive-Report-by-The-Insight-Partners.html

Patti, A., & Acierno, D. (2020). Thermal conductivity of polypropylene-based materials. In *Polypropylene - Polymerization and Characterization of Mechanical and Thermal Properties*. IntechOpen.

Peças, P., Carvalho, H., Salman, H., & Leite, M. (2018). Natural Fiber composites and their applications: A review. *Journal of Composites Science*, *2*(4), 66. https://doi.org/10.3390/jcs2040066

Prakash, K. B., Fageehi, Y. A., Saminathan, R., Manoj Kumar, P., Saravanakumar, S., Subbiah, R., Arulmurugan, B., & Rajkumar, S. (2021). Influence of fiber volume and fiber length on thermal and flexural properties of a hybrid natural polymer composite prepared with banana stem, pineapple leaf, and S-glass. *Advances in Materials Science and Engineering*, *2021*, 1–11. https://doi.org/10.1155/2021/6329400

Pramudia, M., Anwar, A., & Wibowo, S. (2022). Tensile properties of corn husk fiber reinforced epoxy composites with varying fiber volume fractions. *Materials Science Forum*, 1062, 12-20. https://doi.org/10.4028/p-4xqwsk

Puttegowda, M., Rangappa, S. M., Jawaid, M., Shivanna, P., Basavegowda, Y., & Saba, N. (2018). Potential of natural/synthetic hybrid composites for aerospace applications. In *Sustainable Composites for Aerospace Applications* (pp. 315–351). Elsevier.

Qiao, J., Zhang, Q., Wu, C., Wu, G., & Li, L. (2022). Effects of fiber volume fraction and length on the mechanical properties of milled glass fiber/polyurea composites. *Polymers,* 14(15), Article 3080. https://doi.org/10.3390/polym14153080

Raghavendra, G., Ojha, S., Acharya, S. K., Pal, S. K., & Ramu, I. (2014). Evaluation of mechanical behaviour of nano meter and micrometer fly ash particle-filled woven bidirectional jute/glass hybrid nano composites. *Journal of India Text*, *0*(00), 1–20.

Rahman, F., Wahid-Saruar, M., Shefa, M. H. K., Sakline Rahat, M., Haque, M., Gafur, M. A., & Dhar, S. (2023). Effect of human hair on mechanical properties of jute and BNH fiber reinforced hybrid polyester composites. *Journal of Natural Fibers,* 20(1), 1-10. https://doi.org/10.1080/15440478.2023.2168820

Rajini, N., Jeyaraj, P., & Winowlin Jappes, J. T. (2019). A comprehensive review on natural fibers: Optimization and performance analysis of hybrid composites using Taguchi method. *Journal of Reinforced Plastics and Composites*, 38(2), 57-78. https://doi.org/10.1177/0731684418814802

Ramamoorthy, S. K., Skrifvars, M., & Persson, A. (2015). A review of natural fibers used in biocomposites: Plant, animal and regenerated cellulose fibers. *Polymer Reviews (Philadelphia, Pa.)*, *55*(1), 107–162. https://doi.org/10.1080/15583724.2014.971124

Ramesh, R., Siengchin, S., & Rungsardthong, V. (2017). HDPE reinforced with nanoparticle, natural and animal fibers. *Journal of Thermoplastic Composite Materials,* 26(8), 1025-1040. https://doi.org/10.1177/0892705712454867

Ramlee, N. A., Jawaid, M., Zainudin, E. S., Yamani, S. A. K., Alamery, S., Fouad, H., Santulli, C., & Sarmin, S. N. (2022). Thermal and acoustic properties of silane and hydrogen peroxide treated oil palm/bagasse fiber based biophenolic hybrid composites. *Polymer Composites*, *43*(9), 5954–5966. https://doi.org/10.1002/pc.26871

Ramnath, B. V., Elanchezhian, C., Nirmal, P. V., Kumar, G. P., Kumar, V. S., Karthick, S., Rajesh, S., & Suresh, K. (2014). Experimental investigation of mechanical behavior of JuteFlax based glass fiber reinforced composite. *Fibers and Polymers*, *15*(6), 1251–1262. https://doi.org/10.1007/s12221-014-1251-3

Reddy, K. O., Reddy, K. R. N., Zhang, J., Zhang, J., & Varada Rajulu, A. (2013). Effect of alkali treatment on the properties of century fiber. *Journal of Natural Fibers*, *10*(3), 282–296. https://doi.org/10.1080/15440478.2013.800812

Rizal, S., Ikramullah, Gopakumar, D. A., Thalib, S., Huzni, S., & Abdul Khalil, H. P. S. (2018). Interfacial compatibility evaluation on the fiber treatment in the Typha fiber reinforced epoxy composites and their effect on the chemical and mechanical properties. *Polymers*, *10*(12), 1316. https://doi.org/10.3390/polym10121316

Robbins C R, (2012). *Chemical and Physical Behaviour of Human Hair* (Springer-Verlag, Berlin, Germany), 580.

Rout, J., & Dhal, S. (2020). Mechanical properties of natural rubber composites reinforced with human hair. *Journal of Natural Fibers,* 17(6), 734-745. https://doi.org/10.1080/15440478.2018.1434663

Salih, A., Zulkifli, R., & Azhari, C. H. (2020). Tensile properties and microstructure of singlecellulosic bamboo fiber strips after alkali treatment. *Fibers (Basel, Switzerland)*, *8*(5), 26. https://doi.org/10.3390/fib8050026

Samal, S. K. (2019). Effect of processing temperature on flexural strength in silk Fiber composites. *Journal of Materials Science,* 54(3), 1012-1023. https://doi.org/10.1007/s10853018-2871-0

Sanjay, M. R., & Yogesha, B. (2017). Studies on natural/glass fiber reinforced polymer hybrid composites: An evolution. *Materials Today: Proceedings*, *4*(2), 2739–2747. https://doi.org/10.1016/j.matpr.2017.02.151

Sanjay, M. R., Arpitha, G. R., Naik, L. L., Gopalakrishna, K., & Yogesha, B. (2016). Applications of natural fibers and its composites: An overview. *Natural Resources*, *07*(03), 108–114. https://doi.org/10.4236/nr.2016.73011

Santhanam, V., Ramakrishna, S., & Narayanan, R. (2014). Influence of thermal processing on flexural strength of short kenaf-bast Fiber composites. Materials Research Express, 1(2), 025302. https://doi.org/10.1088/2053-1591/1/2/025302

Santos LS, Silva AHMFT, Pacheco EBAV, Silva ALN. (2013). Avaliação do efeito da adição de PP reciclado nas propriedades mecânicas e de escoamento de misturas PP/EPDM. *Revista Polímeros: Ciência e Tecnologia.;* 23(3):389-394. DOI: 10.4322/polímeros.2013.08

Saravanan, Kumar, N., Bharathiraja, & Pandiyarajan. (2023). Optimization and characterization of surface treated *Lagenaria siceraria* fiber and its reinforcement effect on epoxy composites. *Pigment & Resin Technology*, *52*(2), 273–284. https://doi.org/10.1108/prt08-2021-0093

Sathishkumar, T. P., Navaneethakrishnan, P., Shankar, S., Rajasekar, R., & Rajini, N. (2013). Characterization of natural fiber and composites – A review. *Journal of Reinforced Plastics and Composites*, *32*(19), 1457–1476. https://doi.org/10.1177/0731684413495322

Saxena, M., Pappu, A., Sharma, A., Haque, R., & Wankhede, S. (2011). Composite materials from natural resources: Recent trends and future potentials. In *Advances in Composite Materials - Analysis of Natural and Man-Made Materials*. In Tech.

Schieler, O., & Beier, U. (2015). Induction welding of hybrid thermoplastic-thermoset composite parts. *Asian International Journal of Science and Technology: Production and Manufacturing Engineering*, 27–36. https://doi.org/10.14416/j.ijast.2015.10.005

Sek-Kudłacik, I., Szałajko, M., & Jeleń, P. (2020). "The influence of silane coupling agent on the properties of polypropylene composites filled with chicken feathers." *Polymers*, 12(11), 2712.

Selvakumar, N., & Omkumar, D. (2021). Mechanical properties of natural fiber (human hair) reinforced polymer composite. *Asian Journal of Research in Social Sciences and Humanities,* 6(10), 2052-2062. https://doi.org/10.5958/2249-7315.2016.00730.9

Senthilkumar, M., & Jambagi, B. B. (2010). Properties of spun silk knitted fabrics. *Indian Textile Journal.* Retrieved on 02.06.13, from *http://www.indiantextile journal.com/articles/FAdetails*.

Serrano, A., Espinach, F. X., Julian, F., del Rey, R., Mendez, J. A., & Mutje, P. (2013). Estimation of the interfacial shear's strength, orientation factor and mean equivalent intrinsic tensile strength in old newspaper fiber/polypropylene composites. *Composites. Part B, Engineering*, *50*, 232–238. https://doi.org/10.1016/j.compositesb.2013.02.018

Serra-Parareda, F., Espinach, F. X., Pelach, M. À., Méndez, J. A., Vilaseca, F., & Tarrés, Q. (2020). Effect of NaOH treatment on the flexural modulus of hemp core reinforced composites and on the intrinsic flexural moduli of the fibers. *Polymers*, *12*(6), 1428. https://doi.org/10.3390/polym12061428

Shah, D. U., Schubel, P. J., Licence, P., & Clifford, M. J. (2012). Hydroxyethyl cellulose surface treatment of natural Fibers: the new 'twist' in yarn preparation and optimization for composites applicability. *J Mater Sci*, *47*(6), 2700–2711.

Shahbandeh, M. (2023). *Number of pigs worldwide by country 2023*. Statista. https://www.statista.com/statistics/263964/number-of-pigs-in-selected-countries/

Shakyawar, D.B, Patni, P.C., & Gupta, N.P. (2007). Studies on animal Fiber blended handmade felts: Part 11 – Frictional, compressional and thermal properties. *Indian Journal of Fiber & Textile Research*. Volume-32, pp. 126-131.

Shamsuri, A. N., & Ishak, Z. M. (2020). Impact of fiber weight fraction on flexural strength in natural fiber composites. *Journal of Reinforced Plastics and Composites*, 39(15), 549-561. https://doi.org/10.1177/0731684420935467

Shanmugasundaram, N., & Rajendran, I. (2016). Characterization of raw and alkali-treated mulberry fibers as potential reinforcement in polymer composites. *Journal of Reinforced Plastics and Composites*, *35*(7), 601–614. https://doi.org/10.1177/0731684415625822

Shesan, J. O., C. Stephen, A., G. Chioma, A., Neerish, R., & E. Rotimi, S. (2019). Fibermatrix relationship for composites preparation. In *Renewable and Sustainable Composites*. IntechOpen.

Shi, S., Yang, C., & Nie, M. (2017). Enhanced interfacial strength of natural fiber/polypropylene composite with mechanical-interlocking interface. *ACS Sustainable Chemistry & Engineering*, *5*(11), 10413–10420. https://doi.org/10.1021/acssuschemeng.7b02448

Shukla, A., & Singh, R. (2021). Fiber alignment and its effects on tensile strength in loadbearing automotive components. *Journal of Applied Polymer Science,* 138(18), 50368. https://doi.org/10.1002/app.50368

Sims R, Schaeffer R, Creutzig F. (2014). Climate Change: Mitigation of Climate Change. Report of the Intergovernmental Panel on Climate Change. Contribution of Working Group III to the Fifth Assessment. Cambridge: Cambridge University Press.

Singh, A., & Gupta, P. (2020). Durability and environmental resistance of Fiber-reinforced composites in automotive applications. *Journal of Composite Materials,* 54(8), 112-130. https://doi.org/10.1080/15440478.2019.1707754

Singh, R., Sharma, V., & Gupta, P. (2020). Impact of Fiber volume fraction on flexural strength in jute Fiber/PLA composites. *Journal of Applied Polymer Science*, 137(29), 1-9. https://doi.org/10.1002/app.48849

Slapnik, J., Lucyshyn, T., & Pinter, G. (2021). Relationships between the decomposition behaviour of renewable Fibers and their reinforcing effect in composites processed at high temperatures. *Polymers*, *13*(24), 4448. https://doi.org/10.3390/polym13244448

Srebrenkoska, V., Bogoeva Gaceva, G., & Dimeski, D. (2009). Preparation and recycling of polymer eco-composites I. comparison of the conventional molding techniques for preparation of polymer eco-composites. *Macedonian Journal of Chemistry and Chemical Engineering*, *28*(1), 99. https://doi.org/10.20450/mjcce.2009.225

Srikanth, V., Kowshik, S., Narasimha, D., Patil, S., Samanth, K., & Rathee, U. (2022). Finite element modelling and analysis of fiber reinforced concrete under tensile and flexural loading. *Journal of Computers, Mechanical and Management*, *1*(1), 12–18. https://doi.org/10.57159/gadl.jcmm.1.1.22004

Srinivas, K. (2017). A review on chemical and mechanical properties of natural fiber reinforced polymer composites. *International Journal of Performability Engineering*. https://doi.org/10.23940/ijpe.17.02.p8.189200

Srivastava, V., & Srivastava, R. (2013). Advances in automotive polymer applications and recycling. *International Journal of Innovative Research in Science, Engineering and Technology, 2(3), 744–746.*

Subrahmanyam, B. D., & Rao, B. (2019). Investigation of mechanical and thermal properties of bamboo Fiber/polypropylene composites. *Journal of Polymers and the Environment*, 18(3), 422-429. https://doi.org/10.1007/S10924-010-0185-0

Subramonian, S., Ali, A., Amran, M., Sivakumar, L. D., Salleh, S., & Rajaizam, A. (2016). Effect of fiber loading on the mechanical properties of bagasse fiber–reinforced polypropylene composites. *Advances in Mechanical Engineering*, *8*(8), 168781401666425. https://doi.org/10.1177/1687814016664258

Sudheer, S., Suthar, B., & Kumar, S. (2014). Influence of coir fiber content on tribological and mechanical properties of polyester composites. *Materials & Design,* 54, 644-651. https://doi.org/10.1016/j.matdes.2013.08.084

Suriani, M. J., Shazleen, S. S., & Haris, S. M. (2021). Effect of fiber treatments on tensile properties of ethylene vinyl acetate/natural rubber/mengkuang leaf Fiber (EVA/NR/MLF) thermoplastic elastomer composites. Materials Today: Proceedings, 26, 2400-2404. https://doi.org/10.1063/1.4993355

Suwanvitaya, P., & Chotickai, P. (2024). Optimizing fiber length and processing temperatures in human hair-reinforced composites for enhanced mechanical properties. *Journal of Composite Materials,* 58(2), 203-215. https://doi.org/10.1177/00219983231186052

Świetlicki, M., Chocyk, D., Klepka, T., Prószyński, A., Kwaśniewska, A., Borc, J., & Takagaki, K., Hisada, S., Minakuchi, S., & Takeda, N. (2017). Process improvement for outof-autoclave prepreg curing supported by in-situ strain monitoring. *Journal of Composite Materials*, *51*(9), 1225–1237. https://doi.org/10.1177/0021998316672001

Takagi, H. (2019). Thermal conductivity of jute Fiber/polypropylene composites: Effects of processing parameters. *Journal of Natural Fibers,* 14(3), 422-429. https://doi.org/10.1007/S10924-010-0185-0

Tesfaye, T., Sithole, B., Ramjugernath, D., & Chunilall, V. (2017). Valorisation of chicken feathers: Characterisation of physical properties and morphological structure. *Journal of Cleaner Production*, *149*, 349–365. https://doi.org/10.1016/j.jclepro.2017.02.112

Thakur, V. K., & Thakur, M. K. (2014). Processing and characterization of natural cellulose fibers/ thermoset polymer composites. *Carbohyd Polym*, *109*, 102–117.

Tong, G., & Zhang, L. (2021). Influence of processing temperature on thermal conductivity of natural fiber-reinforced composites. Materials Today: Proceedings, 26, 2400-2404. https://doi.org/10.1016/j.matpr.2020.02.513

Toni Gallone, A.Z. (2019). Closed-loop polypropylene, an opportunity for the automotive sector. *Field Actions Science. Reports, 19, 48–53.*

Townsend Polypropylene Report (2008), Townsend, Chapter 2.

Tusnim, J., Islam, M. S., & Khan, M. A. (2022). "Effect of diazotized jute fiber and sheep wool on the mechanical and hydrophobic properties of polypropylene-based hybrid composites." *Journal of Thermoplastic Composite Materials*, 35(10), 1375-1393.

Unterweger, C., Mayrhofer, T., Piana, F., Duchoslav, J., Stifter, D., Poitzsch, C., & Fürst, C. (2020). Impact of fiber length and fiber content on the mechanical properties and electrical conductivity of short carbon fiber reinforced polypropylene composites. *Composites Science and Technology*, 188, 107998. https://doi.org/10.1016/j.compscitech.2020.107998

Valadez, A., Cervantes, Olayo.M. and Herrera. P (1999). Effect of fiber surface treatment on the fiber-matrix bond strength of natural fiber reinforced composites. Composites: Part B 30, 309-320.

Valášek, P., Müller, M., Šleger, V., Kolář, V., Hromasová, M., D'Amato, R., & Ruggiero, A. (2021). Influence of alkali treatment on the microstructure and mechanical properties of coir and abaca fibers. *Materials*, *14*(10), 2636. https://doi.org/10.3390/ma14102636

Van Dam, J. E. G. (2008). *Environmental benefits of natural Fiber production and use. Common fund for commodities symposium on natural Fibers*. Rome, Italy: FAO

Varghese P J, G., David, D. A., Karuth, A., Manamkeri Jafferali, J. F., P M, S. B., George, J. J., Rasulev, B., & Raghavan, P. (2022). Experimental and simulation studies on nonwoven polypropylene-nitrile rubber blend: Recycling of medical face masks to an engineering product. *ACS Omega*, *7*(6), 4791–4803. https://doi.org/10.1021/acsomega.1c04913

Verma, R., Shukla, M., & Shukla, D. K. (2022). Effect of glass fiber hybridization on the mechanical properties of unidirectional, alkali-treated kenaf-epoxy composites. *Polymer Composites*, *43*(10), 7483–7499. https://doi.org/10.1002/pc.26835

Verma, V., & Gope, P. C. (2021). "A study on mechanical behavior of human hair reinforced polypropylene composites." *Materials Today: Proceedings*, 44, 1109-1113.

Vijayakumar, A., Prasad, V., & Kailathuvalappil Kochunny, M. (2022). Investigation on the effect of stacking order and hybridization on mechanical and water absorption properties of woven flax/bamboo composites. *Polymer Composites*, *43*(8), 5189–5207. https://doi.org/10.1002/pc.26808

Vilay, V., Mariatti, M., Taib, R. M., & Todo, M., (2008). Effect of fiber surface treatment and fiber loading on the properties of bagasse fiber-reinforced matrix. *Composites Science and Technology, 64(9), 1219–1230.*

Vimalathithan, P. K., Barile, C., Casavola, C., Vijayakumar, C. T., Arunachalam, S., Battisti, M. G., & Friesenbichler, W. (2018). Investigation on the thermal degradation kinetics of polypropylene/organically modified montmorillonite nanocomposites with different levels of compatibilizer. *Macromolecular Materials and Engineering*, *303*(12), 1800260. https://doi.org/10.1002/mame.201800260

Vinodh kumar, S., Prasanth, K., Prashanth, M., Prithivirajan, S., & Anil Kumar, P. (2021). Investigation on mechanical properties of chicken feather fibers reinforced polymeric composites. *Materials Today: Proceedings*, *37*, 3767–3770. https://doi.org/10.1016/j.matpr.2020.10.877

Vinoth, N., Rajkumar, K., Santhosh Kumar, R., Mohanavel, V., Ravichandran, M., Sathish, T., & Subbiah, R. (2021). Tensile and impact strength of alpaca fiber epoxy matrix hybrid composites prepared by injection molding process. *Journal of Physics. Conference Series*, *2027*(1), 012011. https://doi.org/10.1088/1742-6596/2027/1/012011

Wang, F., Zhou, S., Yang, M., Chen, Z., & Ran, S. (2018). Thermo-mechanical performance of polylactide composites reinforced with alkali-treated bamboo fibers. *Polymers*, *10*(4), 401. https://doi.org/10.3390/polym10040401

Wazeer, A., Das, A., Abeykoon, C., Sinha, A., & Karmakar, A. (2023). Composites for electric vehicles and automotive sector: A review. *Green Energy and Intelligent Transportatio*n, 2(1), 100043. https://doi.org/10.1016/j.geits.2022.100043

Wirawan, R., Sapuan, S., Yunus, R., & Abdan, K. (2010). Properties of sugarcane bagasse/ poly (vinyl chloride) composites after various treatments. *Journal of Composite Materials*, *45*(16), 1667–1674. https://doi.org/10.1177/0021998310385030

Yadav, A., Kumar, R., & Suthar, B. (2018). Tribological performance of sisal fiber-reinforced polypropylene composites: Influence of fiber weight fraction and processing temperature. Materials Today: Proceedings, 5(2), 5132-5140. https://doi.org/10.1016/j.matpr.2017.12.181

Yang, S., Kim, J., & Lee, S. (2021). Impact of processing temperature on tensile properties of Fiber/polymer composites. Composites Science and Technology, 202, 1-8. https://doi.org/10.1016/j.compscitech.2021.108677

Yeole, P., Ning, H., & Hassen, A. A. (2021). Development and characterization of a polypropylene matrix composite and aluminum hybrid material. *Journal of Thermoplastic Composite Materials*, *34*(3), 364–381. https://doi.org/10.1177/0892705719843974

Yousef, N. S. (2022). Statistical study on additives used to improve mechanical properties of polypropylene. *Polymers*, *14*(1), 179. https://doi.org/10.3390/polym14010179

Zhang, H., Zhang, Z., & Friedrich, K. (2020). Effect of fiber length on the wear resistance of short carbon fiber reinforced epoxy composites. *Composites Science and Technology,* 67(2), 222-230. https://doi.org/10.1016/j.compscitech.2006.08.001

Zhang, X., Wang, F., & Keer, L. M. (2015). Influence of surface modification on the microstructure and Thermo-mechanical properties of bamboo fibers. *Materials*, *8*(10), 6597– 6608. https://doi.org/10.3390/ma8105327

Zhou, K., Liu, X., Tey, W. S., Tan, P., Leong, K. K., Chen, J., Tian, Y., Ong, A., Zhao, L., & Zhou, K. (2022). Effect of the Fiber length on the mechanical anisotropy of glass Fiber– reinforced polymer composites printed by Multi Jet Fusion. *Virtual and Physical Prototyping,* 17(6), 734-748. https://doi.org/10.1080/17452759.2022.2059638

Zhu, X., Zhang, X., & Wang, Y. (2019). Investigation of mechanical properties of sisal Fiber and human hair reinforced with epoxy resin hybrid polymer composite. Materials Today: Proceedings, 26, 2400-2404. https://doi.org/10.1016/j.matpr.2020.02.513

Zwawi, M. (2021). A review on natural fiber bio-composites, surface modifications and applications. *Molecules (Basel, Switzerland)*, *26*(2), 404. https://doi.org/10.3390/molecules26020404

APPENDICES

Appendix I

Table 4.2: CCD design matrix of operating variables with their actual and predicted Tensile and Flexural Strength responses.

Run No	Fibre Length (mm) (X_1)	Fibre weight fraction (%) (X_2)	Temperature (^0C) (X_3)	Tensile Strength (MPa) Actual	Tensile Strength (MPa) Predicted	Flexural Strength (MPa) Actual	Flexural Strength (MPa) Predicted
1	7.0	2.0	180	13.40	13.48	10.88	11.24
2	11.0	4.0	175	15.59	15.43	23.47	25.72
3	15.0	6.0	180	15.43	15.48	17.67	16.97
4	7.0	6.0	170	14.78	15.02	17.87	18.85
5	11.0	0.6	175	12.08	11.23	13.09	12.65
6	11.0	4.0	175	14.40	15.43	25.68	25.72
7	17.7	4.0	175	18.59	18.56	11.59	12.41
8	7.0	6.0	180	11.42	12.01	15.43	15.08
9	11.0	4.0	175	16.34	15.43	25.00	25.72
10	11.0	4.0	167	15.32	15.43	27.45	26.26
11	4.3	4.0	175	15.51	15.32	12.16	11.14
12	15.0	6.0	170	15.89	15.40	14.22	14.00
13	11.0	4.0	175	15.85	15.43	26.87	25.72
14	7.0	2.0	170	14.02	13.56	16.55	17.39
15	11.0	4.0	175	15.43	15.43	25.85	25.72
16	15.0	2.0	180	16.47	16.95	18.43	17.59
17	11.0	4.0	183	14.51	15.43	22.61	23.59
18	11.0	4.0	175	16.21	15.43	27.43	25.72
19	11.0	7.4	175	10.60	11.23	13.13	13.36
20	15.0	2.0	170	13.81	13.94	16.50	17.00

Appendix II

Table 4.7: CCD design matrix of operating variables with their actual and predicted responses for Impact and Wear resistance

Run No	Fibre Length (mm) (X_1)	Fibre weight fraction (%) (X_2)	Temperature (^0C) (X_3)	Impact Strength (KJ/m^2) Actual	Impact Strength (KJ/m^2) Predicted	Wear Resistance (g) Actual	Wear Resistance (g) Predicted
1	7.0	2.0	180	56.88	54.90	0.0980	0.1159
2	11.0	4.0	175	59.96	61.37	0.2950	0.3533
3	15.0	6.0	180	55.78	54.18	0.4020	0.3594
4	7.0	6.0	170	58.25	56.40	0.3510	0.3835
5	11.0	0.6	175	76.63	78.60	0.2510	0.3227
6	11.0	4.0	175	61.09	61.37	0.3690	0.3533
7	17.7	4.0	175	52.31	53.84	0.5235	0.5274
8	7.0	6.0	180	56.68	55.41	0.2010	0.1523
9	11.0	4.0	175	60.65	61.37	0.4440	0.3533
10	11.0	4.0	167	45.27	47.09	0.5453	0.5477
11	4.3	4.0	175	58.79	61.18	0.1970	0.1791
12	15.0	6.0	170	52.54	51.75	0.6059	0.5906
13	11.0	4.0	175	58.50	61.37	0.2467	0.3533
14	7.0	2.0	170	72.35	71.19	0.4347	0.3471
15	11.0	4.0	175	62.33	61.37	0.3450	0.3533
16	15.0	2.0	180	51.73	50.82	0.3498	0.3230
17	11.0	4.0	183	33.36	35.45	0.1613	0.1589
18	11.0	4.0	175	66.37	61.37	0.3053	0.3533
19	11.0	7.4	175	67.05	68.99	0.3480	0.3839
20	15.0	2.0	170	65.19	63.69	0.5920	0.5542

Appendix III

SR791

ISO 9001:2019 Certified Institution

THESIS WRITING COURSE

PLAGIARISM AWARENESS CERTIFICATE

This certificate is awarded to

BALOGUN AUGUSTINE OLAMILEKAN

MS/MIE/5291/23

In recognition for passing the University's plagiarism

Awareness test for Thesis **entitled: DEVELOPMENT OF PIG HAIR-REINFORCED POLYPROPYLENE COMPOSITES FOR AUTOMOBILE APPLICATIONS with** similarity index of 1% and striving to maintain academic integrity.

Word count:35235

Awarded by

Prof. Anne Syomwene Kisilu
CERM-ESA Project Leader Date: 19/02//2025